CELLULAR AND MOLECULAR STUDIES OF CILIARY NEUROTROPHIC FACTOR RECEPTOR ALPHA EXPRESSION AND CILIARY NEUROTROPHIC FACTOR MEDIATED NEUROPROTECTION IN THE CANINE RETINA

A Dissertation

Presented to the Faculty of the Graduate School

of Cornell University

in Partial Fulfillment of the Requirements for the Degree of

Doctor of Philosophy

by

William Anthony Beltran

May 2006

CELLULAR AND MOLECULAR STUDIES OF CILIARY NEUROTROPHIC FACTOR RECEPTOR ALPHA EXPRESSION AND CILIARY NEUROTROPHIC FACTOR MEDIATED NEUROPROTECTION IN THE CANINE RETINA

William Anthony Beltran, Ph.D.

Cornell University 2006

Over the past decades, extensive new knowledge on the cellular and molecular mechanisms of vision has been acquired. During the genomic era, numerous genes involved in retinal function have been identified, some of which have been causally associated with various forms of retinal disorders. Despite this rapid progress in the understanding of retinal biology, retinal degeneration, the most common cause of blindness in the developed world remains an untreatable condition. A therapeutic strategy that has been tested in several animal models of retinal degeneration has been to deliver intraocularly a survival factor, ciliary neurotrophic factor (CNTF), in an attempt to rescue photoreceptor cells prior to cell death.

To begin addressing the question about the mechanism of CNTF-mediated neuroprotection, the retinal expression of the specific receptor for CNTF (CNTFRα) was characterized. Using different molecular approaches, we found that photoreceptor cells from non-rodent mammalian species (including dog and human) express CNTFRα. This led to the conclusion that in these species, a CNTF- mediated photoreceptor rescue effect would most likely result from the direct activation of a pro-survival response in rods and cones.

The underlying expectation in testing CNTF as a potential treatment for retinitis pigmentosa (RP) and allied disorders is that it may provide a means of

protecting photoreceptor cells regardless of the genetic and/or environmental causes of the disease. This hypothesis is based on the evidence that CNTF rescues photoreceptors in several non-allelic animal models of RP. One such model has been *rcd1*, a canine form of early-onset and rapidly progressing retinal degeneration caused by a mutation in the *PDE6B* gene. In this work, we evaluated whether CNTF could also rescue photoreceptors in *XLPRA2*, another early-onset canine model of RP caused by a mutation in a different gene (*RPGR* exon ORF15). The characterization of the histological stages of the disease, and the examination of the kinetics of cell death provided time-points to optimally test CNTF's neuroprotective effect in this model. Intravitreal injections of CNTF in *XLPRA2* at these determined ages failed to show any significant rescue from cell death, and caused some abnormal peripheral retina remodeling that was disease- and age-specific.

BIOGRAPHICAL SKETCH

William Anthony Beltran was born in Barnet, United Kingdom, in 1971. After spending part of his childhood in South America (Colombia, Venezuela), he moved with his family to Paris (France). After 4 years of training in veterinary medicine, he graduated in 1994 from the Ecole Nationale Vétérinaire d'Alfort (ENVA; Maisons-Alfort, France). He then enrolled in a two-year internship program in small animal medicine at ENVA. In 1997, he defended his veterinary thesis and was awarded the title of "Docteur Vétérinaire" with honors. That same year, he started a 3-year residency program in veterinary ophthalmology at ENVA and obtained board certification in the European College of Veterinary Ophthalmologists in 2003. In August 2000, he moved to the Unites States to begin a Ph.D. program in Comparative Biomedical Sciences at the Veterinary College at Cornell University. He carried out his graduate studies in Dr Gustavo Aguirre's laboratory, initially at Cornell and then at the School of Veterinary Medicine, University of Pennsylvania. In July 2006 he will join the School of Veterinary Medicine at the University of Pennsylvania as an Assistant Professor of Ophthalmology.

A Gaëlle

ACKNOWLEDGMENTS

During the last several years, I have learned a tremendous amount both on a scientific and personal level, and I am indebted to many people.

First and foremost, I thank my advisor and committee chair, Dr. Gustavo Aguirre, for his exceptional mentoring and the example he sets. He shared with me a lot of his experience, provided his guidance whenever I needed it, but gave me the freedom to explore my own ideas. I am extremely privileged to have learned from him and trained in his laboratory.

During my time in the laboratory, I had the opportunity to work with many very special people, and I wish to express my gratitude to the following individuals:
Dr. Gregory Acland for his openness in sharing scientific questions, as well as his longtime commitment and experience in directing the Retinal Disease Studies Facility. This animal resource was vital to this work.
Drs. Qi Zhang, James Kijas, and Danian Gu for introducing me to the art of molecular biology.
Sue Pearce-Kelling for sharing with me a great deal of her expertise in histology, and for her dedication at always doing her best to create the optimal atmosphere in the group.
Amanda Nickle, Gerri Antonini, and the staff of the Retinal Disease Studies Facility for their commitment and professionalism that was essential to my research.
Julie Jordan and Pamela Hammond for the invaluable technical support they both provided, and for all the enjoyable moments we got to share.
Keith Watamura, and Mary Leonard for the excellence of their graphics support.

The committee members, Drs. Mark Saltzman, Brian Summers, Roy Levine, and Vicki Meyers-Wallen provided useful comments and guidance during the various phases of this project. I thank them for their time and thoughtful evaluation of this work.

My work was also dependent on the contribution of several collaborators. In particular, I am grateful to Dr. Rong Wen who provided me significant amounts of CNTF throughout the course of the project, Dr. Hermann Rohrer for sharing his CNTFRα antibody which was critical for two of my studies.

I would like to thank and acknowledge the contributions made by the College of Veterinary Medicine's Graduate Research Assistantship Program for providing funding for a significant part of my graduate work, and to the Foundation Fighting Blindness for the remainder of my training.

Finally, this enterprise would not have been possible without the initial and continuous support of my wife, Gaëlle. Un très grand Merci.

TABLE OF CONTENTS

LIST OF FIGURES

LIST OF TABLES

LIST OF ABBREVIATIONS

ALS: amyotrophic lateral sclerosis

ARMD: age-related macula degeneration

BDNF: Brain-derived neurotrophic factor

bFGF: basic fibroblast growth factor

cGMP: cyclic guanosine monophosphate

CNTF: ciliary neurotrophic factor

CNTFRα: α subunit of the ciliary neurotrophic factor receptor

CRD: cone-rod dystrophy

CT-1: cardiotrophin 1

DHA: docosahexaenoic acid

ECT: encapsulated cell-based therapy

GCL: ganglion cell layer

GDNF: Glial cell-derived neurotrophic factor

GPI: glycosyl phosphatidylinositol

HD: Huntington's disease

INL: inner nuclear layer

IOP: intraocular pressure

IPL: inner plexiform layer

IS: inner segments

KO: knock-out

LCA: Leber congenital amaurosis

LIFRβ: Leukemia inhibitory factor receptor β

NFL: nerve fiver layer

OCT: optimal cutting temperature medium

ONL: outer nuclear layer

OPL: outer plexiform layer

OS: outer sergments

PAGE: polyacrylamide gel electrophoresis

PCR: polymerase chain reaction

PEDF: Pigment epithelial derived factor

PBS: Phosphate buffered saline

PDE: phosphodiesterase

PRA: Progressive retinal atrophy

PRL: photoreceptor layer

rAAV: recombinant adeno-associated virus

RCD: rod-cone dystrophy

rcd1: rod cone dysplasia type 1

rcd2: rod cone dysplasia type 2

rcd3: rod cone dysplasia type 3

rd: rod degeneration

rds: rod degeneration slow

RD: retinal degeneration

RdCVF: rod-derived cone viability factor

RH: radiation hybrid

RP: retinitis pigmentosa

RPE: retinal pigment epithelium

RPGR: retinitis pigmentosa GTPase regulator

RT-PCR: reverse transcription polymerase chain reaction

VEGF: vascular endothelial growth factor

XLPRA: X-linked progressive retinal atrophy

XLPRA1: X-linked progressive retinal atrophy type 1

XLPRA2: X-linked progressive retinal atrophy type 2

“Dans la Nature…il ne faut rien voir d’impossible,

s’attendre à tout,

et supposer que tout ce qui peut être est. »

Georges-Louis Leclerc, Comte de Buffon, 1788

CHAPTER ONE

INTRODUCTION

Background information

Retinal degenerations (RD) are the major cause of blindness in the developed world. Some forms occur at birth (eg: Leber Congenital amaurosis), during adulthood [numerous forms of Retinitis Pigmentosa (RP)], or in the elderly [eg: age-related macular degeneration (ARMD)]. Retinitis Pigmentosa is a heterogenous group of inherited retinal degenerative diseases, characterized by the progressive death of rod and cone photoreceptors. Over the past decades, numerous genes have been identified as causing RP, yet, the molecular and cellular mechanisms that lead from a mutation in a gene to the death of a photoreceptor cell are still largely unknown. As a consequence, no treatments are currently available to treat patients with these devastating diseases.

Animal models of RP have been critical to understand the function of genes in the retina, as well as to unveil the cellular and molecular events that occur during the disease processes. They have also been used to examine the effects of environmental factors (such as diet, light exposure) on the disease, and finally, have provided an indispensable tool to develop and evaluate the safety and efficacy of novel therapeutic approaches.

The most common therapeutic strategies that are being evaluated for RP can be divided into three groups: 1) approaches aimed at replacing the non-functional photoreceptors or retina, such as grafting of retinal sheets or retinal precursor cells, or the implantation of artificial retinal prostheses. 2) approaches aimed at curing the disease through corrective gene therapy. 3) approaches aimed at delaying the course of

the disease and the onset of photoreceptor death through the use of neuroprotective agents such as vitamin A, anti-apoptotic agents, calcium channel blockers, and survival factors.

Several survival factors have been tested in animal models of RP. These include basic fibroblast growth factor (bFGF), ciliary neurotrophic factor (CNTF), brain-derived neurotrophic factor (BDNF), glial cell-derived neurotrophic factor (GDNF), and pigment epithelium-derived factor (PEDF). Among these, CNTF has been the most extensively studied and has been shown to rescue photoreceptors in rodent as well as large animal species (dog and cat). Because of the side-effects associated with both systemic and intravitreal bolus administration of CNTF, long-term intraocular drug delivery is necessary and can be achieved through gene therapy, as well as by means of an encapsulated cell-based device. This latter technology allows the slow and continuous release of small doses of CNTF into the eye, and has recently been evaluated in experimental animal models, and in Phase I clinical trial in humans.

The molecular mechanisms of CNTF's mediated photoreceptor survival are not fully elucidated. Yet, CNTF is known to trigger several signaling pathways through the binding to CNTFRα, its specific membrane receptor. Determining the mechanism of action of CNTF is critical to 1) optimize the neuroprotective property of this agent. 2) inhibit, or reduce biological properties of this factor that can lead to deleterious side-effects. 3) select the forms of RP that would benefit most from this potential treatment.

Numerous genes cause retinitis pigmentosa in humans

Retinitis pigmentosa is genetically and phenotypically a heterogeneous group of diseases that has an estimated prevalence of approximately 1:4,000.[1-3] It is

classically divided into two clinically distinct group of diseases: rod-cone dystrophies (RCD) and cone-rod dystrophies (CRD).

Most RP diseases are rod-cone dystrophies. They are characterized by an initial loss of rods in the peripheral and mid-peripheral retina that progresses towards the central retina, and may lead to secondary loss of cones. The most common clinical signs are an initial loss of peripheral vision and night blindness. The progressive concentric reduction of the peripheral visual fields causes what patients describe as "tunnel vision".[4] The progression of the disease to the foveo-macular region of the retina leads ultimately to the loss of central vision and complete blindness. Fundus examination of patients with RP usually reveals pigmentary deposits (known as bone spicule pigments) that are caused by the migration of retinal pigment epithelial (RPE) cells into the neurosensory retina.[4] Attenuation of the retinal vessels and pallor of the optic disc are also commonly observed signs.

A smaller group of diseases under the RP rubric are cone-rod dystrophies, in which primary degeneration of cones is followed by the loss of rods.[5] Cone-rod dystrophies are clinically characterized by an early reduction in visual acuity and color vision, photophobia, central or paracentral scotomas, and occasionally fine nystagmus. Fundus examination reveals an early-onset maculopathy characterized by atrophy and pigmentary deposits that occasionally extend to the midperipheral retina at later stages of the disease.

At present, 114 genes responsible for some form of retinal degeneration in man have been cloned and 164 mapped. A listing of these genes is available on the Retnet web site (http://www.sph.uth.tmc.edu/Retnet/home.htm) (see Figure 1.1). Of these, 36 genes and 9 loci cause RCD, and 10 genes and 6 loci cause CRD. Both forms of dystrophies are inherited as either autosomal recessive, autosomal dominant or X-linked diseases (Table 1.1).

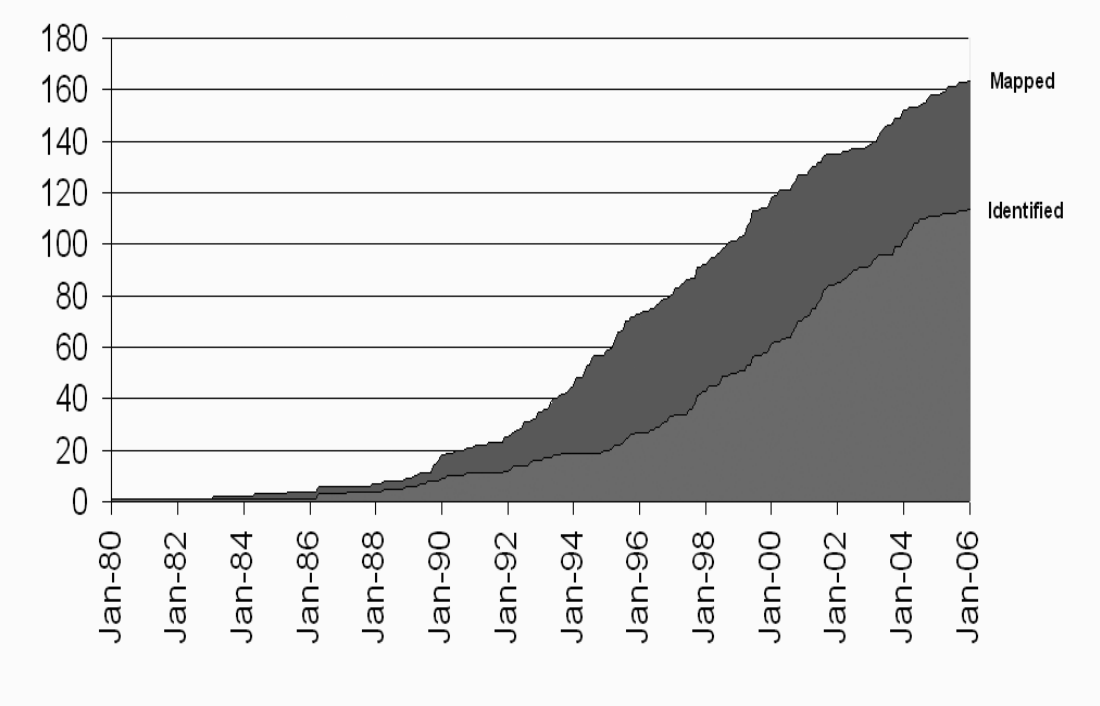

Figure 1.1 Mapped and identified retinal disease genes 1980-2006 as of January 2006 (from RetNet; http://www.sph.uth.tmc.edu/Retnet/home.htm).

Table 1.1 List of cloned and mapped genes associated with retinitis pigmentosa (from RetNet, 01/17/06; http://www.sph.uth.tmc.edu/Retnet/home.htm)

Disease category	Mapped loci (not identified)	Mapped and Identified genes
Retinitis pigmentosa (RCD) autosomal dominant	RP31	CA4, CRX, FSCN2, GUCA1B, IMPDH1, NRL, PRPF3, PRPF8, PRPF31, RDS, RHO, ROM1, RP1, RP9, SEMA4A
Retinitis pigmentosa (RCD) autosomal recessive	RP22, RP25, RP28, RP29, RP32	ABCA4, CERKL, CNGA1, CNGB1, CRB1, LRAT, MERTK, NR2E3, NRL, PDE6A, PDE6B, RGR, RHO, RLBP1, RP1, RPE65, SAG, TULP1, USH2A
Retinitis pigmentosa (RCD) X-linked	RP6, RP23, RP24	RP2, RPGR
Retinitis pigmentosa (CRD) autosomal dominant	CORD4, RCD1	AIPL1, CRX, GUCA1A, GUCY2D, RIMS1, SEMA4A, UNC119
Retinitis pigmentosa (CRD) autosomal recessive	CORD8, CORD9	ABCA4, RDH5
Retinitis pigmentosa (CRD) X-linked	COD2, COD4	RPGR

Despite the identification of several RP-associated genes that encode for proteins involved in the phototransduction pathway, the visual cycle, cell trafficking, the spliceosome complex, the structural integrity of photoreceptor outer segments, or that are transcription factors,[6] little is known about the cascade of molecular events that leads from gene mutation to phenotype in a patient. A final common pathway to most forms of retinal degeneration appears to be the cell death of photoreceptors through apoptosis,[7-10] yet, there is mounting evidence coming from the neurodegeneration field that several distinct cell death pathways may be activated at the same time and lead to an apoptosis-necrosis cell death continuum.[11-14] In such a case, this may account for some of the variability in the phenotype of RP diseases, and must be taken into account when developing and testing therapeutic strategies in patients with different forms of RP.

Animal models are indispensable to understand the pathogenesis of RP and develop new therapies.

Animal models of retinal degeneration have been essential to understand the role of numerous genes/proteins in the normal physiology of the retina, to examine the molecular and cellular events that take place during the course of the disease/degeneration, and to investigate potential therapeutic strategies.

Rodents, mice in particular, have been critical in understanding the function of disease genes in the process of photoreceptor degeneration. Currently, more than 16 mutant strains of mice with a naturally occurring form of retinal degeneration have been identified (http://www.jax.org/mmod/retinal_degen.html). [15] Genetic engineering has allowed the generation of over 50 additional models of RD, through gene knockout (KO), gene overexpression, or the introduction of point mutations.[16]

With the exception of the rhodopsin transgenic pig,[17,18] large animal models of RP occur in the feline[19-21] and canine species (see Table 1.2) and are naturally-occurring disorders. In the absence of a non-human primate model of RP, these large animal models offer advantages over rodents such as a higher cone to rod ratio, and an eye size that are closer to that of the human.[22-25] These anatomical characteristics enable the use in the dog of several non-invasive methods of imaging and functional assessment of the retina that are commonly applied in humans.[26-28] They also allow surgical procedures for the intraocular placement of devices,[29,30] and delivery of large volumes of drugs intravitreally or subretinally.[31] Work originating over the past 30 years, from several research groups, has led to the identification, in the dog, of several non-allelic forms of retinal degeneration collectively termed progressive retinal atrophies (PRA). These have been traditionally subdivided in forms that occur before retinal development is attained (= dysplasia; e.g. *rcd1*) and forms with an age of onset that begins after retinal maturity is achieved (= degeneration; e.g. *prcd*, *XLPRA1*). While the vast majority of PRA forms in the dog are diseases of rods with later involvement of cones, studies also have identified three breeds that are affected by non-allelic forms of RD that resemble human cone rod dystrophy. These have been named *crd1*, *crd2*, and *crd3* .[32] The six genes (*PDE6α*, *PDE6β*, *RHO*, *RPGR*, *RPE65*, and *CNGB3*) that have been identified to this date as causing PRA in the dog are all involved in some form of RP in the human. Progressive retinal atrophy in dogs is most often inherited in an autosomal recessive manner (e.g. *rcd1*, *prcd*), yet -linked PRA (XLPRA) has been described in the Siberian Husky and Samoyed,[42] and a dominant form of PRA caused by a mutation in the *rhodopsin* gene has been recently reported in

Table 1.2 Canine models of retinitis pigmentosa

Animal model	Mutant gene	Affected breeds	References
rcd1	*PDE6B*	Irish setter	33, 34, 35, 36
rcd2	unknown	Collies	37, 38
rcd3	*PDE6A*	Cardigan Welsh corgi	39
rd	unknown	Norwegian elkhound	40
erd	unknown	Norwegian elkhound	41
XLPRA2	*RPGR*	mongrel-derived	42
XLPRA1	*RPGR*	Siberian husky, Samoyed	42, 43
prcd	*PRCD*	American cocker spaniel, English cocker spaniel, Poodles, Labrador retriever, Chesapeake bay retriever, Portuguese water dogs, and others	44, 45, 46
T4R RHO	*RHO*	English mastiff, Bull mastiff	47
crd1	Unknown	American Staffordshire terrier	32
crd2	Unknown	American Bull terrier	32
crd3	Unknown	Glen of Imaal terrier	32
cd	*CNGB3*	Alaskan Malamute	48
canine LCA	*RPE65*	German shorthaired pointer Briard	49, 50

the English and Bull Mastiff breeds.[47]

The typical clinical manifestations of PRA show remarkable similarities with human RCD. Loss of vision in dim light or darkness is one of the earliest signs, and is progressively followed by visual impairment under bright light conditions. Ophthalmoscopically, the earliest alterations are a change in tapetal reflectivity that often takes the appearance of a grayish discoloration in the peripheral tapetal fundus. Concurrently, mild retinal vascular attenuation may also be observed in that region. This progresses to involve the entire tapetal fundus, and is followed at later stages by tapetal hyperreflectivity and marked vascular attenuation that causes optic disc pallor. In the non tapetal fundus, patches of depigmentation are commonly observed. The high genetic and phenotypic homology that exists between canine PRA and human RP, argues for the use of the dog as valuable model system to better understand the mechanisms of disease, and test the safety and efficacy of new therapeutic modalities.

Therapeutic strategies for retinitis pigmentosa

The availability of several animal models of RP and the improved understanding of the genetic and biochemical mechanisms of these diseases has led to the development of therapeutic strategies aimed at either, replacing, curing or sustaining the diseased photoreceptors.

1) *Retinal transplantation*.

The transplantation into the subretinal space of RPE cells, dissociated retinal cells, or full thickness retinal sheets as a way of restoring vision by replacing diseased photoreceptors with new functional cells has been investigated for over 20 years (for review see [51]). Subretinal transplantation of RPE cells or fetal retinal sheets was shown in several studies to promote a morphologic rescue of the host's

photoreceptors,[52] as well as a delay in the deterioration of visual acuity.[53 54] However, it is unclear whether this functional rescue is due solely to the release by the transplanted cells of trophic/survival factors,[55] or to the establishment of synaptic connectivity between the transplant and the host.[56,57]

Recently, the transplantation of neural or retinal progenitor cells has been considered as a novel approach for the replacement of damaged photoreceptors (for review see [58,59]). Although a number of studies in animal models have shown that transplanted progenitor cells are capable of integrating into the recipient retina, and expressing retinal cell markers such as opsin, recoverin, PKCα, or calbindin,[60,61] it is still not known whether they can fully differentiate into functional photoreceptors and establish synapses with the host's cells.

In an attempt to bypass diseased or degenerated photoreceptors, several groups have been developing artificial retinal implants. They are designed to stimulate existing neural circuits in diseased retinas to create a visual signal. There are two kinds of retinal prostheses that have been tested: subretinal and epiretinal implants (for review see [62,63]). A subretinal implant is composed of an array of microphotodiodes that are connected to microelectrodes. The implant is surgically placed in the subretinal space between the RPE and the outer plexiform layer (OPL) of the degenerated retina. Light that enters the eye is converted by the microphotodiodes into small currents that are released by the microelectrodes and stimulate second order neurons (horizontal cells, bipolar cells) in the host retina. The epiretinal implant on the other hand is essentially a readout chip that generates electrical impulses and stimulates directly the ganglion cells and their axons after receiving information from a camera and an image processor that are external to the eye. Surgical implantation and long-term biocompatibility of both types of implants have been evaluated in cats and dogs [64,65 30,66] before being tested in humans.[67,68] Implantation of epiretinal

prosthesis in individuals with RP has shown that light perception could be obtained.[67,68]

Subjective improvement in visual function that included improved perception of brightness, contrast, color, movement, shape, resolution, and visual field size has also been observed in RP patients that were implanted with a subretinal prosthesis, yet the improvements occurred in visual areas that were distant from the implant.[69] It has been suggested that mechanical injury of the retina during the surgical procedure as well as low-level electrical stimulation by the implant may elicit the release of endogenously secreted survival factors that provide a generalized neuroprotective effect to the retina.

2) Corrective gene therapy

Corrective gene therapy has been considered as a promising approach to cure inherited retinal degenerations. The identification of several RP causing genes, and relevant animal models, as well as unique features of the eye (contained organ, small area to treat, easily accessible for examination, gene delivery and functional assessment) have led several groups to develop delivery systems that would allow both safe and efficient transduction of the RPE and/or photoreceptor cells.

Gene therapy can be used in recessive disorders to replace the mutated gene by its wild-type version, and correct the loss of function caused by the mutation. The first demonstration that gene therapy could rescue photoreceptors in an autosomal recessive disorder was conducted ten years ago in the *rd* mouse (*PDE6B* mutation) using a first generation adenovirus.[70] Since then, several studies using different viral vectors have shown in the *rd*,[71-73] *rds*,[74-76] *rd12*,[77] , *LRAT* $^{-/-}$,[78], and *RPGRIP* $^{-/-}$ mice,[79] as well as in the *RCS* rat,[80-82] that transduction of the wild-type gene can delay or prevent photoreceptor cell death and restore function. The most exciting results have come from studies conducted in the *RPE65* $^{-/-}$ dog, a model for Leber congenital

amaurosis (LCA), in which gene replacement by means of a recombinant adeno-associated virus (rAAV) provided long-term restoration of vision.[27,50] Using a similar approach, functional rescue was also obtained in the *rd12* mouse, a model of LCA caused by a nonsense mutation in the RPE65 gene.[77] Biosafety studies in rats, dogs as well as in monkeys are currently being carried out, and a Phase I clinical trial in human patients with RPE65 LCA is expected to begin in 2006.[83]

In autosomal dominant diseases in which a mutation causes a toxic gain of function, the purpose of gene therapy is to inhibit the translation of the gene responsible for the deleterious effects. Gene silencing can be achieved through the use of single-strand antisense oligonucleotides, ribozymes, and more recently by RNA interference. These knock down strategies can be allele-specific (i.e. directed against the mutant gene only) or non-allelic (i.e. directed against both the mutant and wild type gene). Because allele-specificity is often difficult to attain, non-allelic silencing has to be complemented with gene replacement. A hardened target (i.e. wild type copy of the gene that has been modified to be resistant to the silencing) needs to be provided in parallel. To this date, only ribozyme technology has been used to knock down genes involved in retinal degeneration (for review see [84]). This was conducted in a transgenic rat model of autosomal dominant retinitis pigmentosa, the rhodopsin P23H rat, and shown to delay the course of photoreceptor death and the loss of retinal function.[85] The ribozyme rescue was shown to persist for over 6 months, and be equally effective when the gene transfer was done at a late-stage of disease than earlier on.[86] The use of RNA interference technology has not been yet reported in any animal model of RP, yet, it was recently shown to be effective in inhibiting vascular endothelial growth factor (VEGF) expression, and reduce choroidal neovascularization, in a rodent model for age-related macular degeneration (ARMD).[87]

3) Photoreceptor neuroprotection

Although corrective gene therapy offers the potential for curing retinal degeneration, it is a therapeutic approach that is gene-specific. Even with a gene knockdown strategy that would allow inhibition in an allele-independent manner of both the wild type and all mutant forms of a gene, followed by replacement with a resistant wild-type cDNA,[88] identification of the deleterious gene is a pre-requisite. An approach that would circumvent this inherent limitation of corrective gene therapy is the use of neuroprotective agents that could be applicable to a wide range of forms of RP, whether or not the disease-causing mutation is known. Since the gene defect is not corrected, this strategy does not "cure" per se, but intends to slow down the progression of the disease. Numerous agents that include nutrients, ionic channel blockers, anti-apoptotic genes, and neurotrophic factors, have been evaluated over the past decades for their photoreceptor rescue properties.

Vitamin A supplementation (15,000 IU/day) was shown in a randomized, controlled, double-masked clinical trial to slow the rate of decline in ERG amplitudes in patients with RP.[89] Recently, two more studies have shown that supplementation with docosahexaenoic acid (DHA) shortens the time for vitamin A to have a positive effect, only in those patients that were newly started on Vitamin A.[90,91] Although the mechanism by which vitamin A preserves retinal function is unknown, dietary recommendations for RP patients have been made that include the intake of vitamin A palmitate (15,000 IU/day), the supplementation with DHA capsules (600 mg twice/day for 2 years) (if no prior intake of vitamin A), and the consumption of omega 3-rich fish at least once a week.[91]

The beneficial effect of calcium channel blockers as a potential treatment for retinal degenerations has been a matter of debate since the first report that D-cis-diltiazem (a blocker of L-type calcium channels and cGMP-gated channels) rescued

rod photoreceptors in the *rd* mouse.[92] Indeed, while these results were further confirmed by the same group,[93], as well as in a light-induced model of RD,[94] others failed to demonstrate a similar rescue effect in the *rd* mouse,[95] *RCS* rat,[96] *P23H* rhodopsin mutant rat,[97], and *rcd1* dog.[98] Among the other calcium channel blockers tested, a positive photoreceptor rescue effect was observed with nilvadipine in both the *rd* mouse, [99], *RCS* rat,[96], and a rat model of cancer-associated retinopathy.[100] These conflicting results about the neuroprotective effect of calcium channel blockers on photoreceptor cells are most likely explained by differences in experimental conditions such as mouse strains, animal model studied, or type of calcium channel blocker used.

Since numerous forms of RD appear to share a common final pathway of cell death via apoptosis, several groups have investigated whether the overexpression of anti-apoptotic genes of the *Bcl-2* family can rescue photoreceptor cells. When transgenic mice overexpressing *Bcl-2* in their photoreceptors were crossed to four murine models of RD (PDEγ knockout, *rd*, S334ter rhodopsin mutant, and normal albino mice exposed to bright light that causes retinal damage), a limited and transient (2-3 weeks) survival effect was attained.[101,102] A longer suppression of cell death was obtained, in the S334ter mouse when the *Bcl-2* transgene was co-expressed with *BAG-1*,[103] or when transgenic *Bcl-2* mice were crossed with *rds* mice that exhibit a slower form of retinal degeneration.[104] By means of an adenoviral vector, somatic delivery of the *Bcl-2* gene to photoreceptors of the *rd* mouse also provided a transient delay in rod cell death.[105]

Over the past decade, extensive research using different rodent models has shown that various survival factors can slow the course of RD. Work conducted in the early nineties by LaVail's group on bFGF launched the concept of using growth factors/neurotrophic factors as a potential strategy for treating RD.[106] Basic FGF was

shown to protect rat photoreceptors from degeneration in inherited,[106] light-induced,[107,108] and age-related[109] models of RD after intravitreal or subretinal injection. Because an increased incidence of cataracts, retinal macrophages, and retinal neovascularization was observed following intraocular injections of bFGF,[106,107,110,111] the light-damage model was used to screen various growth factors and cytokines with the expectation that novel neuroprotective factors causing minimal side-effects could be identified.[112] Among these agents, CNTF and BDNF were shown to provide structural[112-115] and functional[114] rescue of photoreceptors both *in vivo* in rat and mouse models of RD, as well as in retinal explants.[116,117] Other agents, e.g. GDNF[118-120], PEDF,[121-123] as well as the cytokines IL-1beta,[124] and cardiotrophin-1 (CT-1),[125] have been shown to have a survival-promoting activity in rodents. Rod photoreceptor cells are critical in providing structural and trophic support to cones. Studies conducted in Sahel's group have shown that diffusible factors released by rods promote cone rescue in the retina of the *rd* mouse.[126] Recently, characterization and identification of one of these factors, termed rod-derived cone viability factor (RdCVF), has been reported.[127]

CNTF: a promising agent for photoreceptor neuroprotection?

Ciliary neurotrophic factor was first purified in 1984 from chick eyes and identified as a 20.4 kDa polypeptide that promotes the survival of dissociated 8-day chick embryo ciliary ganglionic (parasympathetic) neurons.[128] Soon after, it was purified in the rat[129] and rabbit[130], and its gene cloned for these species as well as for human.[131,132] The human CNTF gene encodes a protein of 200 amino acids, and shares 83% and 87 % identity with, respectively, the rat and rabbit amino acid sequences.[131] BLAST analysis of the human amino acid sequence of CNTF against the canine genome, revealed a 89% homology with the putative canine CNTF protein.

Following the identification of the biological activity of CNTF on chick parasympathetic ciliary neurons, numerous *in vitro* and *in vivo* studies demonstrated that CNTF also promotes the survival of sensory,[133,134] sympathetic,[135,136] and motor neurons.[137,138] This led to the testing of CNTF as a potential therapy for amyotrophic lateral sclerosis (ALS) in both animal models[139,140] and human patients[141-145] affected with this disease. Because of the limited number of individuals that were included in the two Phase I clinical trials that evaluated the safety of intrathecal long-term delivery of CNTF, no claims were made about its effect on motor neuron loss. Intracerebral long-term delivery of CNTF has also be shown to protect striatal neurons from excitotoxic damage following quinolinic acid intrastriatal injection in a rodent model of Huntington's disease (HD).[146-148] In a primate model of HD, CNTF not only protected neurons from degeneration,[149] but it also restored motor and cognitive function.[150]

The intraocular delivery of CNTF as an approach to treating retinitis pigmentosa has been investigated for the past 14 years since the first report that it rescued rat photoreceptors from cell death in a light-damage model of RD.[112] Numerous studies conducted in transgenic, experimental (light-induced), and naturally occurring animal models of RD have demonstrated the neuroprotective property of CNTF on photoreceptor cells (see Table 1.3). Although CNTF has been effective in all four species in which it has been evaluated, its neuroprotective activity is nevertheless variable and depends on the animal strain, the disease, and the route of delivery.

Despite being a potentially promising therapeutic agent, there are a number of limitations to the use of CNTF in neurodegenerative diseases, and these are related to its pharmacokinetics, bio-availablity, and associated side-effects. After subcutaneous

Table 1.3 Studies of the neuroprotective effect of ciliary neurotrophic factor (CNTF) in animal models of retinal degeneration. (summary)
(PR: photoreceptor; ERG: electroretinographic; I.-vitr.: intravitreal; Subret: subretinal; ND: not determined; AAV: adeno-associated virus; Adv: adenovirus; P: postnatal day)

Animal model	Gene mutated	Delivery mode	CNTF dose	duration	PR rescue	ERG changes	References
Light-damage in Sprague-Dawley rat	None	I.-vitr. CNTF I.-vitr. CNTF	0.5 µg 0.5-1 µg	1 week 1 week	Yes Yes	ND ND	112 115
S334ter-3 (Transgenic rat)	rhodopsin	I.-vitr. CNTF I.-vitr. NTC-201	1 µg ~ 100 ng	P9-P20 P9-P20	Moderate Yes	ND ND	29
S334ter-4 (Transgenic rat)	rhodopsin	I.-vitr. AAV-CNTF	ND	6 months	Yes	↓ b-wave amplitude	153
P23H line 1 (Transgenic rat)	rhodopsin	I.-vitr. AAV-CNTF	ND	6 months	Yes	↓ b-wave amplitude	153
RCS rat	Mertk	Subret. CNTF Subret. Adv-CNTF	0.5 µg ND	P21-P90	Yes Yes	ND ↑ a- and b-wave amplitudes	154
Light-damage in albino BALB/c mouse	None	I.-vitr. CNTF	0.2-0.5 µg	2 weeks	Yes	ND	115
rd/rd mouse	PDE6β	I.-vitr. CNTF I.-vitr. Adv-CNTF	0.2-2 µg ND	1 week P12-P30	Yes Yes	ND ND	115 113
rds/rds mouse	peripherin	I.-vitr. CNTF I.-vitr. Adv-CNTF I.-vitr. AAV-CNTF Subret. AAV-CNTF	0.2-2 µg ND ND ND	3 weeks P21-P73 8.5-9 months P10-6 to 9 weeks later	No Yes Yes Yes	ND ↑ a- and b-wave amplitudes No ↓ b-wave amplitude	115 114 153 155
$rds^{+/-P216L}$ mouse	peripherin	I.-vitr. CNTF I.-vitr. AAV-CNTF Subret. AAV-CNTF	1 µg ND ND	P25-P48 P28-P90 P25-P90/P150	No moderate Yes	No ND ↓ a- and b-wave amplitudes	156

Table 1.3 (continued).

Animal model	Gene mutated	Delivery mode	CNTF dose	duration	PR rescue	ERG changes	References
nr/nr mouse	ND	I.-vitr. CNTF	0.2-2 µg	3-4 weeks	Yes	ND	115
Q344ter mouse (transgenic mouse)	rhodopsin	I.-vitr. CNTF	0.2-2 µg	10 days	Yes	ND	115
pcd/pcd mouse	ND	I.-vitr. CNTF	0.2-2 µg	3-4 weeks	No	ND	115
P23H (transgenic mouse)	rhodopsin	I.-vitr. CNTF	0.2-2 µg	10 days	No	ND	115
VPP (transgenic mouse)	rhodospin	I.-vitr. CNTF	0.2-2 µg	3 weeks	No	ND	115
opsin$^{-/-}$ mouse	rhodopsin	Subret. AAV-CNTF	ND	3 months	Yes	ND	157
Rdy cat	ND	I.-vitr. CNTF (repeated injections)	2.5-5 µg / injection	4-16 weeks	Yes	ND	158
rcd1 dog	PDE6β	I.-vitr. CNTF I.-vitr. ECT-CNTF	10-15 µg (repeated 2X) 0.1-15 ng/day	7 weeks 7-14 weeks	Yes Yes	ND ND	159 29

administration in humans, CNTF is rapidly eliminated from the circulation (half-life: 3.3hrs), and causes acute physiological effects such as elevation in body temperature, activation of the acute phase response,[151,152] and increase in total circulating leucocytes.[142] These non-neurological biological effects of CNTF reflect properties that are shared by most members of the IL-6 family of cytokines. The most common side effects that were observed in more than 5% of the patients receiving 30µg/kg of recombinant human CNTF subcutaneously were, in order of decreasing frequency: pain or other reaction at the injection site, asthenia, nausea, flushing, cough, generalized aches and pains, tachycardia, and mouth sores.[142] In order to by-pass the blood-brain barrier, limit the side-effects associated with systemic administration, and provide a continuous source of the drug, long-term intrathecal delivery of CNTF was tested in Phase I clinical trial in human patients with ALS by means of a drug minipump,[144] or encapsulated genetically modified cells.[143,145] This latest technology, originally developed by CytoTherapeutics Inc., provided nanogram concentrations of CNTF in the patients' cerebrospinal fluid for at least 17 weeks following implantation in the lumbar intrathecal space. No associated side-effects were observed other than a mild cough,[143] and a slightly elevated leucocyte count[145] in some patients.

Preliminary studies conducted in Aguirre's group, in collaboration with Regeneron Inc., showed that intravitreal injection of CNTF in the *rcd1* dog (*PDE6B* deficient) has a very positive photoreceptor rescue effect.[159] In these studies, *rcd1* dogs received an intravitreal injection of a recombinant human mutein of full length CNTF (Axokine®, 10-15 µg / injection) in one eye at 7 and 10 weeks of age. The contralateral eye was vehicle-injected with phosphate buffered saline (PBS). At 14 weeks of age, the animals were killed, and the retinas collected and processed for histological examination. Cell count in the outer nuclear layer showed a significantly higher number of photoreceptors in the CNTF-injected eyes, and suggested that cell

death had been arrested after the 1st injection at 7 weeks of age. Indeed, the number of photoreceptor cells in the treated eyes at 14 weeks was the same as when the treatment was delivered (7 weeks of age). Despite this positive rescue effect, ocular complications such as corneal epitheliopathy, uveitis, and cataracts were generally observed in all CNTF-injected eyes. Similar complications were also reported with CNTF in the cat.[158] The positive neuroprotective effect of intravitreally injected CNTF in the *rcd1* dog prompted Neurotech, a biotechnology company that had recently acquired the Encapsulated Cell Technology (ECT) from CytoTherapeutics Inc., to test the efficacy and safety of this drug-delivery device in a large animal model of retinitis pigmentosa.

A study, conducted in collaboration with Aguirre's group, demonstrated that CNTF delivered intravitreally through the ECT device protects photoreceptors in the *rcd1* dog in a dose-dependent manner.[29] Complete protection is achieved over the 7 week implantation period with devices that release 5-15 ng/day of CNTF. Minimal to no photoreceptor rescue is attained with lower doses (0.2-1 ng/day) of CNTF. A pharmacokinetic study conducted in rabbits showed that ECT devices loaded with a high CNTF-secreting cell line can release therapeutic doses (4.2-19.9 ng/day) of the factor for at least 1 year, and maintain CNTF levels in the vitreous that are between 70 and 490 pg.[160] Although this long-term drug delivery approach eliminates ocular side-effects that are seen with bolus intravitreal injections of CNTF, histologic and electroretinographic changes are observed in rabbits implanted with ECT devices delivering high doses (22 ng/day) of CNTF.[161] Morphologic alterations of rod photoreceptors observed in this study consisted in an increase in nuclear area, and in euchromatin content making them appear more like cones. A similar finding was reported when delivering CNTF subretinally by means of a rAAV vector in mice carrying a dominant-negative point mutation in the *rds* (peripherin) gene.[156] Changes

in rod nuclear size and euchromatin content were not observed in *rcd1* dogs implanted with an ECT device, although it was recently reported that ECT-CNTF causes an elevation of the outer limiting membrane suggestive of intracellular swelling of photoreceptors, Müller cells, or both.[162] Electroretinographic alterations mainly consisting in a decrease in b-wave amplitudes have been described by several groups in the P23H and S334ter rhodopsin transgenic rats,[153] the P216L rds/peripherin and rds/rds mice,[155,156] and in the normal albino rabbit.[97] These ERG changes may be partially caused by a decrease in the expression of rhodopsin and other phototransduction proteins.[162 163] In summary, intravitreal bolus injections, or prolonged-delivery of CNTF through gene therapy or the ECT device promote the survival of photoreceptors in several animal models of RP. Although the severe ocular complications (corneal epitheliopathy, uveitis, cataract) associated with high doses of CNTF are eliminated with the ECT technology, cellular alterations have nevertheless been observed at the lowest therapeutically active doses.

CNTF activates signaling pathways through the binding to its tripartite receptor.

CNTF is structurally and functionally related to members of the IL-6 family of cytokines that includes interleukin-6 (IL-6), interleukin-11 (IL-11), leukemia inhibitory factor (LIF), oncostatin M (OSM), cardiotrophin-1 (CT-1), cardiotrophin-like cytokine [CLC, also known as novel neurotrophin-1/B cell stimulating factor-3 (NNT1/BSF-3)], and neuropoietin.[164 165-167] All these cytokines share a four-α-helix-bundle topology, a molecular weight of approximately 20 kDa, and use the common receptor subunit gp-130 for signal transduction.[168]

The receptor for CNTF is a complex formed by three components: a CNTF-specific α subunit (CNTFRα),[169] and two β subunits (LIFRβ and gp-130) that are shared by receptors of other IL-6-type cytokines.[168,170] The CNTFRα subunit is

located on the cell's surface, and is anchored to the plasma membrane through a glycosyl phosphatidylinositol (GPI) linkage.[169] The binding of CNTF to CNTFRα leads to the recruitment of gp-130 and LIFRβ, and the formation of a tripartite receptor complex. Recent findings support a hexameric model for the complex formed by CNTF bound to its full receptor. The proposed stoichiometry for this model involves the binding of two trimers composed, respectively, of CNTF-CNTFRα- gp-130, and CNTF-CNTFRα-LIFRβ.[171]

The heterodimerization of gp-130 and LIFRβ causes the activation of Jak/tyk kinases that are pre-associated with the two β subunits. This leads to tyrosine phosphorylation of the Jak kinases as well as the cytoplasmic domains of gp-130 and LIFRβ, and the recruitment of SH2-containing signal transducing molecules to these newly formed docking sites (for review see[164]). In addition to members of the STAT family, numerous signaling molecules such as PLCγ, PTP1D, pp120, Shc, Grb2, ras, Raf-1, ERK1 and ERK2 are recruited to the receptor and tyrosine phosphorylated.[172,173] Thus, CNTF binding to its receptor can lead to the activation of the Jak/STAT, ras/MAPK, and PI3K/Akt pathways. Activated STAT molecules dimerize and translocate to the nucleus where they bind specific Response Elements, causing increased transcriptional activity of responsive genes. There is currently limited knowledge about the identity of such genes. A few reports have nevertheless identified neuropeptide genes such as vasoactive intestinal polypeptide (VIP), somatostatin, calcitonin gene-related peptide (CGRP), and immediate early genes such as SOCS-3, c-fos, and Tis-11 as being overexpressed following administration of CNTF.[174,175] Negative regulation of CNTF-Jak/STAT signaling is thought to result from a combination of tyrosine dephosphorylation of Jaks and STATs by protein tyrosine phosphatases (PTP), degradation of phosphorylated STATs by the proteasome, and the inactivation of Jaks and STATS by protein inhibitors such as

suppressors of cytokine signaling (SOCS) and protein inhibitors of activated STATs (PIAS) (for review see [176]).

Müller glial cells have been identified by several groups as the site of endogenous CNTF production in the normal rodent retina.[177,178] Following optic nerve transection, induction of ocular hypertension, or exposure to light damage, an increase in CNTF levels is seen in Müller cells.[178-181] The site of expression of the receptor for CNTF (CNTFRα) in the retina, on the other hand, has been a matter of significant conjecture in the field of retinal degeneration. When I started working in the year 2001 on this topic, Wahlin et al.[182,183] had shown that exogenous administration of CNTF in the rodent eye activates signaling pathways in Müller cells, but not in photoreceptors, thus suggesting that rods and cones do not express CNTFRα. Based on these, and subsequent studies, it was commonly accepted that photoreceptor neuroprotection by CNTF occurred through an indirect mechanism of action that involved the contribution of Müller cells.[184,185] Because CNTFRα mRNA was found by *in situ* hybridization to be expressed only in ganglion, amacrine and horizontal cells in the rat retina,[177] it was proposed that CNTF could mediate the rapid release of CNTFRα from the plasma membrane of these cells. Müller cells would then bind this soluble form of the receptor,[186] and subsequently become a direct target of CNTF. The CNTF-mediated activation of Müller cells would promote the release of other cell survival factors that would initiate a secondary neuroprotective signaling event in photoreceptors.[187] This model of indirect photoreceptor survival by CNTF, nevertheless, was challenged by the findings of two studies that reported the localization of CNTFRα mRNA in the ONL of rat retina after ischemia-reperfusion,[188] and CNTFRα protein in the outer segments (OS) of a subpopulation of chicken photoreceptors.[189] These photoreceptors were recently identified as violet-sensitive cones.[190] These studies suggest that a direct mechanism of CNTF-mediated

photoreceptor rescue may occur in some species, or under certain pathological conditions.

Research aims.

Despite the publication of numerous studies reporting CNTF's photoreceptor rescue effect in several animal models of RD, there is currently a lack of understanding of the cellular and molecular mechanisms of neuroprotection by this survival factor. To begin addressing this issue we used the normal adult canine retina as a model system to characterize the expression of the receptor for CNTF (CNTFRα) and determine whether it is found on rods and cones (see **Chapter 2** and [191]). To determine whether our findings are specific to the dog, or are also present in other mammalian species, we examined the immunolocalization of CNTFRα in the normal retinas of mice, rats, cats, sheep, pigs, horse, monkeys, and in human (see **Chapter 3** and [192]).

Although prolonged intraocular delivery of CNTF is currently being considered as a means of treating human patients with retinitis pigmentosa, there is currently no strong evidence to support or refute the assumption that it will provide a cure for all forms of RP irrespective of the genetic cause of the disease.[193] To begin to address this issue, we evaluated whether CNTF could rescue photoreceptors in *XLPRA2*, an early and rapidly progressive canine model for X-linked retinitis pigmentosa that was recently identified.[42] We selected this model because the severity of disease is comparable to that of *rcd1*, yet the causative mutations are different. For this purpose, we first characterized the morphologic retinal changes that occur during the course of the disease, and determined the kinetics of photoreceptor cell death (see **Chapter 4** and [194]). This enabled us to determine the optimal therapeutic time-windows to test the neuroprotective effect of CNTF in this model (see **Chapter 5**).

References

1. Bunker CH, Berson EL, Bromley WC, et al. Prevalence of retinitis pigmentosa in Maine. *Am J Ophthalmol* 1984;97:357-365.

2. Boughman JA, Conneally PM, Nance WE. Population genetic studies of retinitis pigmentosa. *Am J Hum Genet* 1980;32:223-235.

3. Puech B, Kostrubiec B, Hache JC, et al. Epidemiology and prevalence of hereditary retinal dystrophies in the Northern France. *J Fr Ophtalmol* 1991;14:153-164.

4. Milam AH, De Castro EB, Smith JE, et al. Concentric retinitis pigmentosa: clinicopathologic correlations. *Exp Eye Res* 2001;73:493-508.

5. Klevering BJ, Blankenagel A, Maugeri A, et al. Phenotypic spectrum of autosomal recessive cone-rod dystrophies caused by mutations in the ABCA4 (ABCR) gene. *Invest Ophthalmol Vis Sci* 2002;43:1980-1985.

6. Maubaret C, Hamel C. Genetics of retinitis pigmentosa: metabolic classification and phenotype/genotype correlations. *J Fr Ophtalmol* 2005;28:71-92.

7. Chang GQ, Hao Y, Wong F. Apoptosis: final common pathway of photoreceptor death in rd, rds, and rhodopsin mutant mice. *Neuron* 1993;11:595-605.

8. Portera-Cailliau C, Sung CH, Nathans J, et al. Apoptotic photoreceptor cell death in mouse models of retinitis pigmentosa. *Proc Natl Acad Sci U S A* 1994;91:974-978.

9. Li Z-Y, Milam AH. Apoptosis in retinitis pigmentosa In: Anderson RE, ed. *Degenerative Diseases of the Retina*. New York: Plenum Press, 1995;1-8.

10. Dunaief JL, Dentchev T, Ying GS, et al. The role of apoptosis in age-related macular degeneration. *Arch Ophthalmol* 2002;120:1435-1442.

11. Crowe MJ, Bresnahan JC, Shuman SL, et al. Apoptosis and delayed degeneration after spinal cord injury in rats and monkeys. *Nat Med* 1997;3:73-76.

12. Gwag BJ, Canzoniero LM, Sensi SL, et al. Calcium ionophores can induce either apoptosis or necrosis in cultured cortical neurons. *Neuroscience* 1999;90:1339-1348.

13. Martin LJ. Neuronal cell death in nervous system development, disease, and injury (Review). *Int J Mol Med* 2001;7:455-478.

14. Zeiss CJ. The apoptosis-necrosis continuum: insights from genetically altered mice. *Vet Pathol* 2003;40:481-495.

15. Chang B, Hawes NL, Hurd RE, et al. Retinal degeneration mutants in the mouse. *Vision Res* 2002;42:517-525.

16. Fauser S, Luberichs J, Schuttauf F. Genetic animal models for retinal degeneration. *Surv Ophthalmol* 2002;47:357-367.

17. Petters RM, Alexander CA, Wells KD, et al. Genetically engineered large animal model for studying cone photoreceptor survival and degeneration in retinitis pigmentosa. *Nat Biotechnol* 1997;15:965-970.

18. Li ZY, Wong F, Chang JH, et al. Rhodopsin transgenic pigs as a model for human retinitis pigmentosa. *Invest Ophthalmol Vis Sci* 1998;39:808-819.

19. Curtis R, Barnett KC, Leon A. An early-onset retinal dystrophy with dominant inheritance in the Abyssinian cat. Clinical and pathological findings. *Invest Ophthalmol Vis Sci* 1987;28:131-139.

20. Narfstrom K. Progressive retinal atrophy in the Abyssinian cat. Clinical characteristics. *Invest Ophthalmol Vis Sci* 1985;26:193-200.

21. Rah H, Maggs DJ, Blankenship TN, et al. Early-onset, autosomal recessive, progressive retinal atrophy in Persian cats. *Invest Ophthalmol Vis Sci* 2005;46:1742-1747.

22. Gerke CG, Hao Y, Wong F. Topography of rods and cones in the retina of the domestic pig. *Hong Kong Medical Journal* 1995;1:302-308.

23. Chandler MJ, Smith PJ, Samuelson DA, et al. Photoreceptor density of the domestic pig retina. *Vet Ophthalmol* 1999;2:179-184.

24. Steinberg RH, Reid M, Lacy PL. The distribution of rods and cones in the retina of the cat (Felis domesticus). *J Comp Neurol* 1973;148:229-248.

25. Gilger BC, Reeves KA, Salmon JH. Ocular parameters related to drug delivery in the canine and equine eye: aqueous and vitreous humor volume and scleral surface area and thickness. *Vet Ophthalmol* 2005;8:265-269.

26. Cideciyan AV, Jacobson SG, Aleman TS, et al. In vivo dynamics of retinal injury and repair in the rhodopsin mutant dog model of human retinitis pigmentosa. *Proc Natl Acad Sci U S A* 2005;102:5233-5238.

27. Acland GM, Aguirre GD, Bennett J, et al. Long-term restoration of rod and cone vision by single dose rAAV-mediated gene transfer to the retina in a canine model of childhood blindness. *Mol Ther* 2005;12:1072-1082.

28. Willis CK, Quinn RP, McDonell WM, et al. Functional MRI as a tool to assess vision in dogs: the optimal anesthetic. *Vet Ophthalmol* 2001;4:243-253.

29. Tao W, Wen R, Goddard MB, et al. Encapsulated cell based delivery of CNTF reduces photoreceptor degeneration in animal models of retinitis pigmentosa. *Invest Ophthalmol Vis Sci* 2002;43:3292-3298.

30. Guven D, Weiland JD, Maghribi M, et al. Implantation of an inactive epiretinal poly(dimethyl siloxane) electrode array in dogs. *Exp Eye Res* 2006;82:81-90.

31. Komaromy AM, Varner SE, de Juan E, et al. Application of the new subretinal injection device in the dog. *Cell Transplantation* 2006 (in press).

32. Acland GM, Pearce-Kelling S, Komaromy AM, et al. Three canine cone-rod dystrophies. *Invest Ophthalmol Vis Sci* 2004;45:ARVO E abstract 3587.

33. Suber ML, Pittler SJ, Qin N, et al. Irish setter dogs affected with rod/cone dysplasia contain a nonsense mutation in the rod cGMP phosphodiesterase beta-subunit gene. *Proc Natl Acad Sci U S A* 1993;90:3968-3972.

34. Clements PJ, Gregory CY, Peterson-Jones SM, et al. Confirmation of the rod cGMP phosphodiesterase beta subunit (PDE beta) nonsense mutation in affected rcd-1 Irish setters in the UK and development of a diagnostic test. *Curr Eye Res* 1993;12:861-866.

35. Buyukmihci N, Aguirre G, Marshall J. Retinal degenerations in the dog. II. Development of the retina in rod-cone dysplasia. *Exp Eye Res* 1980;30:575-591.

36. Ray K, Baldwin VJ, Acland GM, et al. Cosegregation of codon 807 mutation of the canine rod cGMP phosphodiesterase beta gene and rcd1. *Invest Ophthalmol Vis Sci* 1994;35:4291-4299.

37. Acland GM, Fletcher RT, Gentleman S, et al. Non-allelism of three genes (rcd1, rcd2 and erd) for early-onset hereditary retinal degeneration. *Exp Eye Res* 1989;49:983-998.

38. Kukekova AV, Nelson J, Kuchtey RW, et al. Linkage Mapping of Canine Rod Cone Dysplasia Type 2 (rcd2) to CFA7, the Canine Orthologue of Human 1q32. *Invest Ophthalmol Vis Sci* 2006;47:1210-1215.

39. Petersen-Jones SM, Entz DD, Sargan DR. cGMP phosphodiesterase-alpha mutation causes progressive retinal atrophy in the Cardigan Welsh corgi dog. *Invest Ophthalmol Vis Sci* 1999;40:1637-1644.

40. Aguirre G. Retinal degenerations in the dog. I. Rod dysplasia. *Exp Eye Res* 1978;26:233-253.

41. Acland GM, Aguirre GD. Retinal degenerations in the dog: IV. Early retinal degeneration (erd) in Norwegian elkhounds. *Exp Eye Res* 1987;44:491-521.

42. Zhang Q, Acland GM, Wu WX, et al. Different RPGR exon ORF15 mutations in Canids provide insights into photoreceptor cell degeneration. *Hum Mol Genet* 2002;11:993-1003.

43. Zeiss CJ, Acland GM, Aguirre GD. Retinal pathology of canine X-linked progressive retinal atrophy, the locus homologue of RP3. *Invest Ophthalmol Vis Sci* 1999;40:3292-3304.

44. Aguirre G, Alligood J, O'Brien P, et al. Pathogenesis of progressive rod-cone degeneration in miniature poodles. *Invest Ophthalmol Vis Sci* 1982;23:610-630.

45. Aguirre GD, Acland GM. Variation in retinal degeneration phenotype inherited at the prcd locus. *Exp Eye Res* 1988;46:663-687.

46. Acland GM, Ray K, Mellersh CS, et al. Linkage analysis and comparative mapping of canine progressive rod-cone degeneration (prcd) establishes potential locus homology with retinitis pigmentosa (RP17) in humans. *Proc Natl Acad Sci U S A* 1998;95:3048-3053.

47. Kijas JW, Cideciyan AV, Aleman TS, et al. Naturally occurring rhodopsin mutation in the dog causes retinal dysfunction and degeneration mimicking human dominant retinitis pigmentosa. *Proc Natl Acad Sci U S A* 2002;99:6328-6333.

48. Sidjanin DJ, Lowe JK, McElwee JL, et al. Canine CNGB3 mutations establish cone degeneration as orthologous to the human achromatopsia locus ACHM3. *Hum Mol Genet* 2002;11:1823-1833.

49. Aguirre GD, Baldwin V, Pearce-Kelling S, et al. Congenital stationary night blindness in the dog: common mutation in the RPE65 gene indicates founder effect. *Mol Vis* 1998;4:23.

50. Acland GM, Aguirre GD, Ray J, et al. Gene therapy restores vision in a canine model of childhood blindness. *Nat Genet* 2001;28:92-95.

51. Aramant RB, Seiler MJ. Progress in retinal sheet transplantation. *Prog Retin Eye Res* 2004;23:475-494.

52. Lopez R, Gouras P, Kjeldbye H, et al. Transplanted retinal pigment epithelium modifies the retinal degeneration in the RCS rat. *Invest Ophthalmol Vis Sci* 1989;30:586-588.

53. Lund RD, Adamson P, Sauve Y, et al. Subretinal transplantation of genetically modified human cell lines attenuates loss of visual function in dystrophic rats. *Proc Natl Acad Sci U S A* 2001;98:9942-9947.

54. Thomas BB, Seiler MJ, Sadda SR, et al. Superior colliculus responses to light - preserved by transplantation in a slow degeneration rat model. *Exp Eye Res* 2004;79:29-39.

55. Mohand-Said S, Hicks D, Simonutti M, et al. Photoreceptor transplants increase host cone survival in the retinal degeneration (rd) mouse. *Ophthalmic Res* 1997;29:290-297.

56. Aramant RB, Seiler MJ. Fiber and synaptic connections between embryonic retinal transplants and host retina. *Exp Neurol* 1995;133:244-255.

57. Kwan AS, Wang S, Lund RD. Photoreceptor layer reconstruction in a rodent model of retinal degeneration. *Exp Neurol* 1999;159:21-33.

58. Sakaguchi DS, Van Hoffelen SJ, Young MJ. Differentiation and morphological integration of neural progenitor cells transplanted into the developing mammalian eye. *Ann N Y Acad Sci* 2003;995:127-139.

59. Klassen H, Sakaguchi DS, Young MJ. Stem cells and retinal repair. *Prog Retin Eye Res* 2004;23:149-181.

60. Klassen HJ, Ng TF, Kurimoto Y, et al. Multipotent retinal progenitors express developmental markers, differentiate into retinal neurons, and preserve light-mediated behavior. *Invest Ophthalmol Vis Sci* 2004;45:4167-4173.

61. Qiu G, Seiler MJ, Mui C, et al. Photoreceptor differentiation and integration of retinal progenitor cells transplanted into transgenic rats. *Exp Eye Res* 2005;80:515-525.

62. Zrenner E. Will retinal implants restore vision? *Science* 2002;295:1022-1025.

63. Weiland JD, Liu W, Humayun MS. Retinal prosthesis. *Annu Rev Biomed Eng* 2005;7:361-401.

64. Majji AB, Humayun MS, Weiland JD, et al. Long-term histological and electrophysiological results of an inactive epiretinal electrode array implantation in dogs. *Invest Ophthalmol Vis Sci* 1999;40:2073-2081.

65. Pardue MT, Stubbs EB, Jr., Perlman JI, et al. Immunohistochemical studies of the retina following long-term implantation with subretinal microphotodiode arrays. *Exp Eye Res* 2001;73:333-343.

66. Guven D, Weiland JD, Fujii G, et al. Long-term stimulation by active epiretinal implants in normal and RCD1 dogs. *J Neural Eng* 2005;2:S65-73.

67. Humayun MS, Weiland JD, Fujii GY, et al. Visual perception in a blind subject with a chronic microelectronic retinal prosthesis. *Vision Res* 2003;43:2573-2581.

68. Mahadevappa M, Weiland JD, Yanai D, et al. Perceptual thresholds and electrode impedance in three retinal prosthesis subjects. *IEEE Trans Neural Syst Rehabil Eng* 2005;13:201-206.

69. Chow AY, Chow VY, Packo KH, et al. The artificial silicon retina microchip for the treatment of vision loss from retinitis pigmentosa. *Arch Ophthalmol* 2004;122:460-469.

70. Bennett J, Tanabe T, Sun D, et al. Photoreceptor cell rescue in retinal degeneration (rd) mice by in vivo gene therapy. *Nat Med* 1996;2:649-654.

71. Jomary C, Vincent KA, Grist J, et al. Rescue of photoreceptor function by AAV-mediated gene transfer in a mouse model of inherited retinal degeneration. *Gene Ther* 1997;4:683-690.

72. Kumar-Singh R, Farber DB. Encapsidated adenovirus mini-chromosome-mediated delivery of genes to the retina: application to the rescue of photoreceptor degeneration. *Hum Mol Genet* 1998;7:1893-1900.

73. Takahashi M, Miyoshi H, Verma IM, et al. Rescue from photoreceptor degeneration in the rd mouse by human immunodeficiency virus vector-mediated gene transfer. *J Virol* 1999;73:7812-7816.

74. Ali RR, Sarra GM, Stephens C, et al. Restoration of photoreceptor ultrastructure and function in retinal degeneration slow mice by gene therapy. *Nat Genet* 2000;25:306-310.

75. Sarra GM, Stephens C, de Alwis M, et al. Gene replacement therapy in the retinal degeneration slow (rds) mouse: the effect on retinal degeneration following partial transduction of the retina. *Hum Mol Genet* 2001;10:2353-2361.

76. Schlichtenbrede FC, da Cruz L, Stephens C, et al. Long-term evaluation of retinal function in $Prph2^{Rd2/Rd2}$ mice following AAV-mediated gene replacement therapy. *J Gene Med* 2003;5:757-764.

77. Pang JJ, Chang B, Kumar A, et al. Gene Therapy Restores Vision-Dependent Behavior as Well as Retinal Structure and Function in a Mouse Model of RPE65 Leber Congenital Amaurosis. *Mol Ther* 2006; 13: 565-572.

78. Batten ML, Imanishi Y, Tu DC, et al. Pharmacological and rAAV gene therapy rescue of visual functions in a blind mouse model of Leber congenital amaurosis. *PLoS Med* 2005;2:e333.

79. Pawlyk BS, Smith AJ, Buch PK, et al. Gene replacement therapy rescues photoreceptor degeneration in a murine model of Leber congenital amaurosis lacking RPGRIP. *Invest Ophthalmol Vis Sci* 2005;46:3039-3045.

80. Vollrath D, Feng W, Duncan JL, et al. Correction of the retinal dystrophy phenotype of the RCS rat by viral gene transfer of Mertk. *Proc Natl Acad Sci U S A* 2001;98:12584-12589.

81. Smith AJ, Schlichtenbrede FC, Tschernutter M, et al. AAV-Mediated gene transfer slows photoreceptor loss in the RCS rat model of retinitis pigmentosa. *Mol Ther* 2003;8:188-195.

82. Tschernutter M, Schlichtenbrede FC, Howe S, et al. Long-term preservation of retinal function in the RCS rat model of retinitis pigmentosa following lentivirus-mediated gene therapy. *Gene Ther* 2005;12:694-701.

83. Hauswirth WW. The consortium project to treat RPE65 deficiency in humans. *Retina* 2005;25:S60.

84. Hauswirth WW, Lewin AS. Ribozyme uses in retinal gene therapy. *Prog Retin Eye Res* 2000;19:689-710.

85. Lewin AS, Drenser KA, Hauswirth WW, et al. Ribozyme rescue of photoreceptor cells in a transgenic rat model of autosomal dominant retinitis pigmentosa. *Nat Med* 1998;4:967-971.

86. LaVail MM, Yasumura D, Matthes MT, et al. Ribozyme rescue of photoreceptor cells in P23H transgenic rats: long-term survival and late-stage therapy. *Proc Natl Acad Sci U S A* 2000;97:11488-11493.

87. Reich SJ, Fosnot J, Kuroki A, et al. Small interfering RNA (siRNA) targeting VEGF effectively inhibits ocular neovascularization in a mouse model. *Mol Vis* 2003;9:210-216.

88. Gorbatyuk MS, Pang JJ, Thomas J, Jr., et al. Knockdown of wild-type mouse rhodopsin using an AAV vectored ribozyme as part of an RNA replacement approach. *Mol Vis* 2005;11:648-656.

89. Berson EL, Rosner B, Sandberg MA, et al. A randomized trial of vitamin A and vitamin E supplementation for retinitis pigmentosa. *Arch Ophthalmol* 1993;111:761-772.

90. Berson EL, Rosner B, Sandberg MA, et al. Clinical trial of docosahexaenoic acid in patients with retinitis pigmentosa receiving vitamin A treatment. *Arch Ophthalmol* 2004;122:1297-1305.

91. Berson EL, Rosner B, Sandberg MA, et al. Further evaluation of docosahexaenoic acid in patients with retinitis pigmentosa receiving vitamin A treatment: subgroup analyses. *Arch Ophthalmol* 2004;122:1306-1314.

92. Frasson M, Sahel JA, Fabre M, et al. Retinitis pigmentosa: rod photoreceptor rescue by a calcium-channel blocker in the rd mouse. *Nat Med* 1999;5:1183-1187.

93. Vallazza-Deschamps G, Cia D, Gong J, et al. Excessive activation of cyclic nucleotide-gated channels contributes to neuronal degeneration of photoreceptors. *Eur J Neurosci* 2005;22:1013-1022.

94. Donovan M, Cotter TG. Caspase-independent photoreceptor apoptosis in vivo and differential expression of apoptotic protease activating factor-1 and caspase-3 during retinal development. *Cell Death Differ* 2002;9:1220-1231.

95. Pawlyk BS, Li T, Scimeca MS, et al. Absence of photoreceptor rescue with D-cis-diltiazem in the rd mouse. *Invest Ophthalmol Vis Sci* 2002;43:1912-1915.

96. Yamazaki H, Ohguro H, Maeda T, et al. Preservation of retinal morphology and functions in royal college surgeons rat by nilvadipine, a Ca(2+) antagonist. *Invest Ophthalmol Vis Sci* 2002;43:919-926.

97. Bush RA, Kononen L, Machida S, et al. The effect of calcium channel blocker diltiazem on photoreceptor degeneration in the rhodopsin Pro23His rat. *Invest Ophthalmol Vis Sci* 2000;41:2697-2701.

98. Pearce-Kelling SE, Aleman TS, Nickle A, et al. Calcium channel blocker D-cis-diltiazem does not slow retinal degeneration in the PDE6B mutant rcd1 canine model of retinitis pigmentosa. *Mol Vis* 2001;7:42-47.

99. Takano Y, Ohguro H, Dezawa M, et al. Study of drug effects of calcium channel blockers on retinal degeneration of rd mouse. *Biochem Biophys Res Commun* 2004;313:1015-1022.

100. Ohguro H, Ogawa K, Maeda T, et al. Retinal dysfunction in cancer-associated retinopathy is improved by Ca(2+) antagonist administration and dark adaptation. *Invest Ophthalmol Vis Sci* 2001;42:2589-2595.

101. Tsang SH, Chen J, Kjeldbye H, et al. Retarding photoreceptor degeneration in Pdegtm1/Pdegtml mice by an apoptosis suppressor gene. *Invest Ophthalmol Vis Sci* 1997;38:943-950.

102. Chen J, Flannery JG, LaVail MM, et al. bcl-2 overexpression reduces apoptotic photoreceptor cell death in three different retinal degenerations. *Proc Natl Acad Sci U S A* 1996;93:7042-7047.

103. Eversole-Cire P, Concepcion FA, Simon MI, et al. Synergistic effect of Bcl-2 and BAG-1 on the prevention of photoreceptor cell death. *Invest Ophthalmol Vis Sci* 2000;41:1953-1961.

104. Nir I, Kedzierski W, Chen J, et al. Expression of Bcl-2 protects against photoreceptor degeneration in retinal degeneration slow (rds) mice. *J Neurosci* 2000;20:2150-2154.

105. Bennett J, Zeng Y, Bajwa R, et al. Adenovirus-mediated delivery of rhodopsin-promoted bcl-2 results in a delay in photoreceptor cell death in the rd/rd mouse. *Gene Ther* 1998;5:1156-1164.

106. Faktorovich EG, Steinberg RH, Yasumura D, et al. Photoreceptor degeneration in inherited retinal dystrophy delayed by basic fibroblast growth factor. *Nature* 1990;347:83-86.

107. Faktorovich EG, Steinberg RH, Yasumura D, et al. Basic fibroblast growth factor and local injury protect photoreceptors from light damage in the rat. *J Neurosci* 1992;12:3554-3567.

108. Masuda K, Watanabe I, Unoki K, et al. Functional Rescue of photoreceptors from the damaging effects of constant light by survival-promoting factors in the rat. *Invest Ophthalmol Vis Sci* 1995;36:2142-2146.

109. Lin N, Fan W, Sheedlo HJ, et al. Basic fibroblast growth factor treatment delays age-related photoreceptor degeneration in Fischer 344 rats. *Exp Eye Res* 1997;64:239-248.

110. Lewis GP, Erickson PA, Guerin CJ, et al. Basic fibroblast growth factor: a potential regulator of proliferation and intermediate filament expression in the retina. *J Neurosci* 1992;12:3968-3978.

111. Perry J, Du J, Kjeldbye H, et al. The effects of bFGF on RCS rat eyes. *Curr Eye Res* 1995;14:585-592.

112. LaVail MM, Unoki K, Yasumura D, et al. Multiple growth factors, cytokines, and neurotrophins rescue photoreceptors from the damaging effects of constant light. *Proc Natl Acad Sci U S A* 1992;89:11249-11253.

113. Cayouette M, Gravel C. Adenovirus-mediated gene transfer of ciliary neurotrophic factor can prevent photoreceptor degeneration in the retinal degeneration (rd) mouse. *Hum Gene Ther* 1997;8:423-430.

114. Cayouette M, Behn D, Sendtner M, et al. Intraocular gene transfer of ciliary neurotrophic factor prevents death and increases responsiveness of rod photoreceptors in the retinal degeneration slow mouse. *J Neurosci* 1998;18:9282-9293.

115. LaVail MM, Yasumura D, Matthes MT, et al. Protection of mouse photoreceptors by survival factors in retinal degenerations. *Invest Ophthalmol Vis Sci* 1998;39:592-602.

116. Ogilvie JM, Speck JD, Lett JM. Growth factors in combination, but not individually, rescue rd mouse photoreceptors in organ culture. *Exp Neurol* 2000;161:676-685.

117. Caffe AR, Soderpalm AK, Holmqvist I, et al. A combination of CNTF and BDNF rescues rd photoreceptors but changes rod differentiation in the presence of RPE in retinal explants. *Invest Ophthalmol Vis Sci* 2001;42:275-282.

118. Carwile ME, Culbert RB, Sturdivant RL, et al. Rod outer segment maintenance is enhanced in the presence of bFGF, CNTF and GDNF. *Exp Eye Res* 1998;66:791-805.

119. Frasson M, Picaud S, Leveillard T, et al. Glial cell line-derived neurotrophic factor induces histologic and functional protection of rod photoreceptors in the rd/rd mouse. *Invest Ophthalmol Vis Sci* 1999;40:2724-2734.

120. McGee Sanftner LH, Abel H, Hauswirth WW, et al. Glial cell line derived neurotrophic factor delays photoreceptor degeneration in a transgenic rat model of retinitis pigmentosa. *Mol Ther* 2001;4:622-629.

121. Cayouette M, Smith SB, Becerra SP, et al. Pigment epithelium-derived factor delays the death of photoreceptors in mouse models of inherited retinal degenerations. *Neurobiol Dis* 1999;6:523-532.

122. Cao W, Tombran-Tink J, Elias R, et al. In vivo protection of photoreceptors from light damage by pigment epithelium-derived factor. *Invest Ophthalmol Vis Sci* 2001;42:1646-1652.

123. Miyazaki M, Ikeda Y, Yonemitsu Y, et al. Simian lentiviral vector-mediated retinal gene transfer of pigment epithelium-derived factor protects retinal degeneration and electrical defect in Royal College of Surgeons rats. *Gene Ther* 2003;10:1503-1511.

124. Whiteley SJ, Klassen H, Coffey PJ, et al. Photoreceptor rescue after low-dose intravitreal IL-1beta injection in the RCS rat. *Exp Eye Res* 2001;73:557-568.

125. Song Y, Zhao L, Tao W, et al. Photoreceptor protection by cardiotrophin-1 in transgenic rats with the rhodopsin mutation s334ter. *Invest Ophthalmol Vis Sci* 2003;44:4069-4075.

126. Mohand-Said S, Deudon-Combe A, Hicks D, et al. Normal retina releases a diffusible factor stimulating cone survival in the retinal degeneration mouse. *Proc Natl Acad Sci U S A* 1998;95:8357-8362.

127. Leveillard T, Mohand-Said S, Lorentz O, et al. Identification and characterization of rod-derived cone viability factor. *Nat Genet* 2004;36:755-759.

128. Barbin G, Manthorpe M, Varon S. Purification of the chick eye ciliary neuronotrophic factor. *J Neurochem* 1984;43:1468-1478.

129. Stockli KA, Lottspeich F, Sendtner M, et al. Molecular cloning, expression and regional distribution of rat ciliary neurotrophic factor. *Nature* 1989;342:920-923.

130. Lin LF, Mismer D, Lile JD, et al. Purification, cloning, and expression of ciliary neurotrophic factor (CNTF). *Science* 1989;246:1023-1025.

131. Lam A, Fuller F, Miller J, et al. Sequence and structural organization of the human gene encoding ciliary neurotrophic factor. *Gene* 1991;102:271-276.

132. Masiakowski P, Liu HX, Radziejewski C, et al. Recombinant human and rat ciliary neurotrophic factors. *J Neurochem* 1991;57:1003-1012.

133. Apfel SC, Arezzo JC, Moran M, et al. Effects of administration of ciliary neurotrophic factor on normal motor and sensory peripheral nerves in vivo. *Brain Res* 1993;604:1-6.

134. Lo AC, Li L, Oppenheim RW, et al. Ciliary neurotrophic factor promotes the survival of spinal sensory neurons following axotomy but not during the period of programmed cell death. *Exp Neurol* 1995;134:49-55.

135. Blottner D, Bruggemann W, Unsicker K. Ciliary neurotrophic factor supports target-deprived preganglionic sympathetic spinal cord neurons. *Neurosci Lett* 1989;105:316-320.

136. Kotzbauer PT, Lampe PA, Estus S, et al. Postnatal development of survival responsiveness in rat sympathetic neurons to leukemia inhibitory factor and ciliary neurotrophic factor. *Neuron* 1994;12:763-773.

137. Sendtner M, Kreutzberg GW, Thoenen H. Ciliary neurotrophic factor prevents the degeneration of motor neurons after axotomy. *Nature* 1990;345:440-441.

138. Forger NG, Roberts SL, Wong V, et al. Ciliary neurotrophic factor maintains motoneurons and their target muscles in developing rats. *J Neurosci* 1993;13:4720-4726.

139. Sagot Y, Tan SA, Baetge E, et al. Polymer encapsulated cell lines genetically engineered to release ciliary neurotrophic factor can slow down progressive motor neuronopathy in the mouse. *Eur J Neurosci* 1995;7:1313-1322.

140. Tan SA, Deglon N, Zurn AD, et al. Rescue of motoneurons from axotomy-induced cell death by polymer encapsulated cells genetically engineered to release CNTF. *Cell Transplant* 1996;5:577-587.

141. The ALS CNTF Treatment Study (ACTS) Phase I-II Study Group. A phase I study of recombinant human ciliary neurotrophic factor (rHCNTF) in patients with amyotrophic lateral sclerosis. *Clin Neuropharmacol* 1995;18:515-532.

142. The ALS CNTF Treatment Study (ACTS) Phase I-II Study Group. The pharmacokinetics of subcutaneously administered recombinant human ciliary neurotrophic factor (rHCNTF) in patients with amyotrophic lateral sclerosis:

relation to parameters of the acute-phase response. *Clin Neuropharmacol* 1995;18:500-514.

143. Aebischer P, Schluep M, Deglon N, et al. Intrathecal delivery of CNTF using encapsulated genetically modified xenogeneic cells in amyotrophic lateral sclerosis patients. *Nat Med* 1996;2:696-699.

144. Penn RD, Kroin JS, York MM, et al. Intrathecal ciliary neurotrophic factor delivery for treatment of amyotrophic lateral sclerosis (phase I trial). *Neurosurgery* 1997;40:94-99; discussion 99-100.

145. Zurn AD, Henry H, Schluep M, et al. Evaluation of an intrathecal immune response in amyotrophic lateral sclerosis patients implanted with encapsulated genetically engineered xenogeneic cells. *Cell Transplant* 2000;9:471-484.

146. Emerich DF, Lindner MD, Winn SR, et al. Implants of encapsulated human CNTF-producing fibroblasts prevent behavioral deficits and striatal degeneration in a rodent model of Huntington's disease. *J Neurosci* 1996;16:5168-5181.

147. de Almeida LP, Zala D, Aebischer P, et al. Neuroprotective effect of a CNTF-expressing lentiviral vector in the quinolinic acid rat model of Huntington's disease. *Neurobiol Dis* 2001;8:433-446.

148. Regulier E, Pereira de Almeida L, Sommer B, et al. Dose-dependent neuroprotective effect of ciliary neurotrophic factor delivered via tetracycline-regulated lentiviral vectors in the quinolinic acid rat model of Huntington's disease. *Hum Gene Ther* 2002;13:1981-1990.

149. Emerich DF, Winn SR, Hantraye PM, et al. Protective effect of encapsulated cells producing neurotrophic factor CNTF in a monkey model of Huntington's disease. *Nature* 1997;386:395-399.

150. Mittoux V, Joseph JM, Conde F, et al. Restoration of cognitive and motor functions by ciliary neurotrophic factor in a primate model of Huntington's disease. *Hum Gene Ther* 2000;11:1177-1187.

151. Schooltink H, Stoyan T, Roeb E, et al. Ciliary neurotrophic factor induces acute-phase protein expression in hepatocytes. *FEBS Lett* 1992;314:280-284.

152. Dittrich F, Thoenen H, Sendtner M. Ciliary neurotrophic factor: pharmacokinetics and acute-phase response in rat. *Ann Neurol* 1994;35:151-163.

153. Liang FQ, Aleman TS, Dejneka NS, et al. Long-term protection of retinal structure but not function using RAAV.CNTF in animal models of retinitis pigmentosa. *Mol Ther* 2001;4:461-472.

154. Huang SP, Lin PK, Liu JH, et al. Intraocular gene transfer of ciliary neurotrophic factor rescues photoreceptor degeneration in RCS rats. *J Biomed Sci* 2004;11:37-48.

155. Schlichtenbrede FC, MacNeil A, Bainbridge JW, et al. Intraocular gene delivery of ciliary neurotrophic factor results in significant loss of retinal function in normal mice and in the Prph2Rd2/Rd2 model of retinal degeneration. *Gene Ther* 2003;10:523-527.

156. Bok D, Yasumura D, Matthes MT, et al. Effects of adeno-associated virus-vectored ciliary neurotrophic factor on retinal structure and function in mice with a P216L rds/peripherin mutation. *Exp Eye Res* 2002;74:719-735.

157. Liang FQ, Dejneka NS, Cohen DR, et al. AAV-mediated delivery of ciliary neurotrophic factor prolongs photoreceptor survival in the rhodopsin knockout mouse. *Mol Ther* 2001;3:241-248.

158. Chong NH, Alexander RA, Waters L, et al. Repeated injections of a ciliary neurotrophic factor analogue leading to long-term photoreceptor survival in hereditary retinal degeneration. *Invest Ophthalmol Vis Sci* 1999;40:1298-1305.

159. Pearce-Kelling SE, Acland GM, Laties A, et al. Survival factors slow inherited retinal degeneration in the rcd-1 and erd dog models. *Invest Ophthalmol Vis Sci* 1998;39:S571.

160. Thanos CG, Bell WJ, O'Rourke P, et al. Sustained secretion of ciliary neurotrophic factor to the vitreous, using the encapsulated cell therapy-based NT-501 intraocular device. *Tissue Eng* 2004;10:1617-1622.

161. Bush RA, Lei B, Tao W, et al. Encapsulated cell-based intraocular delivery of ciliary neurotrophic factor in normal rabbit: dose-dependent effects on ERG and retinal histology. *Invest Ophthalmol Vis Sci* 2004;45:2420-2430.

162. Zeiss CJ, Allore HG, Towle V, et al. CNTF induces dose-dependent alterations in retinal morphology in normal and rcd-1 canine retina. *Exp Eye Res* 2005.

163. Song Y, Zhao L, Liu Y, et al. Negative regulation of phototransduction machinery by CNTF is likely through the photostasis mechanism. ARVO 2005; E-abstract #163.

164. Heinrich PC, Behrmann I, Muller-Newen G, et al. Interleukin-6-type cytokine signalling through the gp130/Jak/STAT pathway. *Biochem J* 1998;334:297-314.

165. Senaldi G, Varnum BC, Sarmiento U, et al. Novel neurotrophin-1/B cell-stimulating factor-3: a cytokine of the IL-6 family. *Proc Natl Acad Sci U S A* 1999;96:11458-11463.

166. Shi Y, Wang W, Yourey PA, et al. Computational EST database analysis identifies a novel member of the neuropoietic cytokine family. *Biochem Biophys Res Commun* 1999;262:132-138.

167. Derouet D, Rousseau F, Alfonsi F, et al. Neuropoietin, a new IL-6-related cytokine signaling through the ciliary neurotrophic factor receptor. *Proc Natl Acad Sci U S A* 2004;101:4827-4832.

168. Ip NY, Nye SH, Boulton TG, et al. CNTF and LIF act on neuronal cells via shared signaling pathways that involve the IL-6 signal transducing receptor component gp130. *Cell* 1992;69:1121-1132.

169. Davis S, Aldrich TH, Valenzuela DM, et al. The receptor for ciliary neurotrophic factor. *Science* 1991;253:59-63.

170. Ip NY, McClain J, Barrezueta NX, et al. The alpha component of the CNTF receptor is required for signaling and defines potential CNTF targets in the adult and during development. *Neuron* 1993;10:89-102.

171. He W, Gong K, Smith DK, et al. The N-terminal cytokine binding domain of LIFR is required for CNTF binding and signaling. *FEBS Lett* 2005;579:4317-4323.

172. Boulton TG, Stahl N, Yancopoulos GD. Ciliary neurotrophic factor/leukemia inhibitory factor/interleukin 6/oncostatin M family of cytokines induces tyrosine phosphorylation of a common set of proteins overlapping those induced by other cytokines and growth factors. *J Biol Chem* 1994;269:11648-11655.

173. Schwarzschild MA, Dauer WT, Lewis SE, et al. Leukemia inhibitory factor and ciliary neurotrophic factor increase activated Ras in a neuroblastoma cell line and in sympathetic neuron cultures. *J Neurochem* 1994;63:1246-1254.

174. Symes AJ, Rao MS, Lewis SE, et al. Ciliary neurotrophic factor coordinately activates transcription of neuropeptide genes in a neuroblastoma cell line. *Proc Natl Acad Sci U S A* 1993;90:572-576.

175. Kelly JF, Elias CF, Lee CE, et al. Ciliary neurotrophic factor and leptin induce distinct patterns of immediate early gene expression in the brain. *Diabetes* 2004;53:911-920.

176. O'Shea JJ, Gadina M, Schreiber RD. Cytokine signaling in 2002: new surprises in the Jak/Stat pathway. *Cell* 2002;109:S121-131.

177. Kirsch M, Lee MY, Meyer V, et al. Evidence for multiple, local functions of ciliary neurotrophic factor (CNTF) in retinal development: expression of CNTF and its receptors and in vitro effects on target cells. *J Neurochem* 1997;68:979-990.

178. Walsh N, Valter K, Stone J. Cellular and subcellular patterns of expression of bFGF and CNTF in the normal and light stressed adult rat retina. *Exp Eye Res* 2001;72:495-501.

179. Chun MH, Ju WK, Kim KY, et al. Upregulation of ciliary neurotrophic factor in reactive Muller cells in the rat retina following optic nerve transection. *Brain Res* 2000;868:358-362.

180. Ji JZ, Elyaman W, Yip HK, et al. CNTF promotes survival of retinal ganglion cells after induction of ocular hypertension in rats: the possible involvement of STAT3 pathway. *Eur J Neurosci* 2004;19:265-272.

181. Ju WK, Lee MY, Hofmann HD, et al. Expression of CNTF in Muller cells of the rat retina after pressure-induced ischemia. *Neuroreport* 1999;10:419-422.

182. Wahlin KJ, Campochiaro PA, Zack DJ, et al. Neurotrophic factors cause activation of intracellular signaling pathways in Muller cells and other cells of the inner retina, but not photoreceptors. *Invest Ophthalmol Vis Sci* 2000;41:927-936.

183. Wahlin KJ, Adler R, Zack DJ, et al. Neurotrophic signaling in normal and degenerating rodent retinas. *Exp Eye Res* 2001;73:693-701.

184. Harada T, Harada C, Kohsaka S, et al. Microglia-Muller glia cell interactions control neurotrophic factor production during light-induced retinal degeneration. *J Neurosci* 2002;22:9228-9236.

185. Wang Y, Smith SB, Ogilvie JM, et al. Ciliary neurotrophic factor induces glial fibrillary acidic protein in retinal Muller cells through the JAK/STAT signal transduction pathway. *Curr Eye Res* 2002;24:305-312.

186. Davis S, Aldrich TH, Ip NY, et al. Released form of CNTF receptor α component as a soluble mediator of CNTF responses. *Science* 1993;259:1736-1739.

187. Peterson WM, Wang Q, Tzekova R, et al. Ciliary neurotrophic factor and stress stimuli activate the Jak-STAT pathway in retinal neurons and glia. *J Neurosci* 2000;20:4081-4090.

188. Ju WK, Lee MY, Hofmann HD, et al. Increased expression of ciliary neurotrophic factor receptor α mRNA in the ischemic rat retina. *Neurosci Lett* 2000;283:133-136.

189. Fuhrmann S, Kirsch M, Heller S, et al. Differential regulation of ciliary neurotrophic factor receptor-α expression in all major neuronal cell classes during development of the chick retina. *J Comp Neurol* 1998;400:244-254.

190. Seydewitz V, Rothermel A, Fuhrmann S, et al. Expression of CNTF receptor-α in chick violet-sensitive cones with unique morphologic properties. *Invest Ophthalmol Vis Sci* 2004;45:655-661.

191. Beltran WA, Zhang Q, Kijas JW, et al. Cloning, mapping, and retinal expression of the canine ciliary neurotrophic factor receptor α (CNTFRα). *Invest Ophthalmol Vis Sci* 2003;44:3642-3649.

192. Beltran WA, Rohrer H, Aguirre GD. Immunolocalization of ciliary neurotrophic factor receptor α (CNTFRα) in mammalian photoreceptor cells. *Mol Vis* 2005;11:232-244.

193. Sieving PA, Caruso RC, Tao W, et al. Ciliary neurotrophic factor (CNTF) for human retinal degeneration: Phase I trial of CNTF delivered by encapsulated cell intraocular implants. *Proc Natl Acad Sci U S A* 2006;103:3896-3901.

194. Beltran WA, Hammond P, Acland GM, et al. A frameshift mutation in *RPGR* exon ORF15 causes photoreceptor degeneration and inner retina remodeling in a model of X-linked retinitis pigmentosa. *Invest Ophthalmol Vis Sci* 2006;47:1669-1681.

CHAPTER TWO

CLONING, MAPPING, AND RETINAL EXPRESSION OF THE CANINE CILIARY NEUROTROPHIC FACTOR RECEPTOR α (CNTFRα) *

INTRODUCTION

Retinal degenerations are a major cause of blindness for which no treatment is currently available. Different therapeutic approaches are being investigated; among these, the use of survival factors that may slow the rate of photoreceptor death and delay the onset of vision loss in various forms of retinal degeneration. Over the past decade, a variety of survival factors have been tested in several animal models of retinal degeneration.[1-4] Ciliary neurotrophic factor (CNTF), a survival factor originally isolated from the chick ciliary ganglion, was shown to promote photoreceptor rescue when delivered intravitreally or subretinally to the rat (Song Y, ARVO abstract # 964, 2000), mouse and cat eye.[2,3,5-7] Our laboratory has shown a similar neuroprotective effect when CNTF was injected into the vitreous of *rcd1* dogs, a canine model of early onset and rapidly progressing retinal degeneration caused by a mutation in the *PDE6B* gene. Similar to observations made in the *rd* mouse,[3,5] a disease model also caused by a mutation in *PDE6B,* a neuroprotective effect was observed in 14 week-old *rcd1* dogs when intravitreal injections of CNTF were performed at 7 and 10 weeks of age (Pearce-Kelling S, ARVO abstract # 2645, 1998). However, side effects such as cataracts were present following intravitreal CNTF injections, but these complications

* Beltran WA, Zhang Q, Kijas JW, Gu D, Rohrer H, Jordan JA, Aguirre GD. *Invest. Ophthalmol. Vis. Sci.* 2003;44 (8):3642-3649.

were eliminated when CNTF was delivered by means of an encapsulated cell based delivery system. In addition, this long-term delivery device allowed prolonged rescue of photoreceptors over a period of 7-14 weeks.[8]

CNTF is thought to trigger a survival signal by binding to the ciliary neurotrophic factor receptor (CNTFR). This receptor is a member of the cytokine receptor superfamily, and is composed of three subunits: an α subunit (CNTFRα)[9] which carries the specific CNTF binding site, and two different β-subunits [gp-130 and Leukemia Inhibitory Factor Receptor (LIFRβ)] [10] that are pre-associated with members of the Jak/Tyk family of cytoplasmic tyrosine kinases. The binding of CNTF to CNTFRα causes heterodimerization of gp-130 and LIFR, and activation of the Jak/Tyk kinases. This, in turn, recruits and activates a variety of downstream signaling molecules, turning on different signaling pathways[11] that promote a cell survival response.

CNTFRα is an extracellular protein that is attached to the plasma membrane by a glycosyl-phosphatidylinositol link. Cleavage of this link by phosphatidylinositol-specific phospholipase C (PI-PLC) releases a soluble form of CNTFRα.[9] CNTFRα has been isolated from a variety of tissues including the retina, central nervous system, peripheral nervous system, muscle, skin, lung, liver, kidney, and testes.[12-14] While CNTF's neuroprotective effect in the retina has been demonstrated in a variety of animal models of retinal degeneration,[2,3,5-7] the site of expression of its receptor, and the mechanism of action by which it rescues photoreceptors, is unknown in mammalian species. Several studies have suggested that CNTFRα is not expressed by photoreceptor cells, and that the neuroprotective effect of CNTF is mediated by Müller cells.[15-17] Because of the dramatic rescue effect of CNTF on *rcd-1* affected photoreceptors, and the lack of knowledge of its cellular targets in the retina, we decided to clone CNTFRα and study its expression in the normal adult canine retina.

METHODS

Primer Design

The human and mouse CNTFRα complete coding sequences (GenBank # M73238, NM016673, respectively) were aligned using the Sequencher program (version 4.0.5, Gene Codes Corp., Ann Arbor, MI) to generate a consensus sequence. PCR primer pairs (Table 1) that amplify the complete coding sequence (exons 3-9) or only fragments of the canine gene were designed based on the consensus sequence.

Reverse Transcription - Polymerase Chain Reaction and cDNA Cloning.

Brain tissue from the frontal cerebral cortex of a 17-week old male beagle dog was used as a source of total RNA. The tissue was homogenized in TRIzol® reagent (Invitrogen, Carlsbad, CA), and total RNA extracted from the aqueous phase with chloroform. First strand cDNA was synthesized using GeneAmp® RNA PCR kit (Perkin Elmer, Foster City, CA); the 20 μl reaction volume contained 1 μg total RNA, 2.5 μM random hexamers, 50 mM KCl, 10 mM Tris-HCl (pH 8.3), 5 mM $MgCl_2$, 1 mM of each dNTP, 20 U RNase inhibitor, and 50 U MuLV reverse transcriptase. After 10 minutes at room temperature, the reaction mixture was incubated at 42°C for 15 minutes, and terminated by incubation at 70°C for 15 minutes followed by 5 minutes on ice. The resulting cDNA was used as a template for a 20 μl PCR reaction containing 0.4 μM of primers CNTFR 1F and CNTFR 1R (Table 1), 1.5 mM $MgCl_2$, 50 mM KCl, 10 mM Tris-HCl (pH 8.3), 200 μM dNTP, and 0.5 U Taq polymerase. PCR amplification with primers CNTFR 1F and CNTFR 1R are expected to generate a 1272 bp DNA fragment that contains the complete canine CNTFRα coding sequence. Reactions were carried out for 36 cycles at an annealing temperature of 53°C for 20 seconds, a polymerization temperature of 72°C for 40 seconds, and a heat-denaturation temperature of 94°C for 20 seconds in a thermal cycler (PTC-200, MJ

Research, Waltham, MA). The PCR-amplified DNA fragment was cloned in a pCR®2.1 vector using the TA-cloning kit (Invitrogen, San Diego, CA) according to the manufacturer's recommendations. Sequencing was done by Taq cycle sequencing using DyeDeoxy terminators in an automated sequencer (ABI prism 3700, Applied Biosystems, Foster City, CA) at the core sequencing facility of Cornell University. The MEGA program (version 2.0, www.megasoftware.net) was used to establish the degree of homology between the canine CNTFRα coding sequence (nucleotide and amino acid) and that of the human (M73238), mouse (NM016673), rat (S54212) and chicken (Z48168).

The transcription of CNTFRα was examined by RT-PCR on 3 μg of total RNA extracted from the retina, brain, spleen, lung, liver, and kidney of a normal adult beagle. PCR amplification of a 369 bp product using primers CNTFR 6F and CNTFR 2R (Table 1) was carried out for 30 cycles at an annealing temperature of 58°C. PCR products were analyzed by electrophoresis on an ethidium bromide-stained polyacrylamide gel (6%).

Radiation Hybrid (RH) Mapping

DNA from the $RH08_{3000}$ canine-hamster radiation hybrid panel was purchased from Research Genetics (Huntsville, AL). The parental mongrel dog cell line was irradiated with 3,000 rads, and fused with A23, a thymidine kinase deficient (TK^-) hamster cell line with a retention estimate of 28%. CNTFRα maps to human chromosome 9p13.[18] We therefore selected six markers (REN142009, REN275M05, IFNA3, IFNA1, REN174D18, REN147002) located on the canine homologous region on canine chromosome 11 (CFA 11) in the RHDF5000 map[19] to generate a framework map, and establish the map position of this gene in the dog. Primers CNTFR 9F and CNTFR 9R (Table 1) were used to amplify a 112 bp fragment of canine-specific CNTFRα. The map was

Table 2.1 PCR primers with position and length of products, and annealing temperature.

Primer ID	Sequence (5'→ 3')	Position	Fragment size (bp)	Annealing temperature (°C)
CNTFR 6F	ATTGTGAAGCCTGATCCTCCAGA	Exon 6-7	369 bp	53
CNTFR 2R	TGGTGGTGCTGGTCGTGGTCT	Exon 9		
CNTFR 1F	GAGGAGGA(T/G)(A/G)A(T/C)ATTGATGTG	5' UTR	1272 bp	58
CNTFR 1R	AAAGGTCCTCCTGCCCGTGTG	3' UTR		
CNTFR 9F	CAGCACCCTTCTTGATCCATG	Exon 9	112 bp	58
CNTFR 9R	GTGCGCTGGCATGTCCCTCAC	3'UTR		

constructed using MultiMap software[20] based on best two-point analysis, placing markers at a lod score of 3.0 for overall order.

Animals and histologic procedures

Retinas from normal adult beagles were used for both the *in situ* hybridization and immunocytochemistry studies. Dogs were anesthetized with intravenous pentobarbital, and the eyes rapidly enucleated in the light. After three hour fixation of the entire globe at 4°C in 4% paraformaldehyde in 0.1 M phosphate buffered saline, the posterior segment was isolated and fixed for an additional 24 hours at 4°C in 2% paraformaldehyde in 0.1 M phosphate buffered saline. The tissue then was trimmed and cryoprotected in a solution of 30% sucrose in 0.1 M sodium phosphate and 0.15 M sodium chloride, pH 7.2 [BupH™, Phosphate Buffered Saline, Pierce, Rockford, IL; (referred in the text as PBS)] at 4°C for 48 hours, and embedded in OCT. Cryosections were cut at 7, 10 or 15 μm thickness. All research conducted was in full compliance with the ARVO Statement for the Use of Animals in Ophthalmic and Vision Research.

***In situ* hybridization**

A 369 bp fragment of canine CNTFRα cDNA encoding exons 7 and 8 was amplified using primers CNTFR 6F and CNTFR 2R (Table 1), and subcloned in the dual promoter vector pCRII®-TOPO (Invitrogen). After purification using the QIAprep miniprep kit (Qiagen, Valencia, CA), the plasmid was linearized using *Hind*III and *EcoR*V restriction enzymes, and single strand sense and antisense digoxigenin-labeled RNA probes were generated by T7 and Sp6 RNA polymerases, respectively, using DIG RNA labeling kit (Roche Molecular Biochemicals, Mannheim, Germany). The slides were air-dried overnight at 40°C, then washed twice for 5 min in PBS, 100 mM glycine in PBS, 0.3% Triton X-100 in PBS, and rinsed with PBS. The 15 μm-thick

sections were then permeabilized with 500 ng/ml Proteinase K in 100 mMTris-HCl, 50 mM EDTA, pH 8.0, for 30 min at 37°C, and post fixed with 4% paraformaldehyde in PBS. After two rinses in PBS, the sections were acetylated twice for 5 min with 0.25% acetic anhydride in 0.1 M triethanolamine, pH 8.0, and incubated for 10 min with deionized formamide in 2 x SSC (1 x SSC: 150 mM NaCl, 15 mM sodium citrate, pH 7.2). The sections were then hybridized with 100 ng of RNA probe in hybridization buffer (In Situ Hyb Buffer, Ambion, Austin, TX) for 16 hours at 50°C in a humid chamber. After hybridization, the slides were washed twice in 2 x SSC, and twice in 1 x SSC at 37°C. They were then treated with RNase A (20 μg/ml in 500mM NaCl, 10 mM Tris, 1 mM EDTA, pH 8.0) for 30 min at 37°C, washed twice in 0.1 x SSC for 30 min at 37°C. RNA hybrids were detected by incubation for 30 min with an alkaline-phosphatase–conjugated antidigoxigenin antibody (1:500), and then for 16 hours with the chromogenic substrates 4-nitroblue tetrazolium chloride (NBT) and 5-bromo-4-chloro-3-indoyl phosphate (BCIP) (DIG nucleic acid detection kit, Roche Molecular Biochemicals). Slides were mounted with Acqua poly mount (Polysciences, Warrington, PA), and examined with a Zeiss Axioplan microscope with or without Differential Interference Contrast (DIC) optics. Images were digitally captured (Spot 3.3, Diagnostic, Instrument, Inc., Sterling Height, MI) and imported into Adobe Photoshop graphics program for display.

Immunoblot analysis

For western analysis, adult canine retina was homogenized in PBS containing a cocktail of protease inhibitors (Sigma, St Louis, MO), and, following sonication, the protein level determined by the Bradford method (Bio-Rad protein assay, Bio-Rad, Hercules, CA). Samples consisting of dog and chicken retinal protein lysates, and recombinant rat CNTFRα (amino acid residues 1-346; R&D systems, Minneapolis,

MN) were placed in the sample buffer containing 4% glycerol, 0.4% sodium dodecyl sulfate, 1% β-mercaptoethanol, 0.005% bromophenol blue in 12.5 mM Tris-HCl buffer (pH 6.8) and heated at 100 °C for 5 minutes. Samples and molecular weight standards were separated by SDS-PAGE (4% stacking gel, 10% separating gel).Transfer of proteins from gels to PVDF membrane (Immobilon, Millipore, Bedford, MA) was performed in pre-chilled transfer buffer (25 mM Tris base, 192 mM glycine, and 15% methanol), and the membrane was then blocked with 10% skim milk in Tris-buffered saline containing 0.5% Tween-20 overnight at 4°C. The membrane was incubated for 1.5 hour with a protein A-purified rabbit anti chick CNTFRα antibody [(1:100,000; developed by one of the authors (HR)], followed by goat anti-rabbit secondary antibody conjugated with horseradish peroxydase (1:10,000, Zymed, San Francisco, CA). The blots were developed using the ECL method according to the manufacturer's recommendations (Amersham Biosciences, Piscataway, NJ).

Immunocytochemistry

Tissue sections (7 or 10 μm thick) were washed three times in a 0.3% hydrogen peroxide solution in 50% ethanol to inhibit endogenous peroxidase. Sections were then treated with 0.25% Triton X-100 in PBS for 5 min followed by 10% normal goat serum (NGS) with 0.25% Triton X-100 and 0.05% sodium azide in PBS for 20 min. They were then incubated with primary antibodies diluted in PBS with 1.5% NGS, 0.25% Triton X-100 and 0.05% sodium azide overnight at 4°C. Primary antibodies used in this study were: an affinity-purified polyclonal rabbit anti chick CNTFRα (1:1,000 dilution), a protein A-purified polyclonal rabbit anti chick CNTFRα (1:2,000 dilution). These two antibodies were raised in the same rabbit after immunization with a large fragment of the chick CNTFRα recombinant protein, as reported previously[21].

Two commercial polyclonal antibodies raised against human CNTFRα and rat CNTFRα (respectively, sc-1913 and sc-1914, Santa Cruz Biotechnology, Santa Cruz, CA) were initially evaluated by immunocytochemistry and showed an intense labeling at the level of the photoreceptor inner segments. Yet, because of significant background labeling on the sections, and the impossibility of blocking the signal on both immunoblots and immunocytochemical sections with their respective blocking peptides (sc-1913 P, sc-1914 P), we did not pursue further investigations with these antibodies.

After washing in PBS, secondary antibody (biotinylated goat anti-rabbit, 1:200 dilution; Vector Laboratories, Burlingame, CA) was applied for 30 min at room temperature. Antibodies were visualized using the avidin biotin complex (ABC) Elite kit (Vector Laboratories) with diaminobenzidine as a substrate. To confirm the cone photoreceptor labeling observed with the CNTFRα antibody, we used serial sections and immunoreacted each sequential section with CNTFRα antibody, a rabbit affinity-purified antibody directed against human cone arrestin[22] (1:10,000 dilution, kindly provided by Dr. Cheryl Craft), and a rabbit affinity-purified antibody directed against mouse phosphodiesterase γ (anti-PDEγ, 1:2,000, kindly provided by D.B. Farber)[23]. The antibodies were applied overnight, and visualized with a biotinylated secondary antibody and the ABC Elite kit. Control sections were treated in the same way with omission of primary antibodies, or replacement by rabbit serum from a non-immunized animal. Slides were mounted with Gelvatol, and examined as described in the previous section.

RESULTS

Cloning of canine CNTFRα cDNA

RT-PCR using primers which hybridise in the 3' and 5' UTR of the CNTFRα gene amplified a single 1272 bp size product from brain derived mRNA. Sequence analysis revealed the CNTFRα coding sequence (1119 bp) and 26 bp of 5' UTR, and 86 bp of 3' UTR (GenBank # AF529215). Alignment of the nucleotide coding sequence (data not shown) showed a cDNA of identical length with human, mouse and rat, and high sequence identity of 93%, 89.5%, and 88.7%, respectively. The alignment of the predicted amino acid sequence of canine CNTFRα with that of human, mouse and rat also showed a high degree of homology between these species (Figure 2.1 B). The canine CNTFRα amino acid sequence is longer than that of the chicken (372 *vs.* 362aa), and the chicken sequence shares a lower degree of homology with dog (69.1%) and other mammals. The amino acid identity was higher between the dog and human, and lower between the rat and the chicken sequences. Hallmarks of cytokine receptors such as clusters of cysteine residues, putative N-glycosylation sites, and the cytokine receptor consensus motif (WSXWS box)[24] were conserved in the canine CNTFRα amino acid sequence (Figure 2.1 A).

Radiation hybrid mapping

Radiation hybrid mapping using the $RH08_{3000}$ canine-hamster panel placed CNTFRα on canine chromosome 11 (CFA11) in a position approximately 70.41 cR3000 telomeric to the microsatellite REN275MO5, and 56.19 cR3000 centromeric from the gene markers IFNA3/IFNA1 (Figure 2.2). Marker order was supported with a lod score of 3.5, and was similar to that obtained with a different radiation hybrid panel made with 5000 rad (RHDF5000 map).[19] CFA 11 exhibits conserved synteny with the

Figure 2.1 Comparison of the dog CNTFRα amino acid sequence with that of the human, mouse and rat, and chicken. (**A**) Alignment of amino acid sequences. Conserved cysteine residues and the conserved cytokine receptor motif (WSXSW box) are underlined. Putative N-glycosylation sites (ArgXSer/Thr) in the dog sequence are boxed. (**B**) Level of homology between sequences are indicated as percentage.

A.

```
dog       MAAPVPWACCAVLAAAAAVVYAQRHSPQEAPHVQYERLGSDVTLPCGTAN   50
human     ..................................................   50
mouse     .T.S.............A..T.K..............A.........S   50
rat       ...S.............A..T.K..............T.........S   50
chicken   ..N...S...V....VVV ....... .QDS.I....V.A...MK..SMD   48

dog       WDAAVTWRVNGTDLALDLLNGSQLVLHGLELGHSGLYACFHRDSWHLRHQ  100
human     ................P.................................  100
mouse     ................P........I.RS.....................  100
rat       ................P........I.RS.....................  100
chicken   .......TA....IDDSH....Y.I.KNVD.TQ..Q.S.YEGS....KY.   98

dog       VLLHVGLPPREPVLSCRSNTYPKGFYCSWHLPTPTYIPNTFNVTVLHGSK  150
human     ..................................................  150
mouse     ..................................................  150
rat       ...............................SA.................  150
chicken   TY.R..V..K....M....N............S......S..IS.I..TR  148

dog       IMVCEKDPALKNRCHIRYMHLFSTIKYKVSISVSNALGHNATAITFDEFT  200
human     ..................................................  200
mouse     ........................................T.........  200
rat       M.......................................T.........  200
chicken   E......IFP........LQ....V....TLT.T....K.S.TL.....A  198

dog       IVKPDPPENVVARPVPSNPRRLEVTWQTPSTWPDPESFPLKFFLRYRPLI  250
human     ..................................................  250
mouse     ..................................................  250
rat       ..................................................  250
chicken   ........S...K...N.......S..N..S...................  248

dog       LDQWQHVELSDGTTHTITDAYAGKEYIIQVAAKDYEIGTWSDWSVAAHAT  300
human     ............A.....................N................  300
mouse     ............A.....................N................  300
rat       ..........N..A.....................N................  300
chicken   ............S.....................ND..........V...  298

dog       PWTEEPRHLTTEAQAPETTTST TSSLAPPPTTKICDPGE LGSGGGPSA  348
human     ..............A...... ..............  ..........  348
mouse     ..................... ..............  ........I  348
rat       ..................... .............. .S......I  348
chicken   ......K.....V.IT... ..S...FM.........K.VGV...A     343

dog       PFLIHVPVTLALAAAAATANSLLI*                          372
human     ...VS..I...........S.....                          372
mouse     L..TS.....V.........N....                          372
rat       ...TS.....V.........N....                          372
chicken      VA.CW.AG.VL..YG  V.F..                          362
```

B.

	dog	human	mouse	rat
human	97.8%			
mouse	94.6%	94.9%		
rat	93.8%	94.1%	97.8%	
chicken	69.1%	69.4%	68.5%	67.7%

cytogenetic p13 region of human chromosome 9 (HSA 9p13).[19] Thus our results are in agreement with human mapping data, which localizes CNTFRα to HSA 9p13.

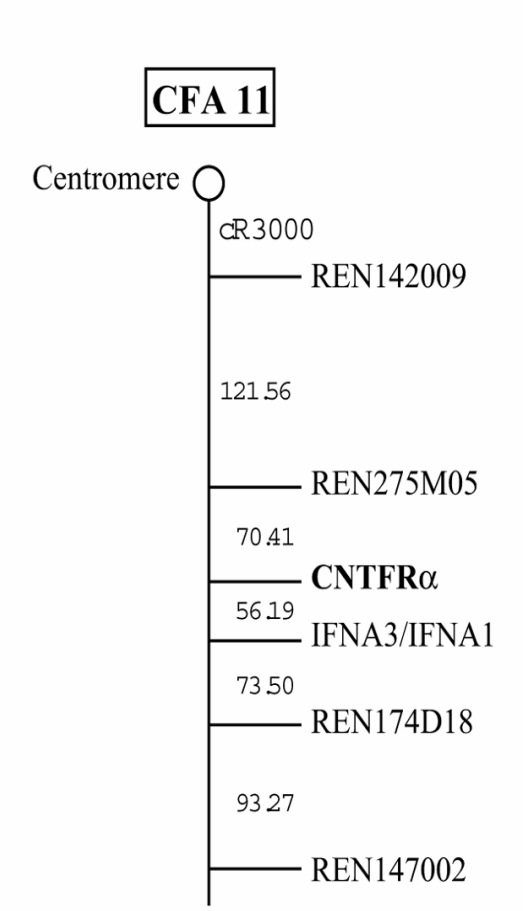

Figure 2.2 Radiation hybrid mapping of CNTFRα. CNTFRα was located on CFA 11 at a lod score of 3.5 for order using MultiMap software. Distances between markers are indicated in cR3000.

Transcription of CNTFRα in different tissues

RT-PCR was used to examine the expression of CNTFRα in various tissues. The transcript was detected in brain, retina, spleen, lung, liver and kidney tissues (Figure 2.3). The specificity of the RT product was based on the product size which was obtained with control retina treated by DNase I digestion, as well as on the absence of any product amplification in tissues processed by omitting the reverse transcriptase enzyme (data not shown).

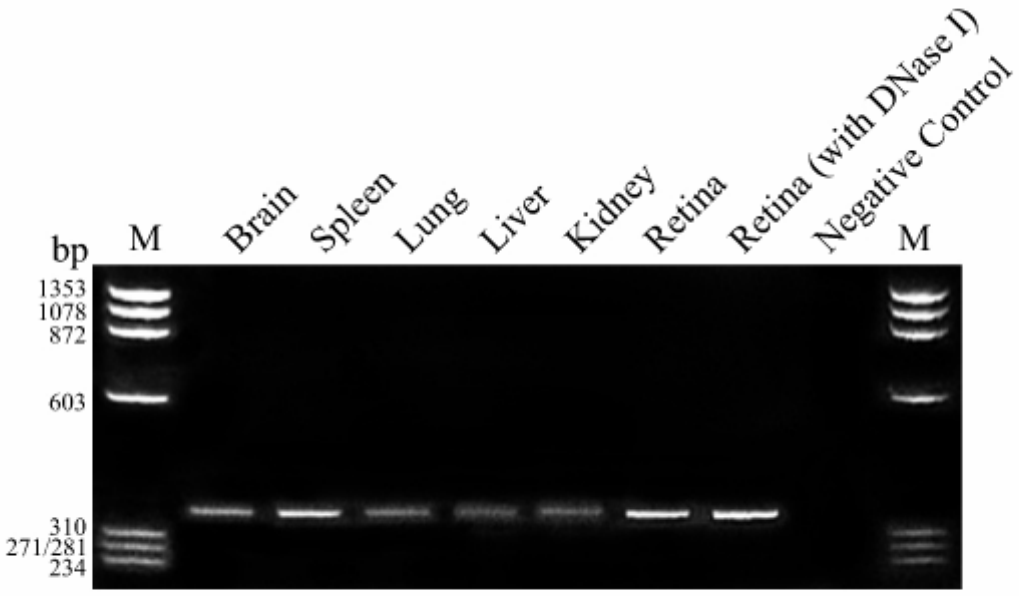

Figure 2.3 Detection of CNTFRα in different canine tissues by RT-PCR. All PCR products contained the DNA fragment of expected size (369 bp). Marker lanes (M) shows DNA markers obtained by digestion of ϕX174 DNA with *Hae*III.

Localization of CNTFRα expression in the adult canine retina.

In situ hybridization was used to determine which retinal cells transcribe canine CNTFRα. With the antisense probe, the CNTFRα message was found in the retinal pigment epithelium (RPE), photoreceptors, inner nuclear layer (INL), and ganglion cells; no labeling was observed with the sense probe, although a very weak background was noticed in some sections (Figure 2.4). The labeling was most intense in the central retina, and decreased towards the periphery. In the visual cells, labeling was present at the level of the external limiting membrane, and in the proximal region of the inner segments (myoid region). Labeling was present throughout the INL but was most intense in the cells located in the vitreal and scleral borders.

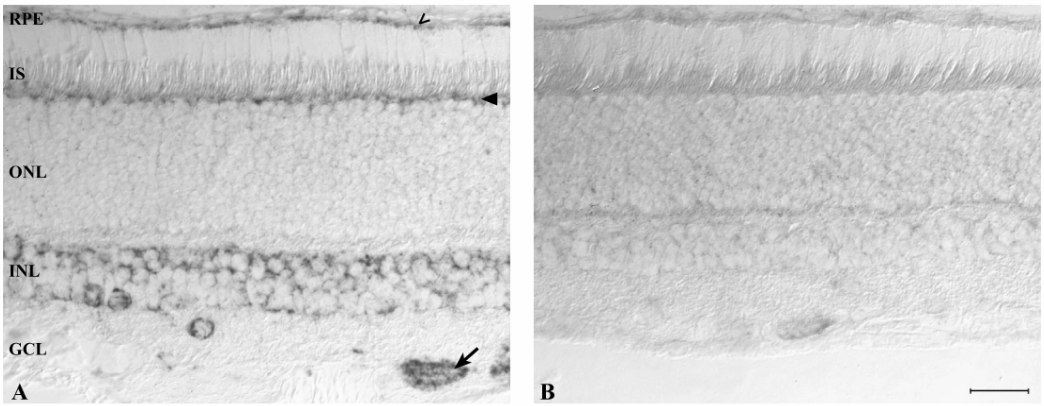

Figure 2.4 Localization of CNTFRα mRNA in the normal adult canine retina (tapetal zone, RPE non-pigmented) by *in situ* hybridization.
(**A**) Expression of CNTFRα mRNA was detected with the antisense probe at the level of the RPE (open arrowhead), photoreceptors (at the level of the external limiting membrane, see arrowhead), INL, and in ganglion cells (arrow). Labeling was present at all levels of the INL but more intense on the scleral and vitreal sides. (**B**) No signal was observed with the sense probe (negative control). RPE: retinal pigment epithelium; IS: inner segments; ONL: outer nuclear layer; INL: inner nuclear layer; GCL: ganglion cell layer. Calibration bar: 25 μm.

To complement the *in situ* hybridization results, we performed immunocytochemical studies using the polyclonal antibodies directed against chick CNTFRα. Both antibodies (affinity-purified, and protein A-purified) produced a similar and consistent pattern of labeling, which was absent in control sections (Figure 2.5 C). There was robust staining of all the inner segments in the photoreceptor layer (Figure 2.5 D-F), and also distinct labeling of the outer and inner plexiform layers (OPL, IPL respectively), cells of the INL, and ganglion cells and their axons (nerve fiber layer, NFL) (Figure 2.5 A, D, F). With the affinity-purified antibody, different populations of cells, predominantly located at the scleral and vitreal borders of the INL, could be identified, but this was not distinct with the protein A-purified antibody (Figure 2.5; compare A, D with F). Labeling of the RPE was present but variable in intensity (Figure 2.5 B, F). Staining of the photoreceptor inner segments was observed, and, in addition, distinct labeling was present throughout a subclass of photoreceptor cells whose nuclei where located at the outermost border of the ONL (Figure 2.5 E, F). The position and cytologic characteristics of these cells, as well as the similar pattern of cone labeling obtained with two antibodies that label only cones (anti human cone arrestin) or cones and rods (anti-PDEγ) (Figure 2.5 G,H), suggest that, in addition to its localization at the rod inner segment, CNTFRα is present throughout most of the cone photoreceptor cell.

To verify the specificity of the protein A-purified anti-chick CNTFRα antibody, we performed immunoblot analysis. When recombinant rat CNTFRα (amino acid residues 1-346) was resolved by SDS-PAGE, the anti-chick CNTFRα antibody identified it at an apparent size of approximately 50 kDa, consistent with the molecular mass indicated by the manufacturer. In protein lysates from dog retina, the antibody recognized a single protein migrating with a molecular weight of approximately 62 kDa (Figure 2.6). A similar result was observed with protein lysates

from retinas of a two week-old chick resolved by SDS-PAGE under reducing conditions (data not shown). This molecular weight was slightly smaller than that reported for the chick under non-reducing conditions,[25] and could be explained by differences in the electrophoresis conditions. Our immunoblot results with the chicken and dog retinal lysates are similar to those reported for rat central nervous system and retina using a different polyclonal antibody.[13] Specificity of the anti-chick CNTFRα antibody has been previously demonstrated both on immunoblots and immunohistochemical sections of chick dorsal root ganglia.[21] The specific labeling was inhibited by preincubating the antibody with the recombinant chick CNTFRα used to generate the antibody. Because the source of the recombinant chick CNTFRα used to block the anti-chick CNTFRα antibody is no longer available, we could not repeat these experiments with the dog tissues.

DISCUSSION

In this study, we cloned the canine CNTFRα cDNA and showed that there was a high level of homology, both at the nucleotide and amino acid levels, when comparing it to that of the human, mouse and rat. The degree of amino acid homology between dog and chicken was lower, however, still sufficient to allow us to use in the dog retina polyclonal antibodies that were raised against chicken CNTFRα. Such a level of conservation, at least for some domains of the protein, suggests that the CNTFRα signaling pathway is conserved across evolution.

Our results show that in the normal adult canine retina, the RPE, photoreceptors, and cells in the INL, and ganglion cell layer (GCL) transcribe the CNTFRα gene. We observed a strict concordance between the retinal cells labeled by *in situ* hybridization, and those stained by immunocytochemistry, particularly with the affinity-purified antibody. This suggests that all cells that transcribe the CNTFRα

Figure 2.5 Immunolocalization of CNTFRα in the normal adult canine retina. (**A**) Labeling pattern of central non-tapetal retina (RPE pigmented) with the affinity-purified anti-chick CNTFRα antibody (**B**) Labeling pattern of mid-peripheral tapetal retina (RPE non-pigmented) with the affinity-purified anti-chick CNTFRα antibody. (**C**) Negative control. (**D**) Labeling pattern of mid-peripheral non-tapetal retina with the affinity-purified anti-chick CNTFRα antibody. (**E**) High power view of (D) (**F, G, H**) Serial sections of mid-peripheral tapetal retina labeled with, the protein-A-purified anti-chick CNTFRα antibody (**F**),the anti-human cone arrestin antibody (**G**), and the anti-PDE γ antibody (**H**). Intense labeling of the entire photoreceptor IS (A, B, D- F) was observed with the two antibodies (E is a high power view of D). Labeling of the OPL, INL, IPL, ganglion cells (arrowhead), and NFL (long arrows) was also present (A, D, F). Labeling of cone perinuclear region (small arrows), axons (arrowheads) and synaptic terminals (open arrowheads) was observed with the anti-chick CNTFRα antibody (E), and resembled that obtained with the anti-PDE γ (G) and anti-human cone arrestin (H) antibodies. RPE: retinal pigment epithelium; OS: outer segments; IS: inner segments; ONL: outer nuclear layer; OPL: outer plexiform layer; INL: inner nuclear layer; IPL: inner plexiform layer; GCL: ganglion cell layer; NFL: nerve fiber layer. Calibration bars: (**A**) 50 μm; (**B**,**C**) 50μm; (**D**) 25 μm; (**E**) 15 μm; (**F**-**H**) 20 μm.

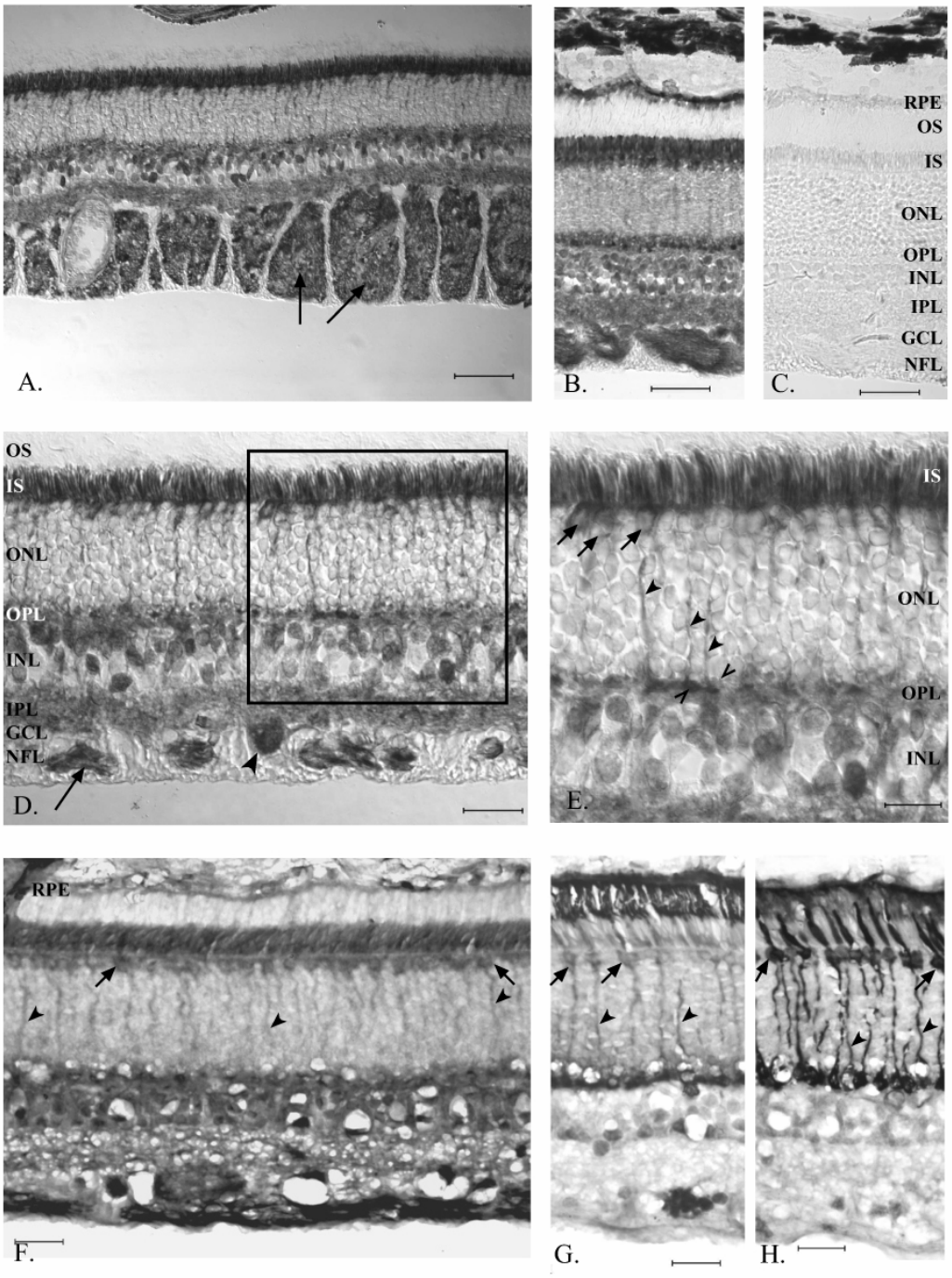
A.
B.
C.
RPE
OS
IS
ONL
OPL
INL
IPL
GCL
NFL
D.
E.
F.
G.
H.

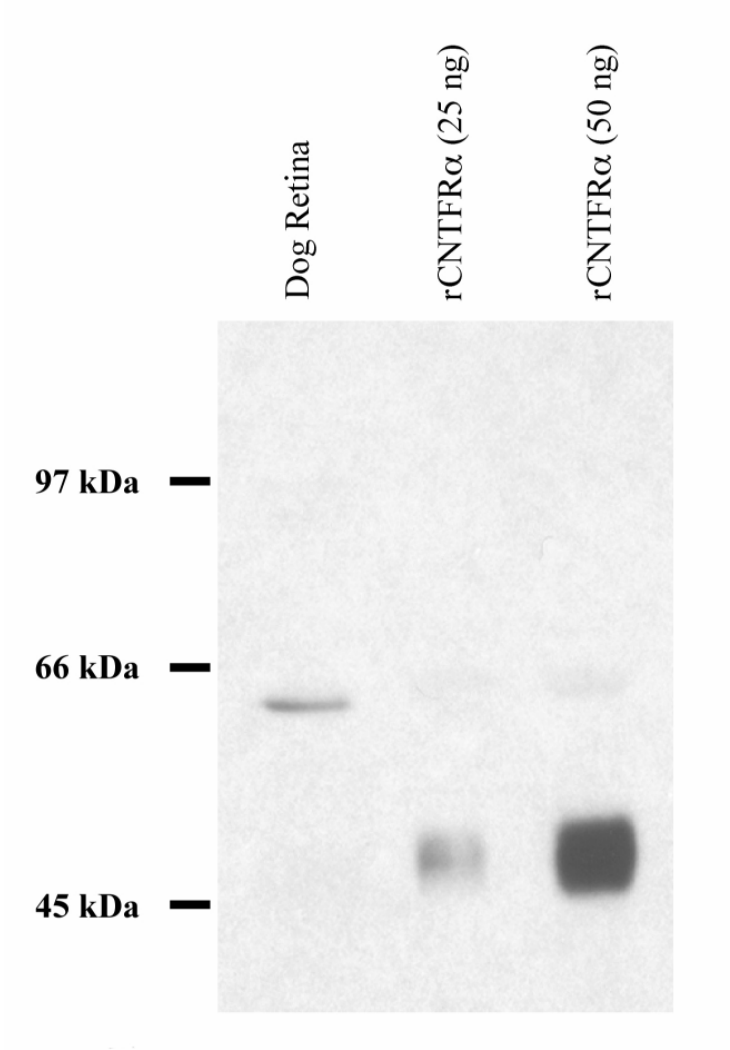

Figure 2.6 Immunoblot analysis of CNTFRα protein expression in the normal adult canine retina. Total protein (14 μg) of adult canine retina (lane 1) and recombinant rat CNTFRα (lane 2: 25 ng, lane 3: 50 ng) were run on a reducing 10% SDS-PAGE gel and immunoblotted using a protein A-purified anti chicken CNTFRα polyclonal antibody. Binding of the anti-CNTFRα antibody was visualized by using enhanced chemiluminescence. Positions and molecular masses (in kilodaltons) of standard proteins are indicated on the left.

gene also express its protein. However, we cannot exclude the possibility that some of these cells also may bind the soluble form of CNTFRα.[26] Such a soluble form could be released by neighboring cells following cleavage of the glycosyl-phosphatidylinositol link by PI-PLC.[9] Labeling of the INL, both by *in situ* hybridization and immunocytochemistry, was more intense in cells located at the outer and innermost part of this layer, suggesting that horizontal, amacrine, and Müller cells express CNTFRα. This was consistent with the location of CNTFRα transcript in the rat INL.[27] However, the use of cell-specific markers, coupled with CNTFRα immunolocalization, will be required to specifically identify the cells in the INL that express this neurotrophic receptor.

The antibodies directed against CNTFRα that were used in our study showed an intense labeling pattern at the level of the RPE, photoreceptors, OPL, INL, IPL GCL and NFL. In addition to the photoreceptor IS labeling, the perinuclear cytoplasm, axon, and synaptic terminal of cones also were intensively labeled with the antibodies raised against chick CNTFR. Although we did not use any antibodies specific to rods, the labeling pattern of the entire IS layer was very different to that obtained with antibodies that solely stain cone photoreceptor cells (see Fig 2.5. H), confirming that CNTFRα is present in both cone and rod inner segments.

Our results show that both rod and cone photoreceptor cells express CNTFRα. It is still to be determined, however, that the two other subunits (gp-130 and LIFR) of the receptor complex are also expressed in photoreceptors. If such were the case, as has been recently suggested by Schulz-Key et al.,[28] our findings would imply that an effect of CNTF on photoreceptors is mediated through a direct rather than indirect mechanism of action. This is in contrast with studies in rodents that suggest that protection of photoreceptors occurs indirectly through the activation of Müller cells or other INL cells.[15-17] The results of those studies, however, are based on the absence of

immunoreactivity for downstream signal transduction molecules, as well as a lack of expression of the immediate early gene c-fos in photoreceptors exposed to CNTF. While a species specificity may explain the discrepancy between these results and ours, it also is possible that binding of CNTF to its receptor in photoreceptors activates signaling pathways other than those examined. A number of *in situ* hybridization studies have examined the expression of CNTFRα mRNA in the retina of the normal adult rat, and have shown labeling at the GCL and INL, but not in the photoreceptors.[27,29] However, after ischemia and reperfusion of the retina, labeling was observed at the outermost part of the ONL,[29] suggesting that rat photoreceptors do express CNTFRα, at least after injury.

In the chick, CNTFRα is expressed in several retinal layers, and was shown by immunocytochemistry to be present in rod outer segments.[25] While a recent study showed the expression of CNTFRα by immunoblot analysis on protein lysates of rat photoreceptor inner and outer segments,[28] to our knowledge there are no reports in the literature characterizing the expression and localization of CNTFRα by immunocytochemistry in mammalian photoreceptors. This lack of information may result from negative immunolocalization results. In this regard, we caution that tissue fixation is critical in these procedures, at least for the canine retina. Our findings are based on using a "very mild" fixation protocol; however, we have observed (data not shown) a reduced to absence of labeling of the inner retina, but not of the photoreceptor inner segments, with more prolonged fixation (24 hours in 4% PAF). In an attempt to evaluate whether the expression of CNTFRα by photoreceptors is specific to the dog or is common to a wide variety of species, we are currently undertaking similar studies in several other mammalian species.

Determining the localization of the expression of the receptor for CNTF is critical since this survival factor is being considered as a potential treatment for retinal

degenerations. Its sustained delivery is currently in late preclinical development and clinical trials are expected to begin in human patients with retinitis pigmentosa (www.neurotech.fr/presse/index.htm). If CNTFRα is also found in human photoreceptors, then evaluating its level of expression during the course of retinal degeneration may be a valid approach for evaluating the potential therapeutic role of CNTF.

In conclusion, we have shown the expression of CNTFRα in photoreceptor cells of the normal, adult canine retina. These results suggest that, at least in the dog, CNTF may act through a direct mechanism to rescue photoreceptors in the *rcd1* model of retinal degeneration. If such a site of action is also present in the human retina, this may lead to novel therapeutic approaches for RP.

REFERENCES

1. Faktorovich E G, Steinberg R H, Yasumura D, Matthes M T, LaVail M M. Photoreceptor degeneration in inherited retinal dystrophy delayed by basic fibroblast growth factor. *Nature.* 1990; 347: 83-86.

2. LaVail M M, Unoki K, Yasumura D, Matthes M T, Yancopoulos G D, Steinberg R H. Multiple growth factors, cytokines, and neurotrophins rescue photoreceptors from the damaging effects of constant light. *Proc Natl Acad Sci U S A.* 1992; 89: 11249-11253.

3. LaVail M M, Yasumura D, Matthes M T, et al. Protection of mouse photoreceptors by survival factors in retinal degenerations. *Invest Ophthalmol Vis Sci.* 1998; 39: 592-602.

4. Frasson M, Picaud S, Leveillard T, et al. Glial cell line-derived neurotrophic factor induces histologic and functional protection of rod photoreceptors in the rd/rd mouse. *Invest Ophthalmol Vis Sci.* 1999; 40: 2724-2734.

5. Cayouette M, Gravel C. Adenovirus-mediated gene transfer of ciliary neurotrophic factor can prevent photoreceptor degeneration in the retinal degeneration (rd) mouse. *Hum Gene Ther.* 1997; 8: 423-430.

6. Cayouette M, Behn D, Sendtner M, Lachapelle P, Gravel C. Intraocular gene transfer of ciliary neurotrophic factor prevents death and increases responsiveness of rod photoreceptors in the retinal degeneration slow mouse. *J Neurosci.* 1998; 18: 9282-9293.

7. Chong N H, Alexander R A, Waters L, Barnett K C, Bird A C, Luthert P J. Repeated injections of a ciliary neurotrophic factor analogue leading to long-term photoreceptor survival in hereditary retinal degeneration. *Invest Ophthalmol Vis Sci.* 1999; 40: 1298-1305.

8. Tao W, Wen R, Goddard M B, et al. Encapsulated cell based delivery of CNTF reduces photoreceptor degeneration in animal models of retinitis pigmentosa. *Invest Ophthalmol Vis Sci.* 2002; 43: 3292-3298.

9. Davis S, Aldrich T H, Valenzuela D M, et al. The receptor for ciliary neurotrophic factor. *Science.* 1991; 253: 59-63.

10. Davis S, Aldrich T H, Stahl N, et al. LIFR beta and gp130 as heterodimerizing signal transducers of the tripartite CNTF receptor. *Science.* 1993; 260: 1805-1808.

11. Boulton T G, Stahl N, Yancopoulos G D. Ciliary neurotrophic factor/leukemia inhibitory factor/interleukin 6/oncostatin M family of cytokines induces tyrosine phosphorylation of a common set of proteins overlapping those induced by other cytokines and growth factors. *J Biol Chem.* 1994; 269: 11648-11655.

12. Ip N Y, McClain J, Barrezueta N X, et al. The alpha component of the CNTF receptor is required for signaling and defines potential CNTF targets in the adult and during development. *Neuron.* 1993; 10: 89-102.

13. Kirsch M, Hofmann H D. Expression of ciliary neurotrophic factor receptor mRNA and protein in the early postnatal and adult rat nervous system. *Neurosci Lett.* 1994; 180: 163-166.

14. Kordower J H, Yaping C, Maclennan A J. Ciliary neurotrophic factor receptor alpha-immunoreactivity in the monkey central nervous system. *J Comp Neurol.* 1997; 377: 365-380.

15. Peterson W M, Wang Q, Tzekova R, Wiegand S J. Ciliary neurotrophic factor and stress stimuli activate the Jak-STAT pathway in retinal neurons and glia. *J Neurosci.* 2000; 20: 4081-4090.

16. Wahlin K J, Campochiaro P A, Zack D J, Adler R. Neurotrophic factors cause activation of intracellular signaling pathways in Muller cells and other cells of the inner retina, but not photoreceptors. *Invest Ophthalmol Vis Sci.* 2000; 41: 927-936.

17. Wahlin K J, Adler R, Zack D J, Campochiaro P A. Neurotrophic signaling in normal and degenerating rodent retinas. *Exp Eye Res.* 2001; 73: 693-701.

18. Donaldson D H, Britt D E, Jones C, Jackson C L, Patterson D. Localization of the gene for the ciliary neurotrophic factor receptor (CNTFR) to human chromosome 9. *Genomics.* 1993; 17: 782-784.

19. Breen M, Jouquand S, Renier C, et al. Chromosome-Specific Single-Locus FISH Probes Allow Anchorage of an 1800-Marker Integrated Radiation-Hybrid/Linkage Map of the Domestic Dog Genome to All Chromosomes. *Genome Res.* 2001; 11: 1784-1795.

20. Matise T C, Perlin M, Chakravarti A. Automated construction of genetic linkage maps using an expert system (MultiMap): a human genome linkage map. *Nat Genet.* 1994; 6: 384-390.

21. Holst A, Heller S, Junghans D, Geissen M, Ernsberger U, Rohrer H. Onset of CNTFRalpha expression and signal transduction during neurogenesis in chick sensory dorsal root ganglia. *Dev Biol.* 1997; 191: 1-13.

22. Zhang Y, Li A, Zhu X, et al. Cone arrestin expression and induction in retinoblastoma cells. *Proceedings of the Ninth International Symposium on retinal Degeneration*. New York: Kluwer Academic / Plenum publishers; 2001, pp. 309-319.

23. Gropp K E, Szel A, Huang J C, Acland G M, Farber D B, Aguirre G D. Selective absence of cone outer segment beta 3-transducin immunoreactivity in hereditary cone degeneration (cd). *Exp Eye Res.* 1996; 63: 285-296.

24. Bazan J F. Structural design and molecular evolution of a cytokine receptor superfamily. *Proc Natl Acad Sci U S A.* 1990; 87: 6934-6938.

25. Fuhrmann S, Kirsch M, Heller S, Rohrer H, Hofmann H D. Differential regulation of ciliary neurotrophic factor receptor-alpha expression in all major neuronal cell classes during development of the chick retina. *J Comp Neurol.* 1998; 400: 244-254.

26. Davis S, Aldrich T H, Ip N Y, et al. Released form of CNTF receptor alpha component as a soluble mediator of CNTF responses. *Science.* 1993; 259: 1736-1739.

27. Kirsch M, Lee M Y, Meyer V, Wiese A, Hofmann H D. Evidence for multiple, local functions of ciliary neurotrophic factor (CNTF) in retinal development: expression of CNTF and its receptors and in vitro effects on target cells. *J Neurochem.* 1997; 68: 979-990.

28. Schulz-Key S, Hofmann H D, Beisenherz-Huss C, Barbisch C, Kirsch M. Ciliary neurotrophic factor as a transient negative regulator of rod development in rat retina. *Invest Ophthalmol Vis Sci.* 2002; 43: 3099-3108.

29. Ju W K, Lee M Y, Hofmann H D, et al. Increased expression of ciliary neurotrophic factor receptor alpha mRNA in the ischemic rat retina. *Neurosci Lett.* 2000; 283: 133-136.

CHAPTER THREE

IMMUNOLOCALIZATION OF CILIARY NEUROTROPHIC FACTOR RECEPTOR α (CNTFRα) IN MAMMALIAN PHOTORECEPTOR CELLS *

INTRODUCTION

Ciliary neurotrophic factor (CNTF) rescues photoreceptors in several genetic[1-7] and in light-induced models of retinal degeneration.[1,8] Its photoreceptor survival effect was demonstrated *in vivo* in a variety of animal species that includes mouse, [1-5] rat,[4,8] cat,[6], and dog,[7] as well as in mouse retinal explants [9,10]. Although its mechanism of action on photoreceptor cells is not fully understood, CNTF is thought to initiate a survival response by binding to the plasma membrane of retinal cells that express its receptor, ciliary neurotrophic factor receptor (CNTFR). CNTFR is composed of an α subunit (CNTFRα) that specifically binds CNTF, and two β subunits (LIFR, gp-130) that are shared by other members of the IL-6 R family.[11] Binding of CNTF to CNTFRα causes heterodimerization of the α and β subunits and activation of various signaling pathways that promote cell survival.[12]

It has been shown that in the rat retina CNTFRα mRNA is expressed in horizontal cells, and in subpopulations of amacrine and ganglion cells, but not in photoreceptors.[13] In addition, intravitreal delivery of CNTF to the rodent eye triggers the activation of signaling pathways predominantly in Müller cells, and also in other

* Beltran WA, Rohrer H, Aguirre GD. *Mol. Vis.* 2005; 11: 232-244

inner nuclear layer (INL) cells, ganglion cells and astrocytes, yet fails to activate photoreceptors. [14-16] These studies suggest that in the rat and mouse retina, the CNTF photoreceptor rescue effect is mediated through an indirect mechanism of action. It has been proposed that microglia-derived CNTF could prevent photoreceptor cells from undergoing degeneration by promoting the release of direct-acting photoreceptor survival factors such as bFGF, and GDNF by Müller cells.[17]

We have recently shown that in the normal adult canine retina both the CNTFRα transcript and protein are expressed by photoreceptors, INL, and ganglion cells.[18] The immunolocalization of CNTFRα to rods and cones suggests that, at least in the dog, the photoreceptor rescue effect observed with CNTF in the *rcd1* model of retinal degeneration [7] may be mediated through a direct mechanism of action.

Determining whether photoreceptors are the direct targets of CNTF has become increasingly important since this survival factor is currently being tested in Phase 1 clinical trials in humans with retinitis pigmentosa (www.neurotech.fr/news_press_100803.asp).To address the differences between dogs and rodents and determine if CNTFRα is localized to photoreceptors in other species, we performed immunocytochemical studies on retinas from a variety of mammalian species.

METHODS

Animals and tissue fixation

Normal adult retinas from the following mammalian species were used for the study: mouse (balb/c, 6 months), rat (AO derived, 6 months), dog (Beagle, adult), cat (DSH, adult), sheep (adult), horse (Pony of America, 7 years), pig (adult), monkey (cynomolgus and rhesus macaques, adult), and human (52-year-old male). In addition, we also collected immature retinas from 3 day-old (PD3) Lewis rats, and 6 day-old

(PD6) AO rats. With the exception of the sheep, horse, and human for which one single individual was available, retinas from at least two individuals were obtained for each of the other species.

While under anesthesia (mouse, rat), or less than 10 minutes after euthanasia (dog, cat, sheep, pig, horse), eyes were enucleated. Retinas were then processed at our facility as follows: a slit was done at the level of the *ora serrata* and the entire globe was fixed for 3 hours in 4 % paraformaldehyde in 0.1 M phosphate buffered saline at 4°C. The posterior segment was isolated and fixed for an additional 24 hours at 4°C in 2 % paraformaldehyde in 0.1 M phosphate buffered saline. The tissue then was trimmed and cryoprotected sequentially for 24 hours in a solution of 15 % and 30 % sucrose in 0.1 M sodium phosphate and 0.15 M sodium chloride, pH 7.2 [BupH™, Phosphate Buffered Saline, Pierce, Rockford, IL; (referred in the text as PBS)] at 4°C, and embedded in OCT. Cryosections were cut at 7 or10 μm thickness and stored at -80°C. The human eye was a surgical specimen that had been enucleated for orbital exenteration of an extraocular tumor. The rhesus macaque and human retina specimens (kindly provided by Drs Bob Fariss and Ann Milam, respectively) were fixed in 4 % paraformaldehyde + 0.5 % glutaraldehyde in 0.1 M phosphate buffered saline for 4 hours followed by 2 % paraformaldehyde in 0.1 M phosphate buffered saline for 2.5 years (monkey), or in 4 % paraformaldehyde in 0.1 M phosphate buffered saline for several days followed by 2 % paraformaldehyde in 0.1 M phosphate buffered saline for approximately 3 years (human). The cynomolgus macaque retina (obtained from the New England Primate Research Center) was fixed for 24 hours in 4 % paraformaldehyde in 0.1 M phosphate buffered saline. Monkey and human retinas were then cryoprotected and processed as indicated above.

For immunoblot analysis, neuroretinas from several adult species (rat, dog, cat, pig, and human) were dissected following death, and stored at -80°C until processed

for total protein extraction. The human retina came from a 68 year-old Caucasian female that died of multi-system organ failure, and was provided by the Cooperative Human Tissue Network which is funded by the National Cancer Institute. All research conducted was in full compliance with the ARVO Statement for the Use of Animals in Ophthalmic and Vision Research, and the tenets of the declaration of Helsinki.

Immunocytochemistry

To visualize the retinal localization of CNTFRα, both immunoenzymatic and immunofluorescence methods were used. For enzymatic immunocytochemistry, tissue sections were washed three times in a 0.3% hydrogen peroxide solution in 50% ethanol to inhibit endogenous peroxidase. Sections were then treated with 0.25% Triton X-100 in PBS for 5 min followed by 10% normal goat serum (NGS) with 0.25% Triton X-100 and 0.05% sodium azide in PBS for 60 min. They were then incubated overnight at 4°C with a protein A-purified polyclonal rabbit anti-chick CNTFRα antibody diluted (1:2,000) in PBS with 1.5% NGS, 0.25% Triton X-100 and 0.05% sodium azide. This antibody was raised in a rabbit after immunization with a large fragment of the chick CNTFRα recombinant protein, and has been described previously.[19] After washing in PBS, secondary antibody (biotinylated goat anti-rabbit, 1:200 dilution; Vector Laboratories, Burlingame, CA) was applied for 30 min at room temperature. Antibodies were visualized using the avidin biotin complex (ABC) Elite kit (Vector Laboratories) with diaminobenzidine as a substrate. A non-specific staining of the photoreceptor layer, and in particular of the outer segments, has been previously reported using this immunoenzymatic method,[20] and was observed in this study on the mouse sections and occasionally in sections from other species as well. To confirm the absence of labeling of mouse photoreceptor cells, and particularly of cones with the CNTFRα antibody, we compared the staining pattern of the

photoreceptor layer to that obtained on a sequential section with an antibody directed against mouse cone arrestin (LUMIJ, 1:10,000; [21]). Conversely, to confirm the cone photoreceptor labeling observed with the CNTFRα antibody in the pig, monkey, and human retinas, we used serial sections and immunoreacted each sequential section with CNTFRα antibody, or a rabbit affinity-purified antibody directed against human cone arrestin (LUMIf, 1:10,000;[22]).

In addition to using the anti-chick CNTFRα antibody, we also tested several commercially available antibodies directed against mammalian CNTFRα. The following antibodies were used on retinal cryosections of the collected species: goat polyclonal anti-human CNTFRα (Cat#: AF303NA, 1: 100; R&D systems Inc., Minneapolis, MN), mouse monoclonal anti-human CNTFRα (Cat#: MAB303, 1:100; R&D systems Inc.), and goat polyclonal anti-rat CNTFRα (Cat#: AF559NA, 1:100; R&D systems Inc.). The ABC immunoenzymatic method was performed as described above using the appropriate biotinylated secondary antibodies.

To further characterize the subpopulation of cones in the dog, pig, monkey, and human retinas that express CNTFRα, we performed double immunofluorescence labeling using antibodies that identify M/L (COS-1, 1:10; [23]), or S wavelength sensitive cones (OS-2, 1:1,000; [23]). For immunofluorescence, sections were permeabilized with 0.25% Triton X-100 in PBS for 5 min, and then blocked with 10% normal goat serum with 0.25% Triton X-100 and 0.05% sodium azide in PBS for 20 min. The sections were then incubated overnight at 4°C with the anti-chick CNTFRα antibody (1:500) followed with a red fluorochrome-labeled goat anti-rabbit secondary antibody (Alexa Fluor 568, 1:200; Molecular Probes, Eugene, OR) for 90 min, and then with the COS-1 or OS-2 antibodies for approximately 5 hours, followed by a FITC-labeled horse anti-mouse secondary antibody (1:50; Vector Labs) for 90 min.

Sequential retinal sections from rats (PD3, PD6, and 6 month-old) were incubated for immunofluorescence with either the anti-chick CNTFRα antibody followed by a red-fluorochrome labeled secondary antibody (as described above), or with polyclonal rabbit anti-rat calbindin D-28 K antibody (C 2724, 1:1,000; Sigma, St Louis, MO) followed by a green fluorochrome-labeled goat anti-rabbit secondary antibody (Alexa Fluor 488, 1:200; Molecular Probes). To better distinguish the location of the photoreceptor layer, rhodamine-labeled peanut agglutinin (1:1,000; Vector Laboratories) was used on some sections as a marker of cone extracellular matrix domain. DAPI nuclear stain (5μM for 15 min) was used to visualize the nuclear layers. Double immunofluorescence labeling of adult rat retinas with the anti-chick CNTFRα antibody and a mouse monoclonal anti-recombinant CRALBP antibody (provided by Dr J. Saari; 1: 40,000) was done to determine whether Müller cells express CNTFRα . To determine labeling specificity, control sections were treated in the same way with omission of primary antibodies, and also by substitution with an unrelated primary antibody. Slides were mounted with gelvatol, a medium composed of polyvinyl alcohol and DABCO (Sigma), and examined with an epifluorescent microscope (Axioplan, Carl Zeiss Meditech, Oberkochen, Germany) with or without Differential Interference Contrast (DIC) optics. Images were digitally captured (Spot 3.3 camera, Diagnostic Instruments, Inc., Sterling Heights, MI) and imported into a graphics program (Photoshop; Adobe, Mountain View, CA) for display.

Western blot analysis

Adult rat, dog, cat, pig, and human retinas were homogenized in PBS containing a cocktail of protease inhibitors (Cat#: P8340, Sigma, St Louis, MO), and, following sonication, the protein levels were determined by the Bradford method (Bio-Rad protein assay, Bio-Rad, Hercules, CA). Protein lysates (60 or 120 μg) were placed in

the sample buffer containing 4% glycerol, 0.4% sodium dodecyl sulfate, 1% β-mercaptoethanol, 0.005% bromophenol blue in 12.5 mM Tris-HCl buffer (pH 6.8), and heated at 100 °C for 5 minutes. Samples and molecular weight standards (Cat#: RPN2107; Amersham Biosciences, Piscataway, NJ) were separated by SDS-PAGE (4% stacking gel, 12% separating gel).Transfer of proteins from gels to PVDF membrane (Immobilon, Millipore, Bedford, MA) was performed in pre-chilled transfer buffer (25 mM Tris base, 192 mM glycine, and 15% methanol), and the membranes were then blocked with 10% skim milk in Tris-buffered saline containing 0.5% Tween-20 overnight at 4°C. The membranes were incubated for 1.5 hour with either a protein A-purified rabbit anti chick CNTFRα antibody (1:100,000), a goat polyclonal anti-human CNTFRα antibody (Cat#: AF303NA, 1:500, R&D Systems Inc.), or a mouse monoclonal anti-human CNTFRα antibody (Cat#: 558783, 1:500; BD Pharmingen, San Diego, CA) followed by the appropriate secondary antibody conjugated with horseradish peroxydase (1:10,000, Zymed, San Francisco, CA). The blots were developed using the ECL method according to the manufacturer's recommendations (Amersham Biosciences), and exposed on autoradiograph film (Eastman Kodak, X-oMAT; Rochester, NY)

RESULTS

Immunolocalization of CNTFRα in mammalian retinas.

Immunolabeling of retinal cells with the polyclonal antibody raised against chick CNTFRα was detected in all species except in the horse in which staining was absent in all retinal layers (data not shown). Results obtained with this antibody are summarized in Table 3.1. A similar pattern of labeling of the nerve fiber (NFL), ganglion cell (GCL), and INL was observed across all species (Figure 3.1 B; Figure

Table 3.1 Pattern of immunolabeling in retinas of mammalian species with the anti-chick CNTFRα antibody.
Intensity of labeling was graded as intense (+++), moderate (+), weak (+), or absent (0); RPE staining was not determined (ND) in some species. In mouse RPE, nonspecific labeling could also be observed on negative control sections. Labeling was intense in PD3 and PD6 rats. Data for "Dog" are taken from a previous study.[18] For dog and human outer nuclear layer (ONL), labeling was limited to cone soma, axon, and pedicle. For cat ONL, labeling was limited to cone soma and some cone axons. For sheep and pig ONL, labeling was limited to cone soma. Retinal pigment epithelium (RPE) pigmentation and autofluorescence precluded assessing the presence of specific labeling in pig, monkey, and human. In pig, inner segments (IS), labeling was limited to the inner portion of the IS.

Retinal layer	**Mouse**	**Rat**	**Dog**	**Cat**	**Sheep**	**Pig**	**Monkey**	**Human**
RPE	ND	0	+++	+++	+++	ND	ND	ND
OS	0	0	0	0	+	0	0	0
IS	0	0	+++	+++	+++	++	+++	+++
ONL	0	0	+++	++	+	+++	++	+++
OPL	++	++	+++	++	++	+++	+++	+++
INL	+++	+++	+++	+++	+++	+++	+++	++
IPL	++	++	+	++	+	+	+	+
GCL	+++	+++	+++	+++	+++	+++	+++	+++
NFL	+++	++	+++	+++	++	+++	+++	+++

3.2 H; Figure 3.3 B; Figure 3.4 C; Figure 3.5 B; Figure 3.6 B). Also, less intense staining of the inner plexiform layer (IPL) was observed in all species (Figure 3.1 B; Figure 3.2 H; Figure 3.3 B; Figure 3.4 C; Figure 3.5 B; Figure 3.6 B). In the INL of the adult mouse, rat, and pig, labeling was predominantly observed in cells located at the vitreal and scleral borders of this layer, suggesting that the cells expressing CNTFRα could be amacrine and horizontal cells, respectively (Figure 3.1 B,C; Figure 3.2 H; Figure 3.4 B).

A significant difference was observed when comparing the labeling pattern of the outer nuclear layer (ONL) and photoreceptor layer in the adult mouse and rat, to that observed in the non-rodent mammals. No labeling of adult rodent photoreceptors was detected by either immunoenzymatic or immunofluorescence methods (Figure 3.1 B,C,E; Figure 3.2 G,H), and this was observed with all four CNTFRα antibodies (see Table 3.2). In the developing rat retina (PD3 and PD6), all cells located in the GCL were labeled (Figure 3.2 B-D). In addition, the CNTFRα antibodies labeled the inner 6-7 rows of cells of the outer neuroblastic layer (Figure 3.2 B-D). A population of cells located at the edge of the presumptive outer plexiform layer (OPL), was also distinctively labeled. These cells were regularly spaced and disposed in a linear fashion from the *ora serrata* to the optic nerve at approximately 50 μm from the external limiting membrane (ELM) (Figure 3.2 B-D). Immunofluorescence studies showed that these cells had extended horizontal processes, suggesting that they could be horizontal cells (Figure 3.2 E,F). To confirm this hypothesis, sequential serial sections were labeled with either the anti-chick CNTFRα antibody or with an antibody directed against calbindin D-28kDa, an epitope located on horizontal, amacrine, and ganglion cells in the adult and developing rat retina [24,25]. We observed a similar pattern of labeling with both antibodies (Figure 3.2 F,G) suggesting that horizontal cells express CNTFRα as early as PD 3. This expression persists in the adult (Figure 3.2

I,J).

In both the developing and mature rat retina, as well as in the adult mouse retina, labeling of CNTFRα was not detected in either the photoreceptor cell bodies in the ONL, in the inner or in the outer segments. Since CNTFRα labeling was not absent in rodents (it was observed in other retinal layers such as NFL, GCL, IPL, INL) the most likely conclusion is that rodent photoreceptors do not express CNTFRα. In the adult rat, double immunofluorescence studies did not show any co-localization of CNTFRα with CRALBP suggesting that Müller cells do not express CNTFRα either (Figure 3.2 K-M).

Recently, we reported that CNTFRα transcript and protein are expressed in dog photoreceptor cells.[18] Here, using a different antibody directed against human CNTFRα we obtained a similar pattern of labeling (Figure 3.7 F). In addition, we show by double immunofluorescence studies that CNTFRα co-localized to both M/L and S wavelength sensitive cones of the dog retina (Figure 3.7 D,E). Similarly to what we have observed in the dog, labeling of sequential sections with CNTFRα or human cone-arrestin antibodies in pig, monkey and human, confirmed that both rod and cone photoreceptors express CNTFRα, and that the cellular distribution of the receptor for CNTF differs between the two classes of photoreceptors (Figure 3.4 C,D; Figure 3.5 C,D; Figure 3.6 B-D). In non-rodent mammals, labeling of rods was limited to their inner segments (IS), while cones showed a distinct pattern of staining that involved their IS, and soma, with variable labeling of their axon and pedicle (Figure 3.7 F, Figure 3.3 B; Figure 3.4 B; Figure 3.5 C,G,H; Figure 3.6 B,C). Like in the dog, double immunofluorescence studies, showed that CNTFRα co-localized to the two subpopulation of cones in pig, monkey and human retinas (Figure 3.4 E,F; Figure 3.5 E,F; Figure 3.6 E,F).

Figure 3.1 Immunolocalization of CNTFRα in the adult mouse retina. (**A**) Negative control. (**B**) Pattern of immunoenzymatic labeling with the anti-chick CNTFRα antibody. (**C**) Pattern of immunoenzymatic labeling with the anti-rat CNTFRα antibody (AF559NA) (**D**) Sequential section to (**B**) labeled with mouse cone arrestin antibody. (**E**) Immunofluorescence labeling (overlaid images) with the anti-chick CNTFRα antibody (green), DAPI (blue), and peanut agglutinin (red). Intense labeling with the CNTFRα antibodies was limited to ganglion cells, nerve fibers, and cells located predominantly at the vitreal and scleral borders of the INL **(B, E**). Less intense labeling was also present at the IPL and OPL. Non-specific staining was observed at the photoreceptor layer (**A, B, C**), and was distinct from the specific cone inner segment labeling (arrows) obtained with the mouse cone arrestin antibody (**D**). Fluorescence immunocytochemistry confirmed the absence of photoreceptor labeling with the anti- chick CNTFRα antibody (**E**). PR: photoreceptor layer; ONL: outer nuclear layer; OPL: outer plexiform layer; INL: inner nuclear layer; IPL: inner plexiform layer; GCL: ganglion cell layer. Scale bars: (**A-D**) 20 μm; (E) 40 μm.

PR
ONL
OPL
INL
IPL
GCL
A
B
C
D
E

Figure 3.2 Immunolocalization of CNTFRα in the developing and adult rat retina. (**A**) Negative control. (**B-C**) Pattern of immunoenzymatic labeling with the anti-chick CNTFRα antibody in the 3- (B), and 6-day old (C) retinas. (**D**) Pattern of immunoenzymatic labeling with the anti-human CNTFRα antibody (AF303NA) (**E**) Immunofluorescence labeling (overlaid images) with the anti-chick CNTFRα antibody (red), and DAPI (blue) on a 6-day-old retina. Intense labeling with the CNTFRα antibodies (**B-E**) was observed in the developing retina at the level of the GCL, RPE, as well as in two distinct areas of the outer neuroblastic layer: the inner 6-7 rows of nuclei (bracket), and in horizontal cells (arrows).(**F**) High power view of (E) showing only CNTFRα labeling. Distinct horizontal processes (arrowheads) were seen extending from the labeled cell bodies (arrows) of the horizontal cells. (**G**) Immunofluorescence labeling of horizontal cells with the calbindin antibody showing a similar pattern as observed in (**F**). (**H**) Pattern of immunoenzymatic labeling with the anti-chick CNTFRα antibody in an adult rat retina. Intense labeling was present at the level of the GCL and cells at the inner and outer most border of the INL. No labeling of photoreceptor cells was observed. (**I**) Immunofluorescence labeling (overlaid images) with the anti-chick CNTFRα antibody (red), and DAPI (blue) on the same adult retina. Absence of staining in photoreceptors and RPE was confirmed. Note that this individual's RPE is pigmented (**H**), but that no labeling is observed by immunofluorescence (**I**). (**J**) Sequential section labeled with the calbindin antibody. (**K-M**) Double immunofluorescence with the anti-chick CNTFRα (**K**) and rCRALBP (**L**) antibodies. Note the absence of co-localization (**M**: overlay) of CNTFRα immunoreactive cells in the INL with the soma of Müller cells (arrows). RPE = retinal pigment epithelium; ONbL = outer neuroblastic layer; ONL = outer nuclear layer; PR = photoreceptor layer; INL = inner nuclear layer; IPL = inner plexiform layer; GCL = ganglion cell layer; NFL = nerve fiber layer. Scale bars: (**A-E, H-J**) 40 μm, (**F, G, K-M**) 20 μm.

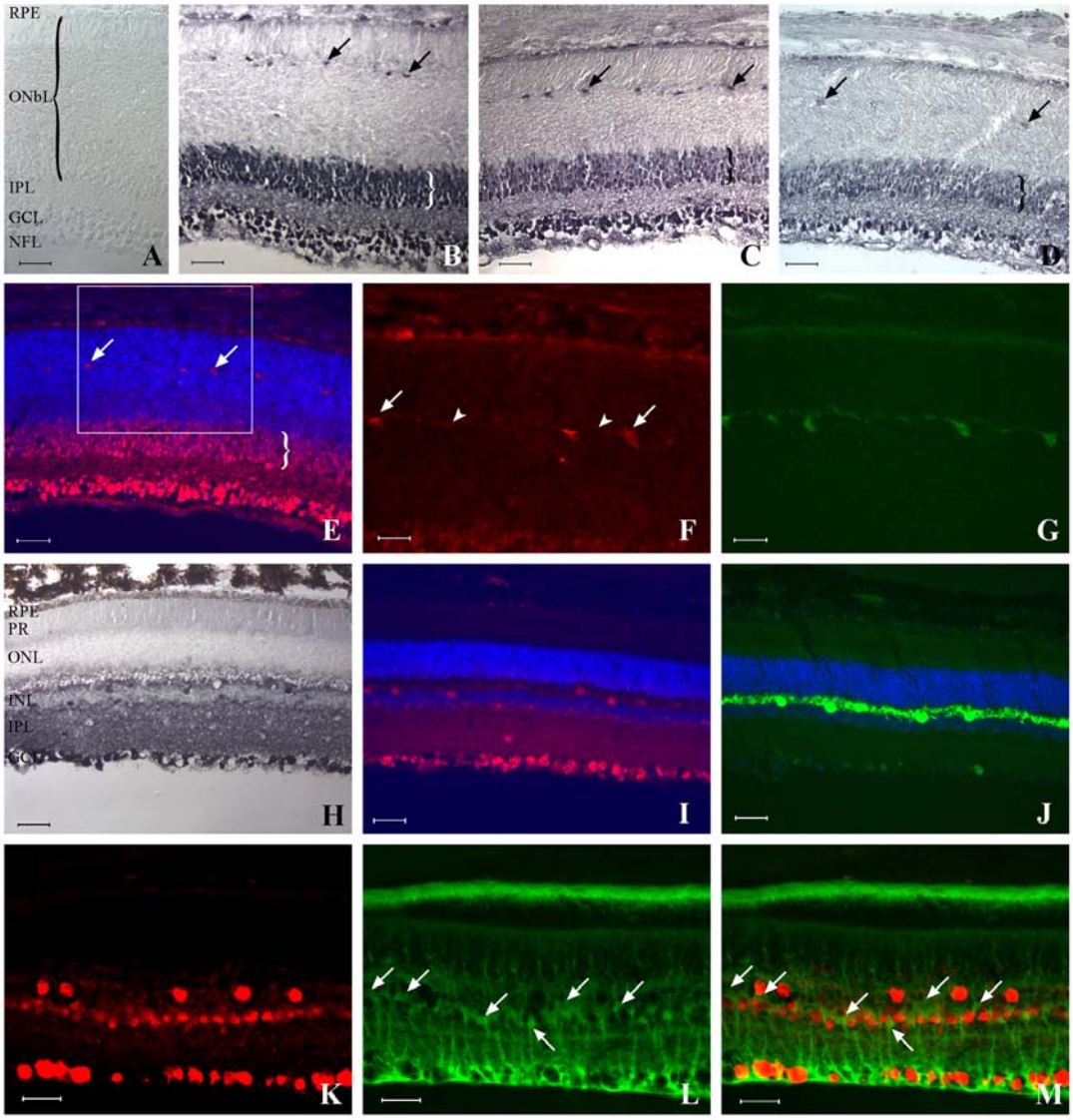
RPE
ONbL
IPL
GCL
NFL
A
B
C
D
E
F
G
RPE
PR
ONL
INL
IPL
GCL
H
I
J
K
L
M

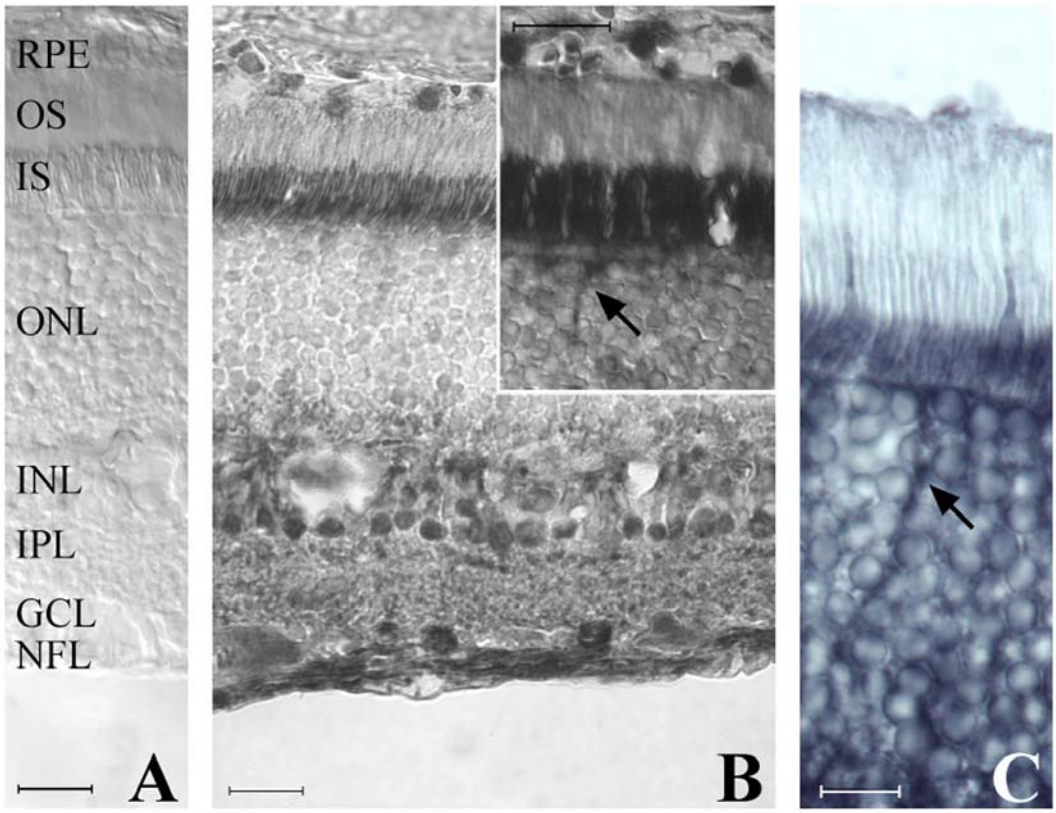

Figure 3.3 Immunolocalization of CNTFRα in the adult cat retina. (**A**) Negative control. (**B**) Pattern of immunoenzymatic labeling with the anti-chick CNTFRα antibody. (**C**) Immunoenzymatic labeling of photoreceptors with the anti-human CNTFRα antibody (AF303NA). Intense labeling with the anti-chick CNTFRα antibody was seen at the RPE, IS, INL, GCL and NFL (B). With longer incubation times in the enzyme substrate (DAB), labeling of cone cell bodies and their extending axons (arrow) could be detected (**inset** to **B** and **C**). RPE = retinal pigment epithelium; OS = outer segments; IS = inner segment; ONL = outer nuclear layer; INL = inner nuclear layer, IPL = inner plexiform layer; GCL = ganglion cell layer; NFL = nerve fiber layer. Scale bars: (**A, B, inset**) 20 μm, (**C**) 10 μm.

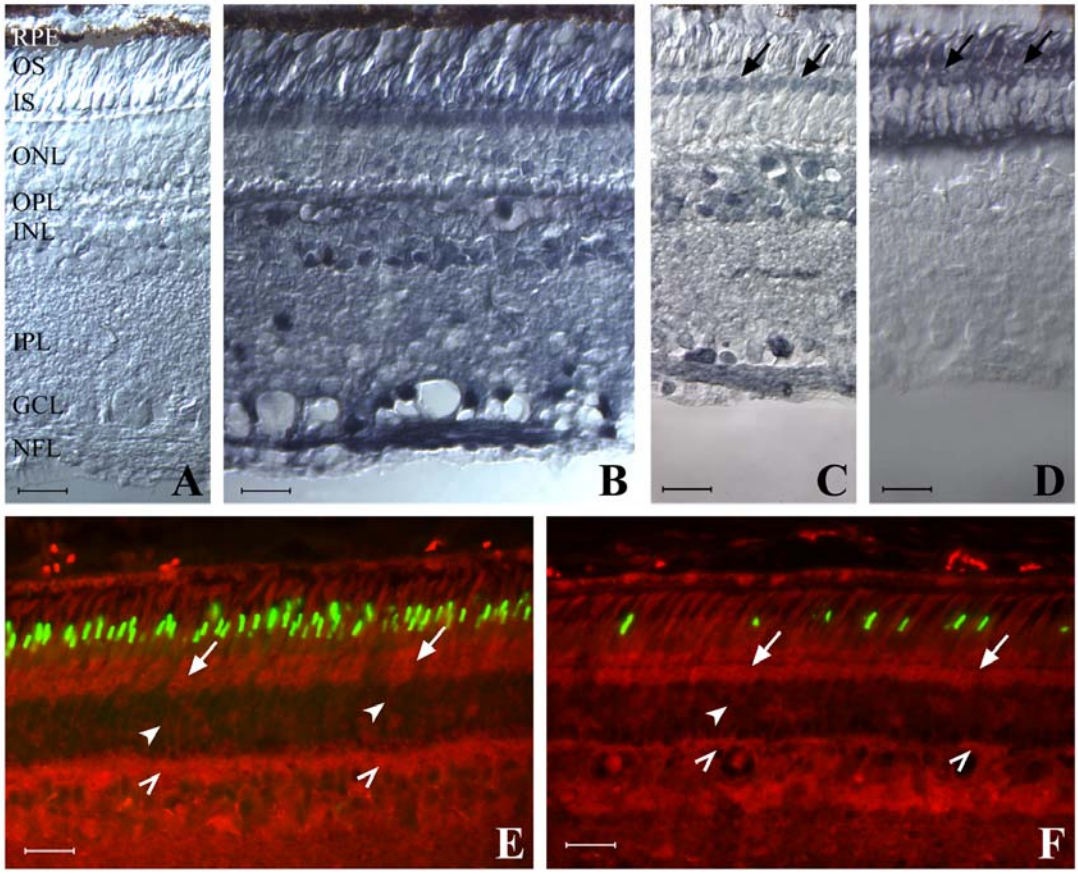

Figure 3.4 Immunolocalization of CNTFRα in the adult pig retina. (**A**) Negative control (pigmented RPE). (**B, C**) Pattern of immunoenzymatic labeling with the anti-chick CNTFRα antibody at 1:2,000 (**B**), or 1: 10,000 (**C**) dilutions. (**D**) Sequential section labeled with human cone arrestin antibody. (**E, F**) Double immunofluorescence labeling (overlaid images) with the anti-chick CNTFRα (red) and COS1 [green, (**E**)] or OS2 [green, (**F**)] antibodies. Intense immunoenzymatic labeling with the CNTFRα antibody (1:2,000 dilution) was seen at the IS, ONL (cone cell bodies), OPL, INL, GCL and NFL (**B**). Labeling with the CNTFRα antibody at a 1:10,000 dilution was still present in the cone cell bodies (arrows) (**C**), and resembled that obtained with the human cone arrestin antibody (arrows) (**D**). CNTFRα immunolabeling of M/L (**E**) and S (**F**) cones was localized to their inner segments, cell bodies (arrows), axons (arrowheads), and pedicles (open arrowheads).
RPE: retinal pigment epithelium; OS: outer segments; IS: inner segments; ONL: outer nuclear layer; OPL: outer plexiform layer; INL: inner nuclear layer; IPL: inner plexiform layer; GCL: ganglion cell layer; NFL: nerve fiber layer. Scale bars: (**A-F**) 20 μm.

Figure 3.5 Immunolocalization of CNTFRα in the adult monkey retina. (**A**) Negative control (pigmented RPE). (**B**) Pattern of immunoenzymatic labeling in the rhesus macaque with the anti-chick CNTFRα antibody. (**C**) High power view of (**B**). (**D**) Sequential section labeled with human cone arrestin antibody. (**E, F**) Double immunofluorescence labeling (overlaid images) in the rhesus macaque with the anti-chick CNTFRα (red) and COS1 [green, (**E**)] or OS2 [green, (**F**)] antibodies. (**G**) Pattern of immunoenzymatic labeling in the cynomolgus macaque with the monoclonal anti-human CNTFRα antibody (MAB303). (**H**) Pattern of immunoenzymatic labeling in the rhesus macaque with the anti-rat CNTFRα antibody (AF559NA). Intense labeling with the CNTFRα antibodies was seen at the IS, ONL (cone cell bodies), OPL, INL, GCL and NFL (**B, G**). Labeling was present at both rod and cone IS, and at cone cell bodies (arrow), axons (arrowheads), and pedicles (open arrowheads) (**C, E, F, G, H**). Both M/L (**E**) and S (**F**) cones were labeled by the CNTFRα antibody.
RPE: retinal pigment epithelium; OS: outer segments; IS: inner segments; ONL: outer nuclear layer; OPL: outer plexiform layer; INL: inner nuclear layer; IPL: inner plexiform layer; GCL: ganglion cell layer; NFL: nerve fiber layer. Scale bars: (**A, B**) 40 μm, (**C**-**H**) 20 μm.

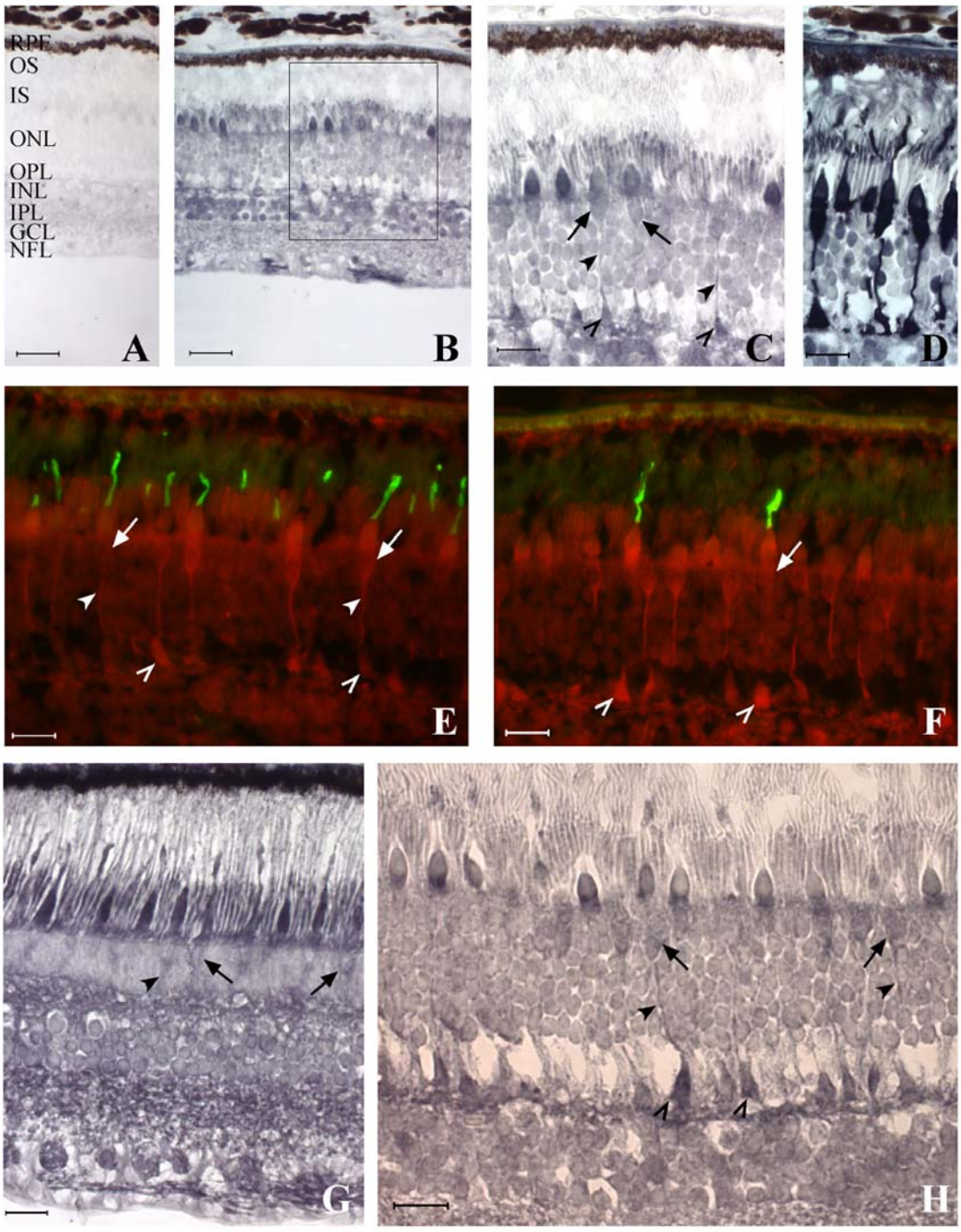
RPE
OS
IS
ONL
OPL
INL
IPL
GCL
NFL
A
B
C
D
E
F
G
H

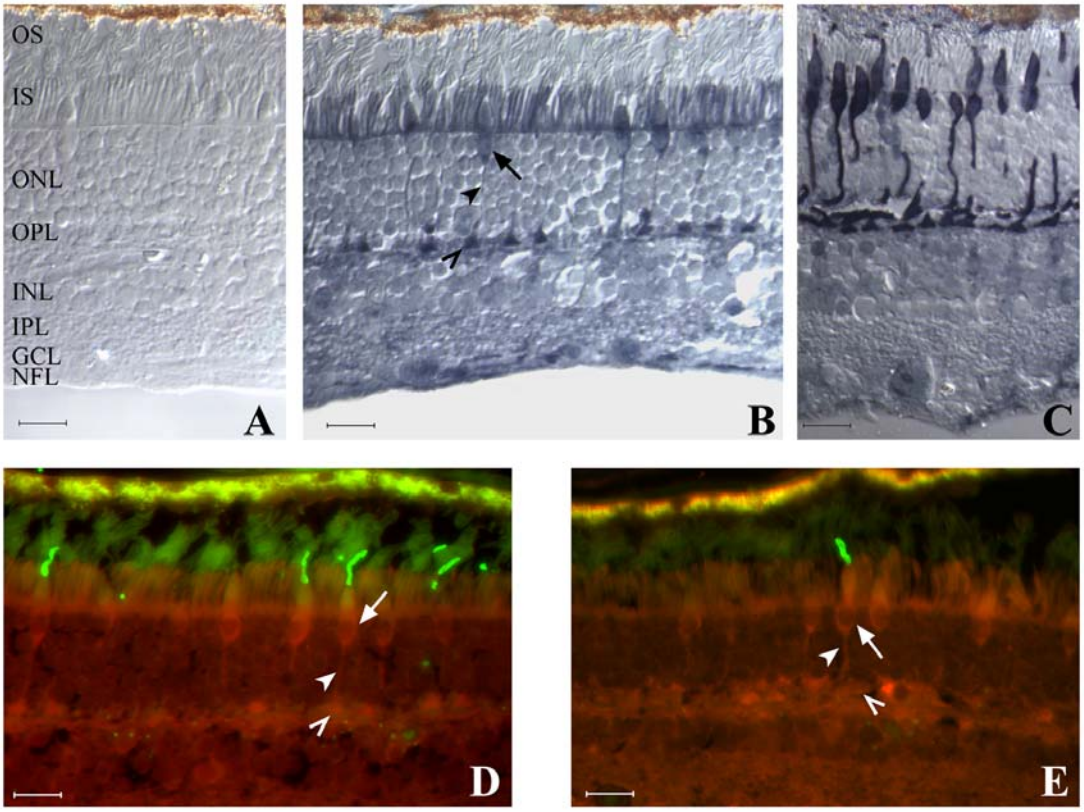

Figure 3.6 Immunolocalization of CNTFRα in the adult human retina. (**A**) Negative control (pigmented RPE). (**B**) Pattern of immunoenzymatic labeling with the anti-chick CNTFRα antibody. (**C**) Pattern of immunoenzymatic labeling with the anti-rat CNTFRα antibody (AF559NA) (**D**) Sequential section to (**B**) labeled with human cone arrestin antibody. (**E, F**) Double immunofluorescence labeling (overlaid images) with the anti- chick CNTFRα (red) and COS1 [green, (**E**)] or OS2 [green, (**F**)] antibodies. Intense labeling with the CNTFRα antibody was seen at the IS, ONL (cone cell bodies), OPL, GCL and NFL (**B**). Labeling was present at both rod and cone IS, and at cone cell bodies (arrow), axons (arrowheads), and pedicles (open arrowheads) (**B, C, E, F**). Both M/L (**E**) and S (**F**) cones were labeled by the anti- chick CNTFRα antibody.
RPE: retinal pigment epithelium; OS: outer segments; IS: inner segments; ONL: outer nuclear layer; OPL: outer plexiform layer; INL: inner nuclear layer; IPL: inner plexiform layer; GCL: ganglion cell layer; NFL: nerve fiber layer. Scale bars: (**A-F**) 20 μm.

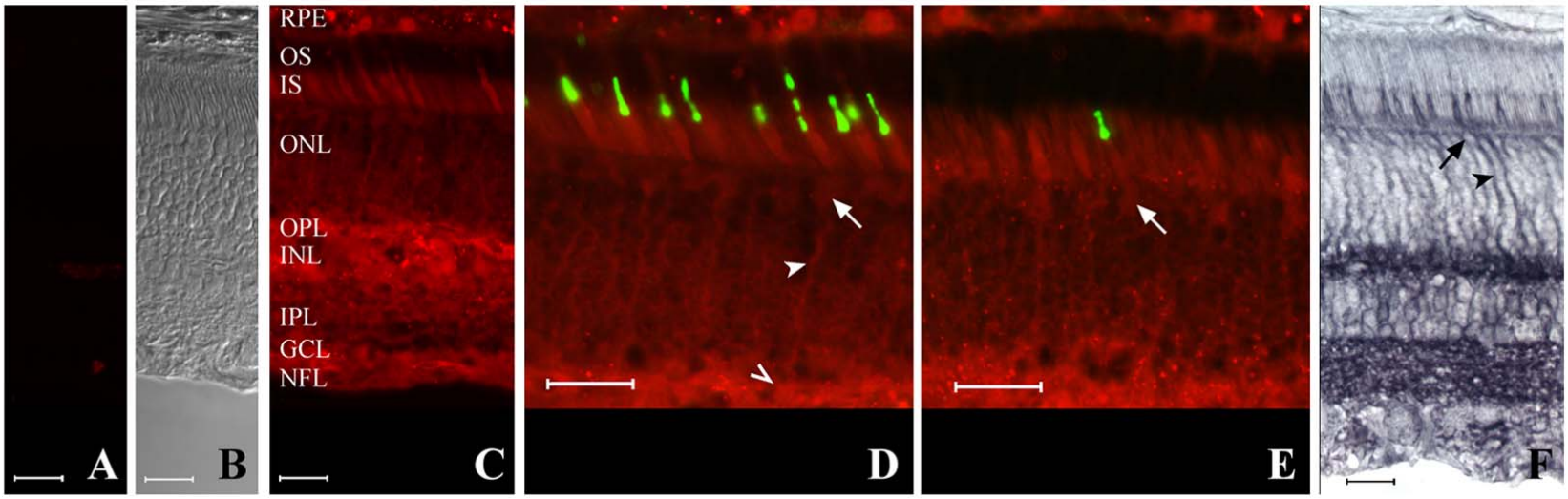

Figure 3.7 Immunolocalization of CNTFRα in cone photoreceptor cells of the dog. (**A**) Negative control. (**B**) Negative control with DIC optics. (**C**) Immunofluorescence labeling with the anti-chick CNTFRα antibody. (**D, E**) Double immunofluorescence labeling (overlaid images) with the anti-chick CNTFRα (red) and COS1 [green, (**D**)] or OS2 [green, (**E**)] antibodies. (**F**) Pattern of immunoenzymatic labeling with the anti-human CNTFRα antibody (AF303NA). Intense labeling was present at the level of the IS of both rod and cones, OPL, INL, GCL, and NFL. CNTFRα immunolabeling of M/L (**D**) and S (**E**) cones was localized to their inner segments, cell bodies (arrows), axons (arrowheads), and pedicles (open arrowheads). Scale bars: (**A-F**) 20 μm.

Western blot analysis of CNTFRα in mammalian retinas.

Using a polyclonal goat anti-human CNTFRα antibody (AF303NA) on total retinal protein extracts of several mammalian species (rat, dog, cat, pig, and human), we detected under reducing conditions a common band at a molecular weight varying between 61 and 64 kDa (Figure 3.8). A similar band was detected in the rat and human when immunoblots were analyzed using the polyclonal rabbit anti-chick CNTFRα, and the monoclonal anti-human CNTFRα antibodies (data not shown). However, with these two antibodies, several additional non-specific bands were detected.

DISCUSSION

We have shown that CNTFRα protein is expressed in the retina in a variety of mammalian species including primates. While a similar pattern of CNTFRα expression could be observed across species in the inner retina, a distinct difference between rodent and non-rodent species was observed in photoreceptors.

Our results (summarized in Tables 3.1, and 3.2) suggest that the mechanism by which CNTF stimulates photoreceptor survival may depend on the expression of CNTFRα by photoreceptor cells, and thus on the animal species examined.

Recently, we reported that normal adult canine photoreceptor cells express CNTFRα when using a polyclonal antibody directed against chick CNTFRα.[18] Here, we have extended our work using this same antibody to examine the expression of CNTFRα in the retina of several other mammals. Since, the degree of homology between the amino acid sequence of chicken CNTFRα and that of dog and other mammals is relatively low,[18] we also used three other antibodies raised against mammalian CNTFRα to verify our results. While the intensity and the quality of the immunolabeling were higher with the anti-chick CNTFRα antibody, a similar pattern

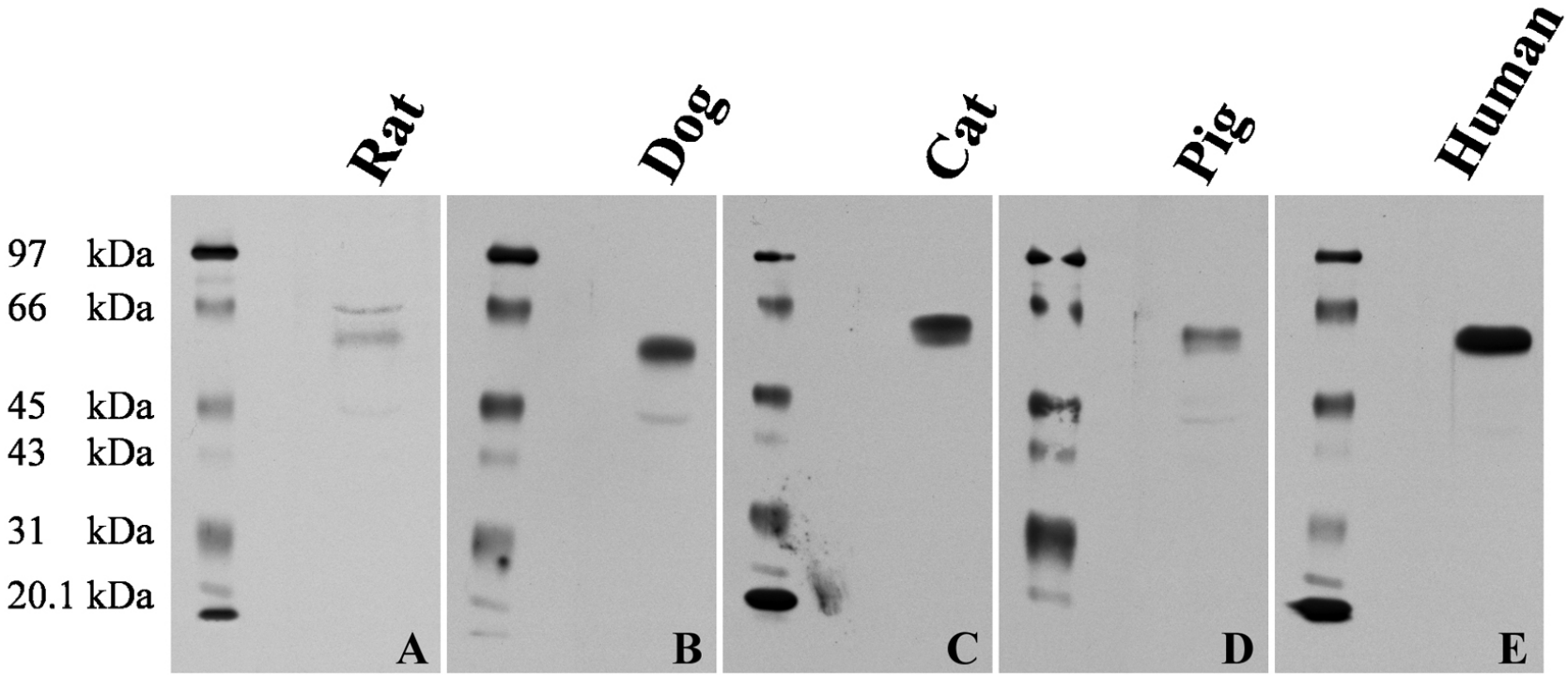

Figure 3.8 Western blot analysis of CNTFRα in retinas of mammalian species.
Total protein extracts were run on a reducing 12 % SDS-PAGE gel and immunoblotted with a polyclonal antibody raised against human CNTFRα (AF303NA). (**A**) Detection in the rat of a major band at approximately 63 kDa. (**B**) Detection in the dog of a major band at approximately 61 kDa. (**C**) Detection in the cat of a band at approximately 64 kDa. (**D**) Detection in the pig of a major band at approximately 63 kDa. (**E**) Detection in the human of a band at approximately 62 kDa.

Table 3.2 Photoreceptor immunolabeling with different CNTFRα antibodies in mammalian retina

The table summarizes the level of immunodetection of CNTFRα in the photoreceptor cells of several mammalian species, with the four antibodies used in this study. Intensity of photoreceptor labeling was characterized as strong (+++), moderate (++), weak (+), absent but with labeling in other retinal layers (0), nonspecific background labeling (BG), nonreactive with an absence of labeling throughout the retina (NR), or indeterminate due to binding of secondary antibody to the tissue (IN).

CNTFRα antibodies	**Mouse**	**Rat 6d**	**Rat adult**	**Dog**	**Cat**	**Sheep**	**Pig**	**Horse**	**Cynomolgus macaque**	**Rhesus macaque**	**Human**
rabbit anti-chick	0	0	0	+ + +	+ + +	+ + +	+ + +	NR	BG	+ + +	+ + +
goat anti-human (AF303NA)	0	0	0	+ +	+ + +	IN	+ +	+ +	+	+	+
mouse anti-human (MAB303)	IN	0	0	BG	+	+ +	+	NR	+ + +	+	+
goat anti-rat (AF559NA)	0	0	0	BG	+ +	IN	+ +	BG	+	+ + +	+ + +

could be observed with the other antibodies, thus confirming the specificity of the labeling detected in mammalian species with the anti-chick CNTFRα antibody. It must be noted, that the manufacturer of these three antibodies (AF303NA, MAB303, AF559NA) does not advertise them for immunocytochemical use, yet we were able to detect some labeling by using the immunoenzymatic method described above.

Our findings support previous observations that suggest that CNTFRα is not expressed by rodent photoreceptors. In both mouse and rat adult retinas, CNTFRα immunolabeling was restricted to some INL, and ganglion cells. This pattern resembled that observed for CNTFRα mRNA in the rat.[13] We showed that photoreceptor expression of CNTFRα was absent in both the mature normal rodent retina as well as in the developing rat retina at PD3 and PD6. This is in contrast to a study that claimed that CNTFRα expression could be detected in photoreceptors at PD5 and PD8.[26] In that report, the authors analyzed on immunoblots the expression of CNTFRα in both the outer and inner retina. Since the horizontal cut made to isolate the outer retina (on flatmounted retinas) was done at a thickness of 140 μm from the vitreal surface, it is likely that the "outer retina" defined by the authors contained a portion of the developing INL that included CNTFRα-expressing horizontal cells. Indeed, on our sections the distance separating the horizontal cells from the internal limiting membrane was approximately 200-250 μm in the PD3 rat, and 170-200 μm in the PD6 rat.

Another study has suggested that rat photoreceptor cells express CNTFRα.[27] While high magnification views showed punctate immunolabeling exclusively limited to the photoreceptor outers segments, no labeling was observed in ganglion, and INL cells. Since negative controls were not performed using a pre-, or non-immunized serum, or an unrelated primary antibody from the same species in which the CNTFRα antibody was raised, it cannot be excluded that outer segment staining was non-

specific and due to “antibody stickiness” to the photoreceptor outer segments. A similar phenomenon has been reported when performing enzymatic immunocytochemistry on the retina,[20] and can be a source of false positive immunolabeling when appropriate antibody controls are not used. We were not able to verify the specificity of the commercial CNTFRα antibody used in that study, as it has not been commercially available for over three years [Personal communication, Research Diagnostics Inc, Flanders, NJ; 11/2003].

In a recent study, Rhee and Yang reported that CNTFRα immunolabeling of the inner and outer segments of mouse photoreceptors could be observed as early as postnatal day 10, and persisted in the mature retina.[28] The commercial goat polyclonal antibody raised against CNTFRα (R-20) (sc-1914, Santa Cruz Biotechnology, Santa Cruz, CA) that the authors used in their study was one that we had tested previously in the dog, rat, mouse, and other mammalian retinas.[18] We had observed (data not shown) in both the mature mouse and rat retinas a similar pattern of labeling as that described by the authors. In addition, by double immunofluorescence, we observed a colocalization of both PNA and the CNTFRα antibody (sc-1914) in the mouse retina, suggesting that murine cones express CNTFRα (data not shown). Yet, as we have reported previously, [18] we were not able to block the labeling obtained with the sc-1914 antibody by preincubating it with its blocking peptide (sc-1914P) on either immunoblots or immunohistochemical sections. We tested two different lots of the blocking peptide as well as a lyophilised peptide preparation provided by the company, at concentrations 5-100 folds higher (10-200 μg/ml) than that of the antibody, and for several different preincubation periods (2 hours-overnight). While we cannot fully exclude the possibility of a manufacturing defect in the preparation of the blocking peptide, we have questioned the specificity of the sc-1914 antibody. In their study, Rhee and Yang [28] have omitted to report the results of the negative

controls used to verify the specificity of the sc-1914 antibody while providing thorough details for the other antibodies tested.

RT-PCR analysis of CNTFRα expression in the ONL of normal and light-reared PD35 rat retinas failed to detect CNTFRα gene expression.[17] Similarly, single cell RT-PCR detected CNTFRα transcript in a fraction of mouse Müller cells but never in rod photoreceptor cells.[29] These results contrast with those from Ju et al.[30] that report increased CNTFRα mRNA expression in rat photoreceptors following retinal ischemia and reperfusion. These apparently contradicting observations may suggest that under normal conditions, mature rodent photoreceptors do not express CNTFRα, but that under conditions of stress such as ischemia and reperfusion, CNTFRα expression occurs.

Several reports have failed to show any CNTF-mediated activation of signaling pathways in juvenile and adult rodent photoreceptor cells,[14-16] and our results support the idea that direct activation of these cells may not occur in the absence of CNTFRα. Yet, very recent studies show that CNTF can trigger the activation of cytokine signaling events in photoreceptor precursor cells and differentiating rods in the early postnatal rodent retina.[31-33] It is therefore possible, that immature photoreceptor cells express low levels of CNTFRα that escape detection by immunocytochemistry, yet are critical to the development of these cells. Alternatively, CNTF may act directly on these photoreceptor precursor cells by binding a different member of the cytokine-receptor family.[34]

A striking difference in the retinal expression of CNTFRα in non-rodent mammals has been the observation that CNTFRα immunolocalizes to photoreceptors. Similarly to our previous findings in the normal adult canine retina,[18] photoreceptors of the adult cat, sheep, horse, pig, monkey and human express CNTFRα. A similar pattern of photoreceptor staining was observed across these species, and is

characterized by the labeling of rod and cone IS, cone soma, axon and pedicle. Labeling with the anti-chick CNTFRα did not appear to be restricted to the cell membrane, particularly at the level of the cone IS and soma. Recently, it was reported that CNTFRα immunostaining of neurons in the rat cochlear nucleus revealed its presence at the level of the cell membrane and at the soma; ultrastructural analysis localized it to the endoplasmic reticulum.[35] The localization of CNTFRα to photoreceptors would suggest that endogenous or exogenously administered CNTF could bind directly to CNTFRα expressed at the surface of these cells. To determine whether CNTFRα is capable of transducing a survival signal to photoreceptors, or whether it plays the role of a CNTF sink, further studies are needed. Examining in non-rodent mammalian photoreceptor cells the expression of the other two β components (LIFR, and gp-130) of the complete CNTF receptor, as well as the downstream signaling pathways is necessary. This would allow characterization of a potential direct mechanism of photoreceptor rescue by CNTF. In parallel, investigations on the indirect mechanism of photoreceptor rescue by CNTF in rodent species need to be pursued. Indeed, at this stage, it cannot be excluded that CNTF protects non-rodent mammalian photoreceptors through both a direct and indirect mechanism of action.

There is evidence that CNTF triggers the activation of signaling pathways in Müller cells of the rodent retina.[14-16,36] Yet, our results fail to identify adult rat Müller cells as a site of CNTFRα expression. In addition, in both the adult rat and mouse, immunolabeling of the INL was mainly restricted to cells located at the vitreal and scleral borders, consistent with the location of horizontal and amacrine cells, respectively. A similar observation has been made when assessing the sites of expression of CNTFRα mRNA in the INL by *in situ* hybridization.[13] This may suggest that Müller cells are also activated indirectly by CNTF, or, as proposed by Peterson

and associates,[14] that Müller cells have the potential to bind the soluble form of CNTFRα. Yet, by single cell RT-PCR, CNTFRα mRNA was detected recently in no more than 30 % of isolated mouse Müller cells.[29] In our study, repeated double immunofluorecence labeling experiments have failed to show any localization of CNTFRα to rat Müller cells. Although this discrepancy may be explained by a species specificity issue, it is also plausible that a low level of CNTFRα expression in Müller cells of normal adult rats is not detected by our current immunofluorecence method. In all other non-rodent mammals, with the exception of the pig in which distinct cell populations predominantly located at the scleral and vitreal borders of the INL were labeled, CNTFRα was found throughout most of the INL. This precluded distinguishing particular cell populations located in the INL, and determining in these species whether Müller cells express CNTFRα.

We previously reported that the anti-chick CNTFRα antibody used in this study detected on immunoblots of canine and chick retina a protein of approximately 62kDa.[18] This value was slightly lower than that previously reported,[13,19] and may be due to different electrophoresis conditions. In the present, we have confirmed our initial finding using antibodies raised against mammalian CNTFRα, and now show that in other mammalian species a protein with a similar molecular weight is detected. Our results are consistent with those of others on rat [37] and bovine [38] tissues.

In summary, we have shown that CNTFRα is expressed as a protein with an apparent molecular weight of approximately 61-64 kDa in the retina of a wide variety of mammalian species. To the best of our knowledge we provide the first immunocytochemical evidence that CNTFRα is not expressed by rodent photoreceptor cells, while it is found on photoreceptors of non-rodent mammalian species. A previous study by one of the co-authors had shown in the chicken retina

that CNTFRα expression was present in photoreceptor cells,[39] and it was recently shown to be restricted to violet-sensitive cones.[40] This further illustrates that caution needs to be used when extrapolating results from one animal species to another.

REFERENCES

1. LaVail MM, Yasumura D, Matthes MT, et al. Protection of mouse photoreceptors by survival factors in retinal degenerations. *Invest Ophthalmol Vis Sci* 1998;39:592-602.

2. Cayouette M, Gravel C. Adenovirus-mediated gene transfer of ciliary neurotrophic factor can prevent photoreceptor degeneration in the retinal degeneration (rd) mouse. *Hum Gene Ther* 1997;8:423-430.

3. Cayouette M, Behn D, Sendtner M, et al. Intraocular gene transfer of ciliary neurotrophic factor prevents death and increases responsiveness of rod photoreceptors in the retinal degeneration slow mouse. *J Neurosci* 1998;18:9282-9293.

4. Liang FQ, Aleman TS, Dejneka NS, et al. Long-term protection of retinal structure but not function using RAAV.CNTF in animal models of retinitis pigmentosa. *Mol Ther* 2001;4:461-472.

5. Liang FQ, Dejneka NS, Cohen DR, et al. AAV-mediated delivery of ciliary neurotrophic factor prolongs photoreceptor survival in the rhodopsin knockout mouse. *Mol Ther* 2001;3:241-248.

6. Chong NH, Alexander RA, Waters L, et al. Repeated injections of a ciliary neurotrophic factor analogue leading to long-term photoreceptor survival in hereditary retinal degeneration. *Invest Ophthalmol Vis Sci* 1999;40:1298-1305.

7. Tao W, Wen R, Goddard MB, et al. Encapsulated cell based delivery of CNTF reduces photoreceptor degeneration in animal models of retinitis pigmentosa. *Invest Ophthalmol Vis Sci* 2002;43:3292-3298.

8. LaVail MM, Unoki K, Yasumura D, et al. Multiple growth factors, cytokines, and neurotrophins rescue photoreceptors from the damaging effects of constant light. *Proc Natl Acad Sci U S A* 1992;89:11249-11253.

9. Ogilvie JM, Speck JD, Lett JM. Growth factors in combination, but not individually, rescue rd mouse photoreceptors in organ culture. *Exp Neurol* 2000;161:676-685.

10. Caffe AR, Soderpalm AK, Holmqvist I, et al. A combination of CNTF and BDNF rescues rd photoreceptors but changes rod differentiation in the presence of RPE in retinal explants. *Invest Ophthalmol Vis Sci* 2001;42:275-282.

11. Davis S, Aldrich TH, Stahl N, et al. LIFR beta and gp130 as heterodimerizing signal transducers of the tripartite CNTF receptor. *Science* 1993;260:1805-1808.

12. Boulton TG, Stahl N, Yancopoulos GD. Ciliary neurotrophic factor/leukemia inhibitory factor/interleukin 6/oncostatin M family of cytokines induces tyrosine phosphorylation of a common set of proteins overlapping those induced by other cytokines and growth factors. *J Biol Chem* 1994;269:11648-11655.

13. Kirsch M, Lee MY, Meyer V, et al. Evidence for multiple, local functions of ciliary neurotrophic factor (CNTF) in retinal development: expression of CNTF and its receptors and in vitro effects on target cells. *J Neurochem* 1997;68:979-990.

14. Peterson WM, Wang Q, Tzekova R, et al. Ciliary neurotrophic factor and stress stimuli activate the Jak-STAT pathway in retinal neurons and glia. *J Neurosci* 2000;20:4081-4090.

15. Wahlin KJ, Campochiaro PA, Zack DJ, et al. Neurotrophic factors cause activation of intracellular signaling pathways in Muller cells and other cells of the inner retina, but not photoreceptors. *Invest Ophthalmol Vis Sci* 2000;41:927-936.

16. Wahlin KJ, Adler R, Zack DJ, et al. Neurotrophic signaling in normal and degenerating rodent retinas. *Exp Eye Res* 2001;73:693-701.

17. Harada T, Harada C, Kohsaka S, et al. Microglia-Muller glia cell interactions control neurotrophic factor production during light-induced retinal degeneration. *J Neurosci* 2002;22:9228-9236.

18. Beltran WA, Zhang Q, Kijas JW, et al. Cloning, mapping, and retinal expression of the canine ciliary neurotrophic factor receptor alpha (CNTFRalpha). *Invest Ophthalmol Vis Sci* 2003;44:3642-3649.

19. Holst A, Heller S, Junghans D, et al. Onset of CNTFRalpha expression and signal transduction during neurogenesis in chick sensory dorsal root ganglia. *Dev Biol* 1997;191:1-13.

20. Milam AH. Immunocytochemical studies of the retina In: Rakoczy PE, ed. *Methods in molecular medicine: vision research protocols*. Totowa, NJ: Humana press, 2001;71-88.

21. Zhu X, Li A, Brown B, et al. Mouse cone arrestin expression pattern: light induced translocation in cone photoreceptors. *Mol Vis* 2002;8:462-471.

22. Zhang Y, Li A, Zhu X, et al. Cone arrestin expression and induction in retinoblastoma cells. Proceedings of the Ninth International Symposium on retinal Degeneration 2001;309-319.

23. Rohlich P, Szel A. Binding sites of photoreceptor-specific antibodies COS-1, OS-2 and AO. *Curr Eye Res* 1993;12:935-944.

24. Uesugi R, Yamada M, Mizuguchi M, et al. Calbindin D-28k and parvalbumin immunohistochemistry in developing rat retina. *Exp Eye Res* 1992;54:491-499.

25. Bastianelli E, Takamatsu K, Okazaki K, et al. Hippocalcin in rat retina. Comparison with calbindin-D28k, calretinin and neurocalcin. *Exp Eye Res* 1995;60:257-266.

26. Schulz-Key S, Hofmann HD, Beisenherz-Huss C, et al. Ciliary neurotrophic factor as a transient negative regulator of rod development in rat retina. *Invest Ophthalmol Vis Sci* 2002;43:3099-3108.

27. Valter K, Bisti S, Stone J. Location of CNTFRalpha on outer segments: evidence of the site of action of CNTF in rat retina. *Brain Res* 2003;985:169-175.

28. Rhee KD, Yang XJ. Expression of cytokine signal transduction components in the postnatal mouse retina. *Mol Vis* 2003;9:715-722.

29. Wahlin KJ, Lim L, Grice EA, et al. A method for analysis of gene expression in isolated mouse photoreceptor and Muller cells. *Mol Vis* 2004;10:366-375.

30. Ju WK, Lee MY, Hofmann HD, et al. Increased expression of ciliary neurotrophic factor receptor alpha mRNA in the ischemic rat retina. *Neurosci Lett* 2000;283:133-136.

31. Zhang SS, Wei J, Qin H, et al. STAT3-mediated signaling in the determination of rod photoreceptor cell fate in mouse retina. *Invest Ophthalmol Vis Sci* 2004;45:2407-2412.

32. Ozawa Y, Nakao K, Shimazaki T, et al. Downregulation of STAT3 activation is required for presumptive rod photoreceptor cells to differentiate in the postnatal retina. *Mol Cell Neurosci* 2004;26:258-270.

33. Rhee KD, Goureau O, Chen S, et al. Cytokine-induced activation of signal transducer and activator of transcription in photoreceptor precursors regulates rod differentiation in the developing mouse retina. *J Neurosci* 2004;24:9779-9788.

34. Schuster B, Kovaleva M, Sun Y, et al. Signaling of human ciliary neurotrophic factor (CNTF) revisited. The interleukin-6 receptor can serve as an alpha-receptor for CTNF. *J Biol Chem* 2003;278:9528-9535.

35. Hafidi A, Decourt B, MacLennan AJ. CNTFRalpha and CNTF expressions in the auditory brainstem: light and electron microscopy study. *Hear Res* 2004;194:14-24.

36. Wang Y, Smith SB, Ogilvie JM, et al. Ciliary neurotrophic factor induces glial fibrillary acidic protein in retinal Muller cells through the JAK/STAT signal transduction pathway. *Curr Eye Res* 2002;24:305-312.

37. Kirsch M, Hofmann HD. Expression of ciliary neurotrophic factor receptor mRNA and protein in the early postnatal and adult rat nervous system. *Neurosci Lett* 1994;180:163-166.

38. Koh SW. Ciliary neurotrophic factor released by corneal endothelium surviving oxidative stress ex vivo. *Invest Ophthalmol Vis Sci* 2002;43:2887-2896.

39. Fuhrmann S, Kirsch M, Heller S, et al. Differential regulation of ciliary neurotrophic factor receptor-alpha expression in all major neuronal cell classes during development of the chick retina. *J Comp Neurol* 1998;400:244-254.

40. Seydewitz V, Rothermel A, Fuhrmann S, et al. Expression of CNTF receptor-alpha in chick violet-sensitive cones with unique morphologic properties. *Invest Ophthalmol Vis Sci* 2004;45:655-661.

CHAPTER FOUR

A FRAMESHIFT MUTATION IN *RPGR* EXON ORF15 CAUSES PHOTORECEPTOR DEGENERATION AND INNER RETINA REMODELING IN A MODEL OF X-LINKED RETINITIS PIGMENTOSA*

INTRODUCTION

X-linked retinitis pigmentosa (XLRP) is a group of diseases that comprises some of the most severe and early-onset forms of inherited retinal degeneration in humans with partial or complete blindness in the third or fourth decade of life, or earlier.[1-3] Mutations in the retinitis pigmentosa GTPase regulator (*RPGR*) gene account for more than 70% of patients with XLRP, and most of these mutations are found in exon ORF15.[4] A spectrum of disease phenotypes is associated with *RPGR* mutations. The most common reflect the typical rod-cone degeneration encountered in most forms of RP and consist first in night blindness and loss of mid-peripheral visual field followed by loss of day vision and central visual acuity.[1,2] Yet, some other mutations result in equal rod-cone abnormalities,[5] cone-rod dystrophies,[6] or macular degeneration.[7]

To understand the retinal function of the RPGR protein, as well as the pathogenic mechanisms that link mutations in *RPGR* with the death of photoreceptor cells, several animal models have been used. These comprise two transgenic murine

* Beltran WA, Hammond P, Acland GM, Aguirre GD. *Invest. Ophthalmol. Vis. Sci*. 2006; 47 (4): 1669-1681.

models (*RPGR* knockout mouse,[8] and a dominant gain-of-function mutant[9]), and two naturally-occurring canine mutations in exon ORF15[10] that cause two forms of X-linked progressive retinal atrophy (*XLPRA*).

In *XLPRA1*, a five-nucleotide deletion (del1028-1032) in exon ORF15 causes an immediate premature stop codon that results in a protein truncated of its 230 C-terminal amino acids. This mutation causes a loss of function of *RPGR*. Morphological characterization showed that photoreceptor cells develop and function normally, but then undergo progressive rod-cone degeneration. The earliest histological signs of rod degeneration are detected at 11 months of age, and are followed at later stages by cone death.[10,11]

In *XLPRA2*, preliminary results from our group have shown that the disease is a much more severe and earlier form of retinal degeneration than *XLPRA1*.[10] A two nucleotide deletion (del 1084-1085) in exon ORF15 results in a frameshift that changes the deduced peptide sequence by the inclusion of 34 additional basic residues and increases the isoelectric point of the truncated protein.[10] In addition, the mutant ORF15 protein was also shown to accumulate in the endoplastic reticulum of transfected COS7 cells. These results suggest that the mutation in *XLPRA2* causes a toxic gain of function and is comparable to the severe human phenotype resulting from microdeletions that cause a frameshift.[12]

Although the precise subcellular location of the RPGR ORF15 protein in photoreceptor cells is still debated,[13,14] findings in the null mutant mouse suggest that it may play a role in maintaining a polarized distribution of proteins between inner (IS) and outer (OS) segments.[8] Yet, it is still unclear how the loss of function of *RPGR* or the expression of a toxic mutant RPGR protein in *XLPRA2*, may initiate a cascade of molecular events that ultimately lead to photoreceptor cell death. To begin to address this question, we examined the retinal structural alterations that occur in

XLPRA2 and characterized the time course of photoreceptor disease, degeneration, and death and the subsequent alterations that occur in the inner retina. We found an early onset of photoreceptor disease leading to cell death, as well as early inner retina remodeling. Our results identify the critical stages in the pathogenesis of the disease and define the time windows for testing novel therapies.

METHODS

Animals

Thirty-five dogs were used in the study (Table 4.1). This included 25 crossbred *XLPRA2* affected dogs (age range, 2-40.6 weeks), and 10 nonaffected beagles that were used as normal control subjects (age range, 2-24 weeks). All affected dogs (11 hemizygous males, 14 homozygous females) were bred at the Retinal Disease Studies Facility (RDSF; University of Pennsylvania, New Bolton Center, Kennett Square, PA), and their genotype was determined either from the known status of their progenitors or from genetic testing for the disease-causing mutation.[10] All nonmutant beagles came from the Baker Institute colony of specific pathogen-free dogs. After an ocular examination to identify abnormalities not associated with the primary retinal disease, all animals were anesthetized by intravenous injection of pentobarbital sodium, the eyes enucleated, and the dogs euthanatized. All procedures involving animals were done in compliance with the ARVO Statement for the Use of Animals in Ophthalmic and Vision Research.

Retinal histology

The left eyes of 16 *XLPRA2* dogs (age range, 2-40.6 weeks) were used for morphologic examination of disease expression using plastic embedding (Table 4.1, morphology). The retinas of 3 normal beagles (ages: 2.3, 5.4, and 8.3 weeks) were

used as control specimen. By 8 weeks of age the canine retina is structurally mature.[15,16] Immediately after enucleation, the posterior segments were isolated and fixed, using a triple fixative protocol (3% glutaraldehyde-2% formaldehyde; 2% glutaraldehyde-1% osmium tetroxide; and 2% osmium tetroxide) as previously reported.[15] The posterior segments were then trimmed into pieces that extended from the optic nerve to the *ora serrata* along the superior and inferior meridians, dehydrated, and embedded in epoxy resin (PolyBed 812, Polysciences, Warrington, PA). Tissues were sectioned with glass knives at 1 μm with a supercut microtome (Reichert Jung model 2065; Leica, Deerfield, IL), stained with azure II-methylene blue and a paraphenylenediamine counterstain.

Sections from both the superior and inferior meridians were examined with a 40X objective under light microscopy (Axioplan; Carl Zeiss Meditech GmbH, Oberkochen, Germany). The sections were examined in contiguous fields from the optic disc to the *ora serrata*. This included evaluation of the retinal pigment epithelium (RPE), the rod and cone OS and IS, and the thickness and density of the outer (ONL) and inner (INL) nuclear layers. For each dog, a single section from both quadrants was used for quantitative evaluation of the photoreceptor cells, and INL cells at three specific locations: S1, 2,000 ± 500 μm from the optic nerve; S3, 2,000 ± 500 μm from the *ora serrata*; and S2 midway (± 500 μm) between these 2 points. At each of these sites, the number of rows of nuclei in the ONL and INL were counted in at least 3 areas of a 40X field and averaged. For the same areas, the thickness (in μm) of the ONL and INL were measured on digitally captured images.

The kinetics of photoreceptor cell loss were analyzed by fitting the ONL thickness data to solutions of the following differential equations reported by Clarke et al.[17]. We are also reporting below the integral equations used for the statistical analysis, since we found typographical errors confirmed by the authors (Geoff Clarke,

personal communication, 11/29/05) in the integral equations provided in the supplementary information that accompanied their paper (http://www.nature.com/nature/journal/v406/n6792/suppinfo/406195a0.html).

Constant risk:

$$\frac{dONL(t)}{dt} = -\mu_0 \times ONL(t) \xrightarrow{\text{integral}} ONL(t) = ONL(0)e^{-\mu_0 t}$$

Exponentially decreasing risk:

$$\frac{dONL(t)}{dt} = -\mu_0 e^{-At} \times ONL(t) \xrightarrow{\text{integral}} ONL(t) = ONL(0)e^{\left[\frac{\left(e^{-At}-1\right)\mu_0}{A}\right]}$$

Exponentially increasing risk:

$$\frac{dONL(t)}{dt} = -\mu_0 e^{At} \times ONL(t) \xrightarrow{\text{integral}} ONL(t) = ONL(0)e^{\left[-\frac{\left(e^{At}-1\right)\mu_0}{A}\right]}$$

Data-fitting was performed with nonlinear regression analysis (with PROC NLIN in SAS 9.1 software; SAS Institute Inc., Cary, NC, USA). This is a least-squares procedure for estimating parameters in nonlinear models. The parameter estimates (using the Gaussian method) and 95% confidence intervals, along with probabilities (based on the Wald test) were computed. The R^2 was used to assess the overall goodness of fit of the model. Please note that it was not possible to fit our data to mathematical models that account for the time period between birth and onset of cell death (called the "delay" parameter by Clarke et al.[17]), because there were insufficient data at early time points, which prevented us from getting an estimate for the "delay" parameter.

Phagocytic cells present in the photoreceptor layer were counted throughout the entire length of both the superior and inferior retinal meridians and expressed as the number of phagocytic cells per unit length of retina. The unit length was set as 10,000 μm. Pyknotic photoreceptor nuclei were counted in the ONL in both the superior and inferior meridians and expressed as the number of pyknotic nuclei per unit area of ONL. The unit area was set as 1 million μm^2 (1 M μm^2) of ONL. A similar count was used to quantify TUNEL-positive photoreceptor cells.

TUNEL assay

In 18 *XLPRA2*-affected dogs, one eye was processed immediately after enucleation for TUNEL assays and/or immunohistochemistry (Table 4.1: TUNEL, IHC). After enucleation, a slit was made through the globe at the level of the *ora serrata*, and the entire globe was fixed for 3 hours in 4% paraformaldehyde in 0.1 M phosphate-buffered saline at 4°C. The posterior segment then was isolated, the vitreous gently removed, and the eyecup fixed for an additional 24 hours at 4°C in 2% paraformaldehyde in 0.1 M phosphate-buffered saline. The tissue then was trimmed, cryoprotected sequentially for 24 hours in a solution of 15% and 30% sucrose in 0.1 M sodium phosphate and 0.15 M sodium chloride, pH 7.2 (BupH™, Phosphate Buffered Saline, Pierce, Rockford, IL; referred in the text as PBS) at 4°C, and embedded in OCT medium.

Cryosections (7 μm thick) along the superior meridian of 17 *XLPRA2* dogs (age range, 3.9-40.6 weeks) were used for TUNEL assay, according to the manufacturer's protocol (*In situ* cell death detection kit, Roche, Indianapolis, IN) and stained with DAPI. Sections along the superior meridian of three normal beagles (ages, 4, 5, and 6 weeks) were also used. Positive control specimen included sections pretreated with DNAse I (3 U/ml in 50 mM Tris-HCl, pH 7.5, 1 mg/ml BSA for 10

Table 4.1: Status, gender and age of dogs used for the morphologic, TUNEL, and immunohistochemical (IHC) studies. M: male; F: female; +: done.

ID	Gender	Age (weeks)	Morphology	TUNEL	IHC
Affected					
Z215	F	2	+		
Z210	M	2	+		+
Z201	M	3.9	+	+	+
Z266	F	4.1		+	
Z212	M	4.9	+		
Z202	M	5	+	+	+
Z203	F	6	+	+	+
Z253	F	6.1		+	
Z254	F	6.7		+	
Z255	F	6.7		+	
Z207	F	7.9	+	+	+
Z250	M	8		+	
Z251	M	8		+	
Z216	M	8.3	+		
Z211	M	11.9	+	+	+
Z219	F	12.1		+	
Z226	F	16	+	+	+
Z194	M	17.3	+		
Z195	F	17.3	+		
Z193	M	17.7	+		
Z208	F	19.9	+		
Z204	M	19.9		+	
Z209	F	23.7		+	
Z181	F	26	+	+	+
Z178	F	40.6	+	+	+
Normal					
7304	F	2			+
2327-2	M	2.3	+		
7306	F	4		+	+
7307	M	5		+	
2297-1	F	5.4	+		
7308	F	6		+	+
7310	F	8.1			+
2298-1	M	8.3	+		
7312	F	12			+
7299	M	24			+

min at room temperature). For negative control subjects, the terminal transferase enzyme was omitted from the TUNEL reaction mixture. Sections were examined from the optic disc to the *ora serrata* by epifluorescence microscopy with the 40X objective. TUNEL-labeled cells in the ONL were counted throughout the entire length of the section (i.e., from disc to *ora serrata*). In determining the proportion of photoreceptor cells that undergo cell death as a function of time, we expressed our results as the number of TUNEL-labeled photoreceptor cells per 1 M μm^2 of ONL. The area of the ONL of each section was obtained by measuring the entire length of the ONL from optic disc to *ora serrata*, and multiplying it by the average thickness of the ONL throughout the section (mean value of the thickness measured in the three locations S1, S2, and S3). This method may slightly underestimate, in areas of decreased photoreceptor density, the proportion of cell that are TUNEL positive. Yet, it was selected because individual cell count could not be determined on 7-µm-thick DAPI-stained cryosections. For each dog, this procedure was performed in triplicate with sequential sections from the superior meridian. The values were averaged and reported as the mean ± SD.

Immunohistochemistry

Sections along the superior retinal meridian of 9 *XLPRA2* dogs (age range, 2-40.6 weeks) and 6 normal dogs (age range, 2-24 weeks) that were processed as described earlier were used for fluorescent immunohistochemistry. We used a battery of cell-specific primary antibodies[9,18-30] of which more than half worked on canine retina (see details in Table 4.2). Because of the lack of specific antibodies directed against all subpopulation of ganglion cells in the dog, our study did not include assessment of their density or morphology. Because previous testing of RPGR and RPGRIP antibodies conducted in our laboratory failed to show any cross-reactivity or

Table 4.2: List of primary antibodies tested and used in this study.

Antigen	Host	Source, catalog # or name	Working concentration	Normal retinal localization (reported in rodents)	Refs.
RPE65	Rabbit	T.Michael Redmond	1:10,000	Retinal pigment epithelium	[18]†
Human cone arrestin	Rabbit	Cheryl Craft, LUMIF	1:10,000	Cone photoreceptors	[19]†
M/L cone opsin	Rabbit	Chemicon, AB5405	1:10,000	OS of M/L cones	[20]*
S cone opsin	Rabbit	Chemicon, AB5407	1:5,000	OS of S cones	[20]*
Rod opsin	Mouse	Paul Hargrave, R2-12N	1:300	OS of rods	[21]†
Synaptophysin	Rabbit	DakoCytomation, A0010	1:100	Neuron synapses, OPL, IPL	[22]†, [23]*
Calbindin D-28K	Rabbit	Sigma, C2724	1:1,000	Horizontal, amacrine cells	[24]†, [23]*
Protein Kinase C (PKCα)	Mouse	BD Biosciences, 610107	1:100	Rod bipolar cells	[25]*, [24]*
Goα	Mouse	Chemicon, MAB3073	1:5,000	ON (rod and cone) bipolar cells	[26]†
Tachykinin receptor 3 (=NK3R, NKBR)	Rabbit	Novus biologicals, NLS4043	1:100	Cone bipolar cells	[24]†
	Rabbit	Abcam, ab13278	1:50		
Metabotropic glutamate receptor (GRM6)	Rabbit	Abcam, ab13362	1:10 – 1:200	Postsynaptic sites of ON bipolar cells	[24]*, [25]*
γ-amino butyric acid (GABA)	Rabbit	Chemicon, AB5016	1:50	GABAergic amacrine cells	[27]*
Choline acetyl transferase (ChAT)	Rabbit	Chemicon, AB143	1:500	Cholinergic amacrine cells	[28]†, [29]*
	Rat	Oncogene, NB05L	1:100		
Tyrosine hydroxylase (TH)	Rabbit	Chemicon, AB152	1:500	Dopaminergic amacrine cells	[24]†, [25]†
Disabled 1 (Dab1)	Rabbit	Chemicon, AB5840	1:50 - 1:100	AII amacrine cells	[25]*
CRALBP	Mouse	John Saari,	1:5,000	Müller cells, RPE	[9]†
Glial Fibrillary acidic protein (GFAP)	Rabbit	DakoCytomation, Z0334	1:1,000	Astrocytes, Müller cells (reactive)	[30]†
Glutamine synthetase	Mouse	Chemicon, MAB302	1:20,000	Müller cells	[25]†

Highlighted in gray are the antibodies that cross-reacted on canine retina, and were successfully used as cell-specific markers in this study. The other antibodies (non-highlighted) were tested but did not cross react on canine retina when used overnight at the indicated concentrations.

†: This same antibody was used in this reference.

*: A different antibody raised against the same antigen was used in this reference.

specificity on canine retina, we did not include them in this study.[10] Cryosections (7-10 μm-thick) were incubated overnight with the primary antibodies after a blocking step with 10% normal serum from the appropriate species. The antigen-antibody complexes were visualized with fluorochrome-labeled secondary antibodies (Alexa Fluor, 1:200; Molecular Probes, Eugene, OR). DAPI stain was used to detect cell nuclei. Slides were mounted with a medium composed of polyvinyl alcohol and DABCO (1,4 diazobizyklo-[2.2.2]oktan) (Gelvatol; Sigma-Aldrich, St Louis, MO), and examined with an epifluorescent microscope (Axioplan; Carl Zeiss Meditec). Images were digitally captured (Spot 4.0 camera; Diagnostic Instrument, Inc.) and imported into a graphics program (Photoshop; Adobe, Mountain View, CA) for display.

RESULTS

Photoreceptor Disease

Gross examination of the eyes at the time of enucleation did not reveal significant differences in size between affected and normal dogs. Measurements of retinal length between the optic disc and the *ora serrata* along the superior meridian confirmed that in *XLPRA2* the growth of the eye was not affected by the disease (data not shown).

Normal retinal development in the dog is complete at approximately 7 to 8 weeks of age.[15,16] At birth, photoreceptor cells have not completely differentiated and are located in the sclerad portion of the outer neuroblastic layer, which then give rise to the outer nuclear layer (ONL). Maturation of photoreceptors occurs in waves from central to peripheral retina.[31] IS are first seen as short bulges of cytoplasm protruding from the external limiting membrane between 1 day and 1 week after birth.[32] At approximately 2 weeks of age, IS are visible throughout the entire length of the retina, and OS formation is underway centrally (Figure 4.1 A). By 5.4 weeks of age, OS are

formed and begin to elongate (Figure 4.1 B). Full maturation of photoreceptors is reached at approximately 8 weeks of age, at which time the retina resembles that of the adult (Figure 4.1 C). Pyknotic figures in the ONL were extremely rare (0 to 1 per 1 M μm^2 of ONL) at all ages examined. Concurrent with the maturation of the photoreceptors, there are changes in the inner retinal layers which are most prominent in the INL. These primarily consist of a decrease in the number of nuclei, presumably because of an increase in eye size (see Figure 4.1 A-C).

Disease stages of *XLPRA2* were defined at early time points on the basis of the structural changes observed in the photoreceptor layer (IS, OS). At later ages, reduction in ONL thickness was also taken into account. Because no major differences in the course of the disease were observed between the superior and inferior retina, the description is provided for the superior meridian (Figure 4.1). Table 3 provides more specific details (phagocyte count, ONL thickness, pyknosis in ONL, and INL thickness) for both the superior and inferior meridians.

The earliest time point examined in the affected dogs was 2 weeks of age (Figure 4.1 D), and no evidence of abnormal development or arrested differentiation was observed (Stage 0; normal). The typical layering of the neuroretina was preserved from the optic disc to the *ora serrata* along both superior (tapetal) and inferior (nontapetal) meridians. Nuclei in the ONL were elongated, which is a normal characteristic of immature photoreceptor cells. Nuclear pyknosis was negligible in the ONL (Table 4.3). Cone and rod IS were present throughout the photoreceptor layer. In the central retina, elongating IS, with budding OS, were observed, whereas in the periphery, short IS were in close contact with the apical RPE.

At 3.9 weeks of age, there was a moderate increase in the number of pyknotic cells in the ONL (Table 3), and very subtle changes in the morphology of the OS. This early stage of OS disruption and misalignment was better seen when dogs were

Figure 4.1: Stages of development and photoreceptor degeneration in normal and mutant retinas. Images are from the mid-periphery of the superior meridian. (**A-C**) Normal retina. (**A**) By 2.3 weeks, photoreceptor nuclei were elongated, IS were visible, and short OS began to form. (**B**) By 5.4 weeks, OS were formed and elongated, and (**C**) photoreceptor maturation was complete by 8.3 weeks. (**D-I**) *XLPRA2* mutant retina. (**D**) Stage 0, 2.2 weeks. Photoreceptor development was normal and comparable to the control. (**E**) Stage 1, 5 weeks. OS were misaligned and partially fragmented (*). Pyknotic nuclei were visible in the ONL (*arrow*). (**F**) Stage 2, 7.9 weeks. OS were disintegrating (*), and there was pyknosis in the ONL (*arrows*). ONL, eight t nine rows of nuclei. (**G**) Stage 3, 16 weeks. The subretinal space was narrowed, rod IS were very short (*arrow*), and remaining but distorted rod and cone OS were visible. Phagocytic cells were present in the subretinal space (*arrowhead*). ONL, six rows of nuclei. (**H**) Stage 4, 26 weeks. The subretinal space wass narrowed further, but distorted OS remained (*arrow*). Both rod and cone IS were shortened, and cone IS were broader than normal. Spaces were visible in the IS layer secondary to rod loss (*arrowheads*). ONL, five rows of nuclei with increased spacing between photoreceptor somas (*). (**I**) Stage 5, 40.6 weeks. The interphotoreceptor space had open areas, yet some photoreceptors appeared to retain their distorted OS (*arrows*). ONL, two to three rows of nuclei. RPE, retinal pigment epithelium; PR, photoreceptor layer; OS, outer segments; IS, inner segments; ONL, outer nuclear layer; OPL, outer plexiform layer; INL, inner nuclear layer. Scale bar: 20 μm.

NORMAL
AFFECTED
AFFECTED
RPE
PR
ONL
OPL
INL
OS
IS
A
B
C
D
E
F
G
H
I

Table 4.3: Changes in the *XLPRA2* retina associated with disease stages.
[a]: Number of phagocytic cells in the subretinal space per 10,000 μm of retinal length;
[b]: Thickness of the ONL or INL measured in number of rows of nuclei;
[c]: Number of pyknotic nuclei in the ONL per 1 million μm^2 of ONL;
S1: central retina (2,000 μm ± 500 μm from optic disc); S3: peripheral retina (2,000 μm ± 500 μm from ora serrata); S2: mid-peripheral retina (midpoint of S1 and S3, ± 500 μm).

	Stage 0		Stage 1			Stage 2	Stage 3		Stage 4	Stage 5
	2 wk (Z215)	**2 wk** (Z210)	**3.9 wk** (Z201)	**4.9 wk** (Z212)	**5 wk** (Z202)	**7.9 wk** (Z207)	**11.9 wk** (Z211)	**16 wk** (Z226)	**26 wk** (Z181)	**40.6 wk** (Z178)
A. Superior retina										
Phagocytic cells [a]	0	0	0	0	0	0	3	13	31	27
ONL thickness [b]										
S1	10	10	14	10	10	7	7	7	5	3
S2	10	11	12	9	11	9	6	6.5	5	3
S3	11.5	11	15.5	9	14	8	5.5	5	3.5	2
Pyknosis (ONL) [c]	0	0	9	105	81	65	27	23	33	15
INL thickness [b]										
S1	4	5	6	4	4	3.5	3.5	3.5	3	3
S2	5	5	5	3	3	3	3	2.5	2	2
S3	5.5	6	5	3	4	3	2.5	1.5	2	1.5
B. Inferior retina										
Phagocytic cells [a]	0	0	0	0	0	0	6	28	31	17
ONL thickness [b]										
S1	10	11	15	9	11	9	6.5	6	4.5	3.5
S2	10	11	14	8.5	9	8.5	6	6	3.5	3
S3	10	11	15	9	9	10	5	5	3	2.5
Pyknosis (ONL) [c]	0	2	15	101	68	42	23	24	41	13
INL thickness [b]										
S1	5	5	5	4	4	4	3	2	3	3
S2	5.5	4.5	5	3	3	3.5	3	2	2.5	2
S3	6	4.5	5	3	3	4	2	1.5	2	2

slightly older (≈ 5 weeks of age; Stage 1; Figure 4.1 E). At that age, nuclear pyknosis had increased in the ONL (Table 3).

By 7.9 weeks of age (Stage 2; Figure 4.1 F), there was severe OS disintegration, with abundant disorganized and disoriented membranous material persisting in the photoreceptor layer. ONL thickness was moderately reduced, and the number of pyknotic nuclei in the ONL had decreased (Table 3). A similar decline in INL thickness as seen in the normal retina was observed between 2 and 7.9 weeks of age (see Figure 4.1 A-F) and reached approximately 3 to 4 rows of nuclei (Table 3).

By 11.9 and 16 weeks, there was narrowing of the subretinal space with shortening or loss of rod IS, and these abnormalities were comparable at both time points (Stage 3; Figure 4.1 G). Distorted OS persisted in the photoreceptor layer. There was marked rod loss, with the ONL reduced to approximately 60 % of its original thickness. Pyknosis in the ONL was further reduced. A few phagocytic cells located in the subretinal space in close apposition to the RPE were first seen in the 11.9-week-old retina. Their number increased at 16 weeks (Table 4.3). Disease-associated thinning of the INL was observed at both ages and was most pronounced in the peripheral retina (Table 4.3).

There was a clear decrease in the density of both rod and cone photoreceptors by 26 weeks of age (Stage 4; Figure 4.1 H). This decrease was seen at the level of the photoreceptor layer, where there were areas devoid of any rod and cone IS, and also in the ONL where internuclear spacing was increased. ONL thickness was less than 50 % of its original thickness. In the photoreceptor layer, the remaining rod and cone IS appeared broader and, although the subretinal space was severely narrowed, shortened, and distorted OS were still present. Cone nuclei displaced into the IS and extruding into the subretinal space were first seen at this age. Phagocytic cells persisted in the subretinal space.

The latest stage of disease examined was at 40.6 weeks (Stage 5; Figure 4.1 I). At that time point, there were approximately 2 to 3 rows of nuclei left in the ONL, and the remaining cone and rod IS were short and broad. Numerous photoreceptor cells maintained a shortened and misaligned OS, and RPE cytoplasmic processes extended towards them. Phagocytes remained in the subretinal space, but were not migrating in the ONL or inner retina. Nuclear pyknosis persisted in the ONL but was not observed in the INL, despite a decrease in its thickness (Table 4.3).

To illustrate the rate of photoreceptor cell loss that occurs during the course of the disease along both the superior and inferior retinal meridians, we plotted the average thickness of the ONL (expressed as either the number of nuclei per column, or in μm) as a function of age. These graphs (Figure 4.2) show a major and rapid early cell loss occurring from 4 to 12 weeks of age. Subsequently, the number of remaining photoreceptors continued to decrease but at a slower rate. The kinetics of photoreceptor cell loss was best described by a model of constant risk of cell death when the ONL thickness was measured as number of nuclei. When the ONL thickness was measured in μm, the data was best fit by both a model of constant risk and of decreasing risk of cell death.

To determine whether the disease and degeneration of photoreceptor cells was uniformly distributed throughout the retina, or if there was a topographic distribution of the disease, we examined all sections from optic disc to *ora serrata*. We observed that a comparable disease process occurred throughout the entire length of the retina along both the superior and inferior meridians. In the normal retina, there is a normal gradient in ONL thickness from central (10-14 nuclei) to peripheral (3-6 nuclei) retina.[33] A similar trend in ONL thickness occurred in young mutant retinas and therefore should not be considered as several different stages of the disease coexisting along the same retinal meridian.

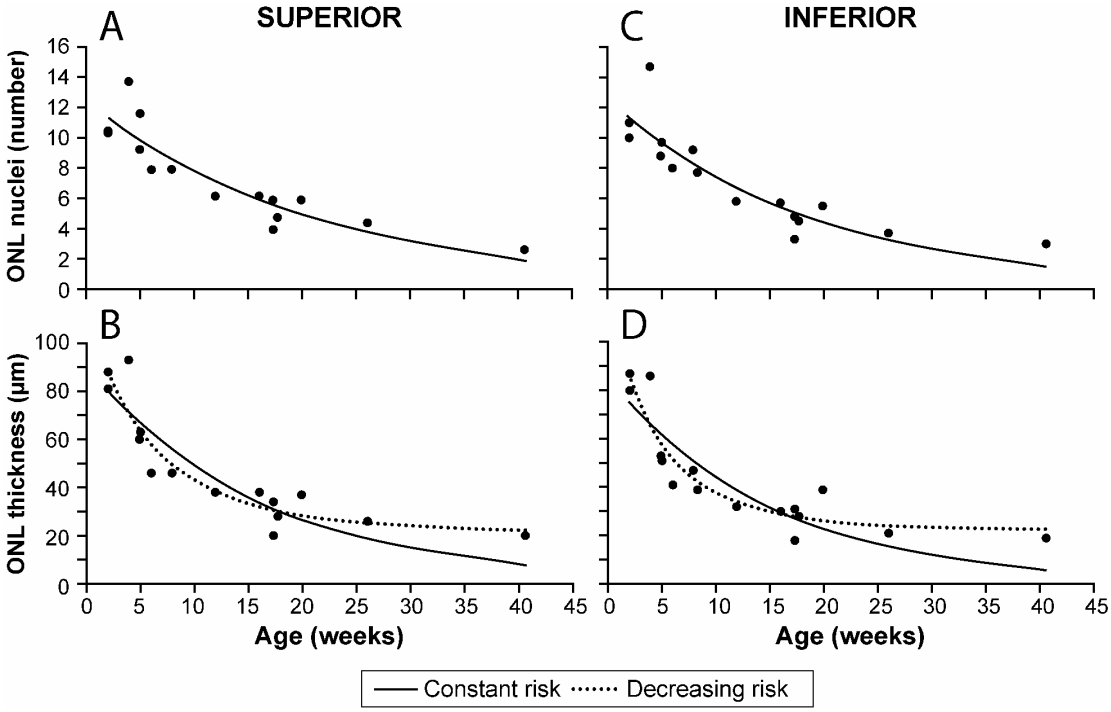

Figure 4.2: Rate of photoreceptor cell loss in mutant retinas as a function of age. ONL thickness was measured as the number of rows of photoreceptor nuclei (**A, C**) or in µm (**B, D**) along both the superior (**A, B**) and inferior (**C, D**) retinal meridians. Reported values are the mean of three measurements taken in the central, midperipheral and peripheral region of the superior or inferior retinal meridian. The kinetics of photoreceptor cell loss are best fit by a model of constant or exponentially decreasing risk of cell death. ONL: outer nuclear layer.

Cell Death

Because of the uniform distribution and rate of disease along the superior and inferior meridians, we determined cell death by using TUNEL assays in sections from the superior meridian. The earliest age when cell death was examined by TUNEL assay was 3.9 weeks, because this was the age when the first morphological signs of disease were detected. Approximately 31 to 48 TUNEL-labeled cells per 1 M μm^2 of ONL were counted. The proportion of photoreceptors undergoing cell death was higher at 5 and 6 weeks, and reached a peak value of more than 300 TUNEL-positive cells per 1 M μm^2 of ONL at 6.7 weeks of age. In normal retinas of 4, 5, and 6 week-old beagles, the number of TUNEL-positive cells per unit area of ONL was significantly lower and did not exceed six per 1 M μm^2 of ONL. At 8 weeks of age, the proportion of photoreceptors undergoing cell death in the mutant retina had decreased to about half that occurring at 6.7 weeks (approximately 150 TUNEL-positive cells per 1 M μm^2 of ONL). At any given time after 12 weeks of age, the proportion of dying photoreceptors was significantly reduced and close to 80 cells / 1 M μm^2 of ONL (Figure 4.3). TUNEL-labeled cells were equally distributed throughout the length of the retina, but it appeared that at the earlier ages, there were more dying cells located in the vitreous half of the ONL. (Figure 4.4 A1) Yet, although, TUNEL-positive photoreceptors were seen in the outer half of the ONL, it was extremely rare before 26 weeks of age to detect any labeling in the outermost row of ONL nuclei where cone somas are located (Figure 4.4 A1, A2). In 26-and 40.6-week-old *XLPRA2* retinas, it was frequent to observe, particularly in the retinal periphery, cone nuclei that were ectopically located in the IS (Figure 4.4 A3). Double fluorescent labeling showed that a few displaced cone nuclei were TUNEL-positive (Figure 4.4 A4). Rare TUNEL-positive cells were also present in the INL and GCL in both mutant and normal young retinas (4-6 weeks), and this was therefore considered a normal finding not associated

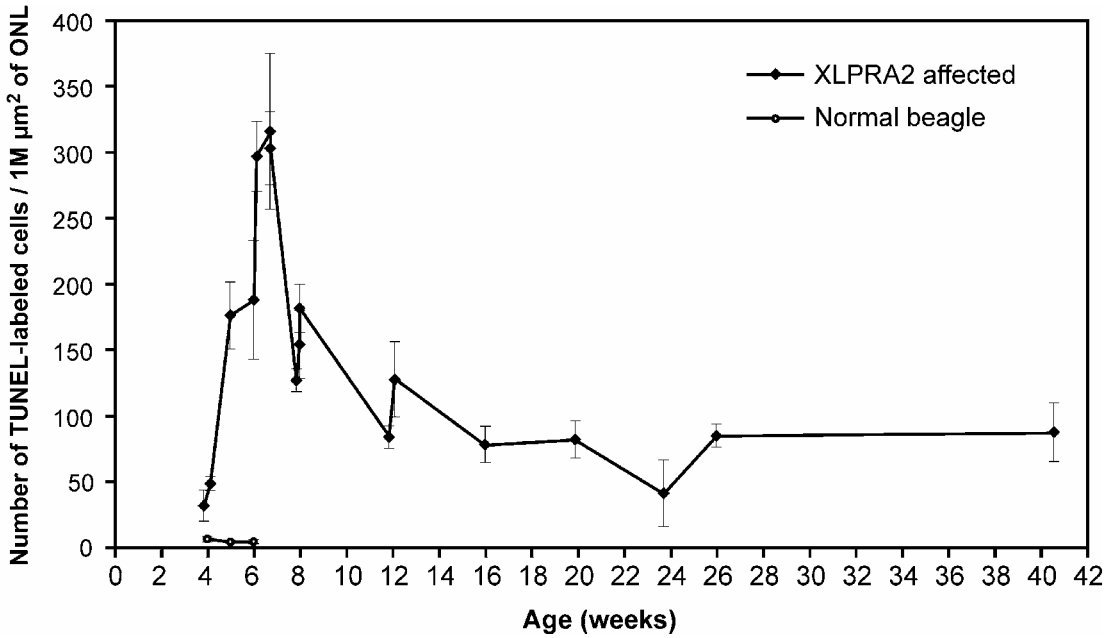

Figure 4.3: Number of TUNEL-labeled photoreceptor cell nuclei per unit area (1 million μm^2) of ONL as a function of age in the superior retinal quadrant of affected and normal dogs. *Symbols* : the mean ± SD of 3 counts made on three sections from the superior retinal meridian of each animal.

with disease. At later time points in the mutants, there was a relative absence of TUNEL-labeling in those layers.

Immunohistochemical analysis of photoreceptors and inner retinal changes with disease.

To further characterize the effects of the disease on the morphology, location, and density of several retinal cell populations, we tested a battery of antibodies that are commonly used as cell-specific markers (see Table 4.2) on retinas of mutants and normal age-matched control subjects.

The integrity of the RPE was evaluated with an antibody directed against RPE65. There was no loss in RPE65-immunoreactivity in 16- and 26-week-old mutant retinas and the numerous phagocytic cells present in the subretinal space were not labeled by the RPE65 antibody (data not shown). Double-fluorescence immunolabeling with rod opsin and human cone arrestin antibodies showed partial mislocalization of the rod photopigment to the ONL as early as 2 weeks of age in mutant retinas (data not shown). Although rod opsin labeling was restricted to the OS in normal subjects (Figure 4.4 B1), distinct staining of the plasma membrane around the rod somas also was visible throughout the entire length and thickness of the ONL in affected dogs at all ages (Figure 4.4 B2). In the 7.9-week-old mutant retina, short rod-opsin-positive neurites originating from rod somas extended into the inner retina (Figure 4.4 B2), and, in older animals, the sprouting was more prominent and extended deeper into the inner retina, reaching the inner plexiform layer (IPL; Figure 4.4 B3; 40.6 weeks of age). In contrast, cone neurite sprouting was not observed at any stages of the disease examined.

To confirm further that these opsin-positive projections were rod neurites, we performed double immunofluorescence labeling with rod opsin and synaptophysin

antibodies (Figures 4.4 C). Anti-synaptophysin labeled both plexiform layers in normal subjects (Figure 4.4 C1), but, in mutant retinas, outer plexiform layer (OPL) labeling was thinned, and punctuate staining in the INL colocalized with the rod-opsin-positive neurites (Figure 4.4 C2). Colocalization occurred at beaded varicosities along the neurites and at their terminals. These had either a bulb-shaped appearance or that of a typical rod spherule (Figure 4.4 C3). Although rod opsin and cone arrestin labeling persisted in the 40.6-week-old affected retina, we observed a decrease in cone arrestin immunoreactivity at the level of the cone axons and pedicles (Figure 4.4 B3) that was first visible at 26 weeks of age. Because of the thinning of the ONL at that age (approx 3 rows of nuclei), the lengths of the remaining rod and cone axons were significantly shorter than in a normal adults. Even though thinning and disruption of the photoreceptor layer caused occasional retinal separation artifacts during tissue fixation and processing in older retinas, distinct rod opsin and arrestin labeling was observed, respectively, in some of the remaining rods and cone OS (Figure 4.4 B3).

To characterize better the two subpopulations of cone photoreceptor cells during the course of disease, we used antibodies raised against short (S)- and medium (M)/long (L)- wavelength cone opsin on retinas at various ages and disease stages. Both S and M/L cone opsin labeling were present in young and older (40.9 weeks) affected dogs. In normal retinas, labeling was restricted to the cone OS (Figures 4.4 D_1, D_3), but in mutant retinas there was partial mislocalization of the two types of cone opsins to the IS, perinuclear area, axon, and pedicles (Figures 4.4 D_2, D_4). Mislocalization of S opsin was observed in some S cones, distributed throughout the entire length of the retina, as early as 3.9 weeks of age. By 6 weeks, S opsin mislocalization was found mainly in some peripheral cones (Figure 4.4 D_2). At later ages S opsin localization was normal. Although the M/L opsin antibody that we used caused some non-specific background staining of the INL and faint labeling of cone

somas and axons, we observed a similar transient and partial mislocalization of the photopigment, particularly in the peripheral retina of 3.9 and 6-week-old affected dogs (Figure 4.4 D_4). At 8 weeks of age, M/L opsin mislocalization was essentially restricted to the perinuclear area of the cones and did not extend into the axons and pedicles; in older animals, M/L opsin localization was normal.

Because we observed OPL thinning and rod neurite sprouting, we decided to use several inner retina cell markers to determine whether photoreceptor disease and degeneration were also associated with inner retinal changes. A variety of antibodies that label subpopulations of horizontal, bipolar, and amacrine cells, as well as Müller cells were tested in either single or double immunofluorescence analysis.

Anti-calbindin antibody labeled horizontal cells and, to a lesser extent, amacrine and RPE cells in both affected and normal retinas at 4 weeks of age. At later time points in disease, immunostaining was predominantly found in horizontal cells somas and processes. This pattern persisted throughout the course of the disease. Because of the variability in the intensity of calbindin-labeling in the dog we were not able to quantify with certainty the number of horizontal cells present throughout the length of a retinal section and compare these counts at different stages of the disease. Nevertheless, we were able to observe in older affected retinas a flattening of their axonal arborization associated with the thinning of the OPL (Figures 4.5 A1-3).

PKCα staining of rod bipolar cells showed that these second-order neurons develop normally (Figure 4.5 B_1) in the diseased retina (data not shown). At 11.9 weeks of age there was a mild reduction in the density of their dendritic arborization, which was followed by progressive shortening and total atrophy at later stages (Figures 4.5 B_2, B_3). By performing double-immunofluorescence experiments with PKCα and Goα (a cell-marker for ON bipolar cells) antibodies, we were able to distinguish rod bipolar cells that coexpress PKCα and Goα from ON-cone bipolar

Figure 4.4: Characterization of photoreceptor cell death and disease in *XLPRA2*.
(**A**) Photoreceptor cell death in *XLPRA2*. (**A1**) TUNEL-labeling (*green*) of rod photoreceptor cells in a 5-week-old affected retina with DAPI nuclear counterstain (*blue*). (**A2**) TUNEL-labeling (*green*) of a cone nucleus in a 40.6-week-old retina (*arrow*). An ectopically located cone nucleus that is not TUNEL-positive is highlighted (*arrowhead*). Cone photoreceptors were labeled with anti-human cone arrestin (*red*), and DAPI (*blue*) was used as a nuclear counterstain. (**A3**) Plastic section from peripheral retina of a 26-week-old retina shows a morphologically normal cone nucleus displaced in the IS (*arrow* and *inset*). (**A4**) TUNEL-labeling (*green*) of a fragmented ectopic cone nucleus (*arrow*) in a 40.6-week-old retina. Cone photoreceptors were labeled with anti-human cone arrestin (*red*), and DAPI (*blue*) was used as a nuclear counterstain.
(**B**) Double immunofluorescent labeling of rod and cones with, respectively, anti-rod opsin (*green*) and anti-human cone arrestin (*red*) in normal (**B1**, 8.1 weeks) and affected (**B2**, **B3**) retinas. (**B2**) In 7.9 week-affected rod opsin was mislocalized to the IS and ONL, and there was early rod neurite sprouting (*arrows*). (**B3**) In a 40.6-week affected, rod opsin-positive neurites extended deep into the inner retina. Rod opsin and cone arrestin expression persisted at this stage of disease, but there was a decrease in cone arrestin immunoreactivity at the level of the cone axons and pedicles, even though the cone IS and OS were present.
(**C**) Double immunofluorescent labeling with anti-rod opsin (*green*) and anti-synaptophysin (*red*) in normal (**C1**) and affected (**C2**, **C3**) retinas. (**C1**) In a 12-week normal retina, both the OPL and IPL were labeled with the synaptophysin antibody. (**C2**) In a 12-week affected retina, there was OPL thinning and punctuate synaptophysin-positive labeling that colocalized with rod opsin-positive neurites (*arrows*). (**C3**) A 40.6-week affected retina. A higher-magnification view showing colocalization of synaptophysin and rod opsin along beaded varicosities of rod neurites (*arrowheads*) and at their terminal ends (*arrows*).
(**D**) Immunofluorescent labeling of cones with anti-S opsin (**D1**, **D2**), and anti-M/L opsin (**D3**, **D4**). (**D1**) In a 4-week normal retina, S opsin labeling was restricted to the OS of S cones. (**D2**) In a 3.9-week affected retina, S opsin was mislocalized to the IS (*horizontal arrows*), soma (*vertical arrows*), and axons (*arrowheads*) of some S cones. (**D3**) In a 6-week normal retina, M/L opsin labeling wass predominantly restricted to the OS of M/L cones, although faint background labeling of the M/L cone somas and axons was present. (**D4**) In a 6-week affected retina, M/L opsin was mislocalized to the somas (*vertical arrows*), axons (*arrowheads*), and pedicles (*oblique arrows*) of most M/L cones in the peripheral retina. Scale Bars: (**A1**) 40 μm; (**A3**) 10 μm; (**A2, A4, B-D**) 20 μm.

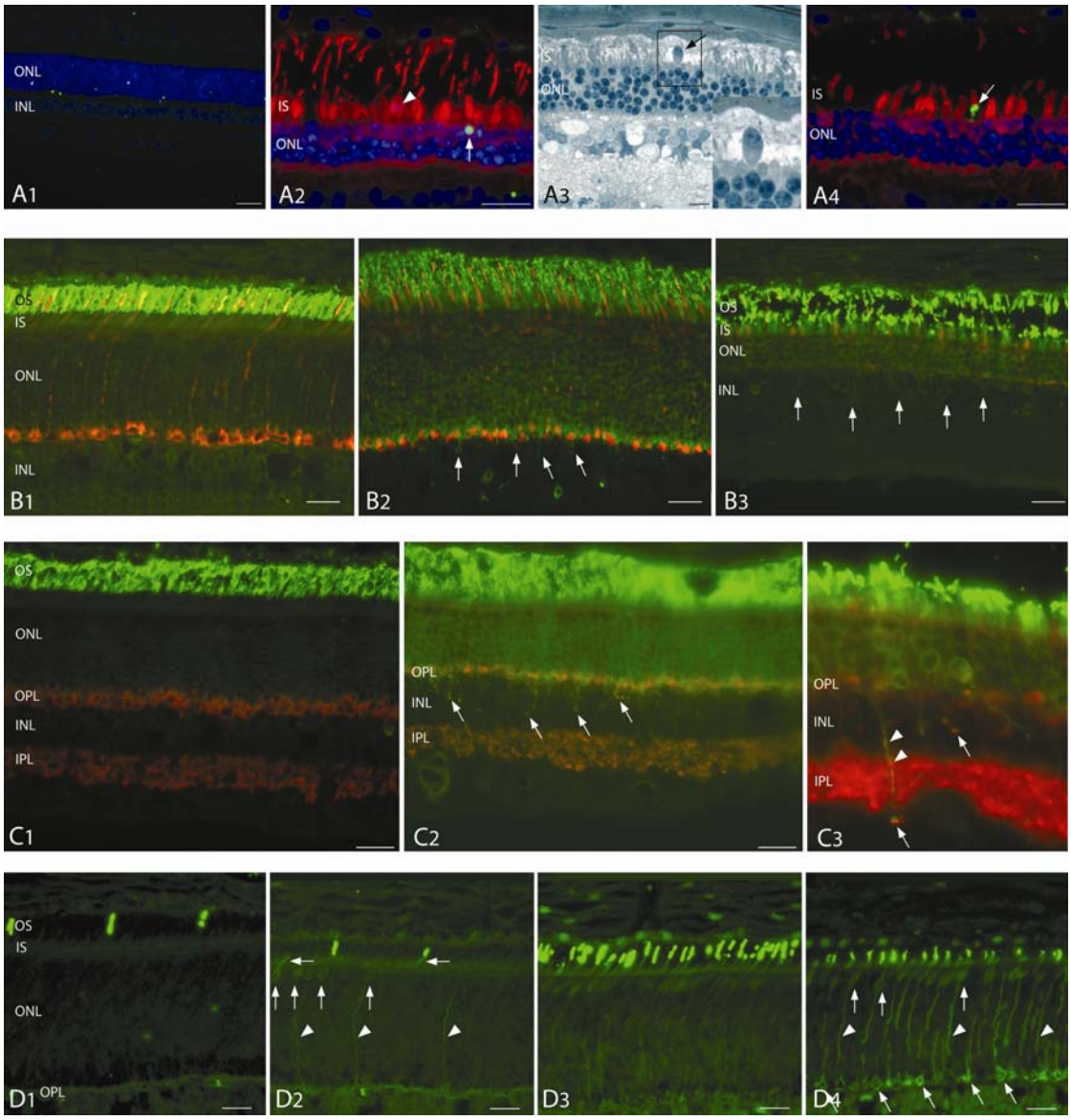
ONL
INL
A1
IS
ONL
A2
IS
ONL
A3
IS
ONL
A4
OS
IS
ONL
INL
B1
B2
OS
IS
ONL
INL
B3
OS
ONL
OPL
INL
IPL
C1
OPL
INL
IPL
C2
OPL
INL
IPL
C3
OS
IS
ONL
D1
OPL
D2
D3
D4

cells that are only Goα immunoreactive (Figure 4.5 C_1). We confirmed that rod bipolar cell dendrites underwent retraction with time, but did not observe a similar change in ON-cone bipolar cells (Figures 4.5 C_2-C_4). Indeed, even at the latest time-point examined (40.6 weeks), there was distinct labeling of the dendrites of cone bipolar cells that appear as a continuous layer in the OPL (Figure 4.5 C_4).

Although we tested a variety of antibodies (anti-ChAT, anti-TH, anti-Dab1, anti-γ-aminobutyric acid [GABA], see Table 2) reported to label different subpopulations of amacrine cells in rodents, we were successful only in detecting GABAergic amacrine cells in the canine retina. Labeling of amacrine cell bodies with the GABA antibody was limited to the central retina in the normal adult, yet intense staining of the IPL laminae was seen throughout the entire retina (Figure 4.5 D1). A similar pattern was seen in the mutant retina until 11.9 weeks of age. Thereafter (26 and 40.6 weeks), there was a significant increase in the number of GABA-immunoreactive amacrine cells. These were located both at the inner border of the INL as well as displaced into the ganglion cell layer (GCL), and they were found all along the length of the retina. In addition, there was a thinning of the IPL and a loss of its normal lamination (Figures 4.5 D2, D3). The GABA antibody also labeled the somas and processes of horizontal cells in the normal canine retina (Figure 4.5 D1). This was also observed in young affected retinas until 8 weeks of age. In the 11.9-week-old mutant retina there was decrease in the intensity of the labeling, and, after 26 weeks, no staining of any horizontal cell was observed, although it was distinct in the normal. (Figure 4.5, compare D1 with D2, D3).

Because the cellular retinaldehyde-binding protein (CRALBP) antibody that we used to examine Müller cells did not label canine retina, we used instead an antibody directed against glutamine synthetase. With this antibody, we found a decrease in Müller cell length in mutant retinas associated with the thinning of the ONL; however,

there was no apparent reduction in their density at 11.9 weeks of age. By 26 weeks of age there was a significant reduction in Müller cell immunoreactivity, and by 40.6 weeks, immunolabeling was almost absent (data not shown). This precluded assessment of glial cell loss at later stages of the disease. GFAP immunolabeling was used to evaluate the level of glial reactivity in Müller cells. GFAP staining was limited to astrocytes and Müller cell end feet in normal retinas of all ages (Figure 4.5 E1) as well as in the youngest (3.9 weeks) retina. A gradual increase in GFAP immunoreactivity began at 5 weeks and peaked at 8–12 weeks of age (Figure 4.5 E2). Minimal GFAP reactivity was seen in older retinas when outer retinal atrophy was more advanced (Figure 4.5 E3).

DISCUSSION

XLPRA2 is a severe canine retinal degeneration of early onset that affects both rods and cones. The two nucleotide deletion in *RPGR ORF15* causes a frameshift in the translation of the putative protein that changes the glutamic-acid-rich ORF15 domain to one containing many arginine residues.[10] This, presumably, causes a toxic gain of function in photoreceptor cells that results in early and severe disease. Although signs of disease are detected in both classes of photoreceptor cells before their complete maturation, rods start dying at a much earlier stage than do cones. Furthermore, early remodeling of the OPL and INL suggest that photoreceptor disease and death alter the synaptic connections with inner retinal neurons.

Evaluation of mutant retinas showed that this was a very early-onset disease characterized by visible abnormalities in both rods and cones before their maturation. At 3.9 weeks of age, the earliest signs of OS disruption were detectable on 1-µm-thick plastic-embedded sections, and mislocalization of rod and cone opsins was seen by immunohistochemistry. At this same age, there was clear evidence of rod

Figure 4.5: Inner retina remodeling in *XLPRA2*.
(**A**) Immunofluorescent labeling of horizontal cells with anti-calbindin (*green*) in normal (**A1**; 12 weeks) and affected (**A2**, **A3**) retinas. In the 12-week affected retina (**A2**), the horizontal cell processes were flattened by the narrowing of the OPL. This was more evident at 40.6 weeks of age, although there was persistent labeling of the horizontal cell somas (**A3**). DAPI (*blue*) was used as a nuclear counterstain.
(**B**) Immunofluorescent labeling of rod bipolar cells with anti-PKCα (*green*) in normal (**B1**, 12 weeks) and affected (**B2**, **B3**) retinas. (**B2**) 12-week affected. There was early retraction of the dendritic arborization of rod bipolar cells (*arrows*); (**B3**) 40.6-week affected. Note the almost total loss of dendritic arborization in OPL (*arrows*). DAPI (*blue*) was used as a nuclear counterstain.
(**C**) Double immunofluorescent labeling of ON bipolar cells with anti-Goα (*red*), and rod bipolar cells with anti-PKCα (*green*) in the normal (**C1**, 12 weeks) and affected (**C2**, **C3**, **C4**) retinas. Rod bipolar cells were colabeled with both Goα and PKCα and appear yellow-orange, whereas ON cone bipolar cells were only labeled with Goα and appeared *red*; (**C1**) 12-week normal. Note the extensive yellow-orange dendritic arborization of rod bipolar cells (*arrowheads*), and just below, the dendrites of ON cone bipolar cells that form a continuous *red* layer (*arrows*). (**C2**) 12-week affected. Note the shortening of the rod bipolar cell dendrites (*arrowheads*) in comparison to the age-matched normal. (**C3**) In a 26-week affected retina, there was an overall decrease in PKCα immunoreactivity in rod bipolar cells and a significant retraction of their dendritic arborization (*arrowheads*). (**C4**) In a 40.6-week affected retina, there was weak labeling of rod bipolar cell somas and axons with PKCα and complete retraction of dendrites. There was persistence of Goα-IR in rod bipolar and ON cone bipolar cells, as well as the presence of the cone bipolar cell dendrites (*arrows*).
(**D**) Immunofluorescent labeling with anti-GABA in normal (**D1**, 24 weeks) and affected (**D2**, **D3**) retinas. (**D1**) GABA-IR was present in the mid-peripheral retina in several laminae of the IPL and in horizontal cells (*arrowheads*) and their processes. There was no labeling of amacrine cells, other than in the central region of the normal retina. (**D2**) 26 week affected midperipheral retina. There was loss of the IPL lamination, but increased immunoreactivity of putative amacrine cells located at the vitreal border of the INL and displaced in the GCL (*arrows*). There was also loss of horizontal cell labeling. (**D3**) In a 40.6 week affected mid peripheral retina, IPL thickness was significantly reduced, and GABA-IR was increased in amacrine cells (*arrows*).
(**E**) Immunofluorescent labeling of Müller cells with GFAP (*red*) in normal (**E1**, 12 weeks) and affected (**E2**, **E3**) retinas. (**E1**) 12-week normal. GFAP labeling was weak and limited to astrocytes and Müller cell end feet (*arrow*). (**E2**) In a 12-week affected retina, intense GFAP-IR was present throughout the entire length of Müller cells. (**E3**) In a 40.6-week affected, GFAP labeling was almost absent. Scale Bars: 20 μm.

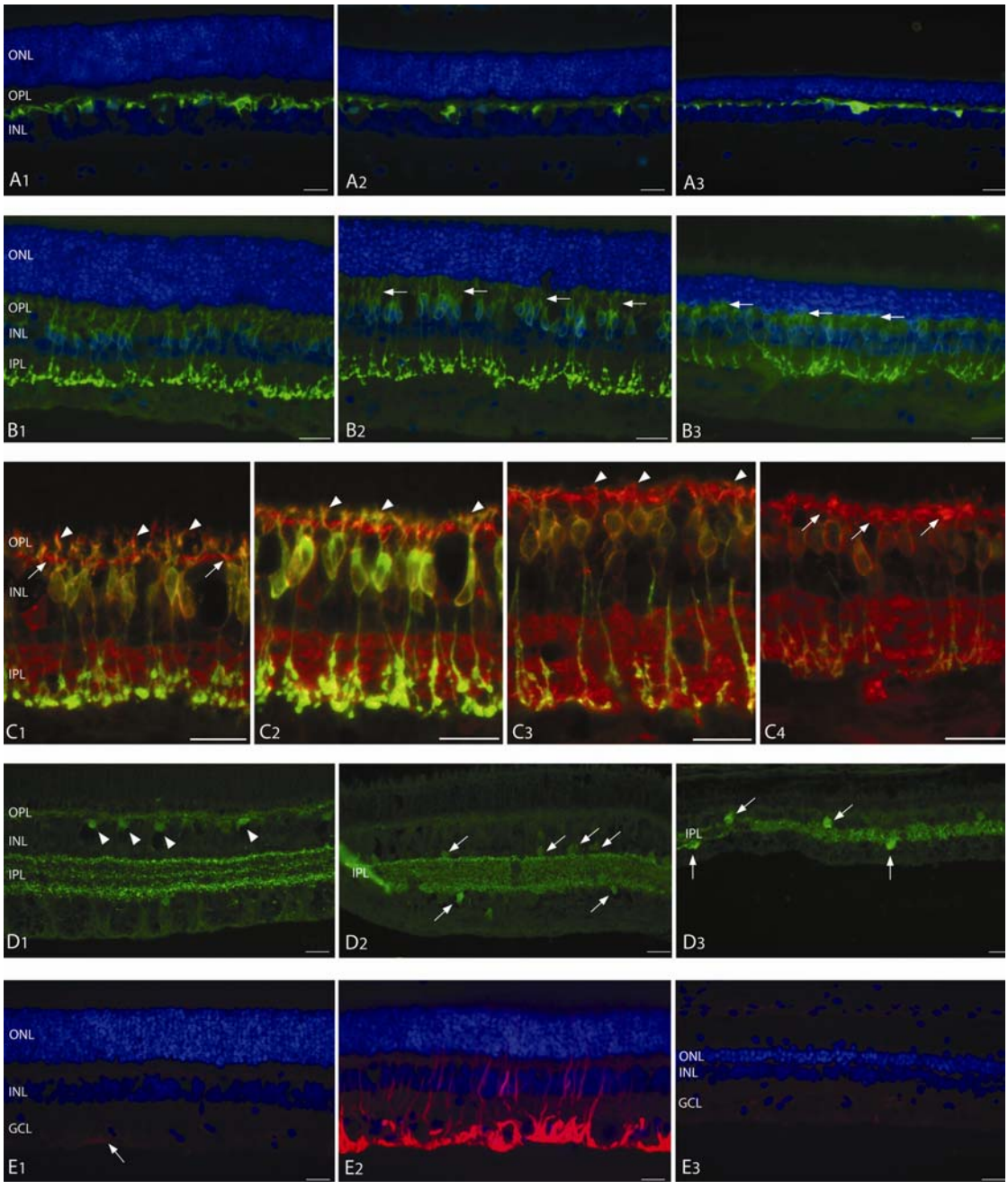
ONL
OPL
INL
A1
A2
A3
ONL
OPL
INL
IPL
B1
B2
B3
OPL
INL
IPL
C1
C2
C3
C4
OPL
INL
IPL
D1
IPL
D2
IPL
D3
ONL
INL
GCL
E1
E2
ONL
INL
GCL
E3

photoreceptors undergoing cell death. We confirmed that this differed from the normal developmental cell death process, which was found at 2 weeks of age in both normal and mutant retinas (data not shown). In the mutant retina the number of TUNEL-labeled photoreceptor cells was significantly higher than in age-matched control subjects. Over the ensuing weeks, there was an increase in the proportion of TUNEL-labeled photoreceptors that resulted in a peak of cell death between 6 and 7 weeks. After this early burst of cell death, the rate was significantly decreased after 12 weeks of age. Our findings are similar to that reported in the *Rdy* cat, a model of autosomal dominant rod/cone dysplasia, in which an early onset of photoreceptor death begins at 5 weeks of age and peaks at about 9 weeks of age.[22] Our results clearly suggest that the risk of death in a single photoreceptor cell is not the same at all ages and that the mathematical model of a constant or decreasing risk of photoreceptor death, as suggested by Clarke et al.[17], may not be applicable to this class of *RPGR* mutations, at least during the initial course of the disease.

Although the data on the ONL thickness (Figure 4.2, Table 4.4) are best fit with an exponentially declining curve that would be consistent with the kinetics of a constant or decreasing risk of photoreceptor death in *XLPRA2*, the TUNEL data (Figure 4.3) do not support this model. We saw (Figure 4.3) two distinct phases of cell death. An initial phase, from 3.9 to 7 weeks of age, showed an increased risk for photoreceptors to die (peak of TUNEL-positive cells at 6 to 7 weeks of age). This was followed by a second phase of rapid (from 7 to 12 weeks) and then a more gradual decrease (after 12 weeks) in the number of TUNEL-positive cells per unit area of ONL. It is therefore possible that the limited number of observations between 3.9 and 7 weeks of age fails to show an early sigmoidal decline in photoreceptor cell number, which we would have expected to observe with an increased risk of cell death. This initial phase of photoreceptor death does not appear to be unique to *XLPRA2*. Indeed,

a group of investigators used TUNEL assay to look at the kinetics of cell death in the *rd* mouse and recorded a similar increase in photoreceptor death that reached its peak by 16 days of age.[34] Not surprisingly, in their study, Clarke et al. reported that the *rd* mouse was the only animal model for which an increased risk of cell death could not be excluded, since the data fit equally well to mathematical models of constant and exponentially increasing risk.[17,35]

Several hypotheses may explain this biphasic pattern of cell death in *XLPRA2*: (1) the coexistence of two populations of photoreceptor cells that differ in their response to a same death stimulus. (2) the existence of a single population of photoreceptors that acquire an increased resistance to death after the early degeneration of some cells. Supporting this hypothesis is evidence for the endogenous release of survival factors (bFGF, CNTF) in the degenerating retina that protect the remaining photoreceptors from undergoing cell death[36,37]; and (3) the existence of a single population of photoreceptors that is affected at different ages by two distinct cell death stimuli. Based on the toxic gain-of-function hypothesis as being causal to the disease mechanism,[10] it may be that during photoreceptor maturation, rods are particularly sensitive to the toxicity of the mutant RPGR protein. This may lead to a burst of rod photoreceptor death, the release of survival factors, and the acquired resistance of the remaining photoreceptors to the endogenous mutant toxic protein. The second phase of death, after 12 weeks of age, could then be the result of either an incomplete resistance to the toxic mutant RPGR protein, or of sensitivity to the absence of the normal isoform. In this case, photoreceptor cells may be dying through a mechanism caused by the loss of function of the normal RPGR retinal isoform. If such is the case, this may open the possibility of rescuing photoreceptor cells that have survived the first phase of cell death in *XLPRA2* through a gene replacement approach.

The mislocalization of opsins in both rods and cones at the early stages of the disease suggests that *RPGR* is expressed in both populations of photoreceptors, and lends additional support to the hypothesis that RPGR is involved in the trafficking of proteins from the IS to the OS, or in their retention in the OS.[13] A similar mislocalization of both rod and cone opsins has been reported recently in a human carrier (Adamian M, et al. *IOVS* 2005;46:ARVO E-Abstract 3400), yet, in the mouse, only cone opsins appear to mislocalize.[8] In the present study, we found early signs of cone disease both in plastic-embedded sections and in cryosections treated for immunohistochemistry; however, we did not detect any features of cone cell death before the age of 26 weeks. This raises the question of whether the mechanism of cone death is directly caused by the *RPGR* mutation or is non-cell-autonomous and secondary to rod degeneration. In animal models of retinitis pigmentosa caused by mutations in rod-specific genes, the delayed cone loss is thought to be caused by the death of rods that induces structural alterations in the photoreceptor layer and ONL, the release of toxic by-products, and/or a decrease in the secretion of cone survival factors.[38,39]

Contrary to implications of the results in immunocytochemical studies on human retinas with advanced stages of retinitis pigmentosa,[23,40] inner retinal remodeling is not, at least in the dog, a late response to photoreceptor degeneration. Our observations showed that synaptic connectivity in the OPL was altered at early stages of the disease. Rod neurite sprouting was first apparent within 1 to 2 weeks after the peak of photoreceptor cell death that occurred at approximately 7 weeks of age. Although this is the first report of rod neurite sprouting in the canine retina, it has been observed in two other animal models of retinitis pigmentosa: the rhodopsin transgenic pig,[41] and the *Rdy* cat with autosomal dominant rod/cone dysplasia.[22] Neurite sprouting of cones has been described in the *rd* mouse as an early-onset

change that starts at P8, when rod degeneration begins.[42] Neither this abnormality, nor elongation and branching of cone axons as previously described in humans[40] were observed in the *XLPRA2* retina at any studied age, but these changes may occur in much older animals with more advanced disease. Concomitant to the onset of rod neurite sprouting, there was a loss in synaptophysin immunoreactivity of the OPL as early as 7.9 weeks of age. This illustrates the possible rapid and early disorganization in synaptic connectivity that could seriously hamper retinal function at a stage of disease when photoreceptor loss is limited.

Another early change that occurred throughout the entire thickness of the neuroretina was the increased reactivity of Müller cells. An increase in GFAP labeling of Müller cells occurred approximately two weeks before the peak of photoreceptor cell death and reached its highest level in the following weeks. These glial cells, which somas are located in the INL, have apical radial processes extending to the external limiting membrane (ELM). It is therefore possible that Müller cells detect early structural or chemical modifications in the photoreceptor layer and/or ONL caused by the degeneration of photoreceptor cells and relay this change in the outer retina environment to deeper retinal layers. GFAP reactivity in Müller cells had decreased at 26 weeks of age and was like normal by 40.6 weeks. These findings are different from those reported in human retinas with advanced disease where GFAP reactivity persists.[43] This difference may be explained by the fact that we did not collect retinas from the very advanced stages of disease. Thus, it may be that GFAP reactivity in Müller cells occurs both at the onset of photoreceptor degeneration and during the terminal stages of retina atrophy.

After these early changes in the inner retina, there was progressive retraction of rod bipolar cell dendrites that began by approximately 12 weeks of age. Contrary to what had been described in the *rd* mouse,[44] rod bipolar cells developed dendritic

arborizations. This may be because in *XLPRA2*, unlike in the *rd* mouse, most photoreceptor cells reach a stage of functional and structural maturation, albeit abnormal, that allows the formation of synapses with second-order neurons. We did not observe any significant loss in the arborization of ON-cone bipolar cells, as occurs in the *rd* mouse at later stages of the disease, when cones undergo cell death.[25] The most probable explanation of this difference is that, at the latest time point that we examined ON-cone bipolar cells (40.6 weeks), there was still a significant number of cone photoreceptors in the ONL that had not degenerated. This may suggest that the cone-mediated pathway remains functional at more advanced stages of the disease. Although more extensive electroretinographic testing is needed to verify this hypothesis, our previous study has shown the presence of robust cone signals at a time when there is significant loss of rod-mediated responses.[10]

Information on the histopathologic changes that occur in retinas of human patients with *RPGR* exon ORF15 mutations has currently only been reported in a carrier.[12] Yet, it appears that frameshift mutations in *RPGR* exon ORF15 have a comparably severe phenotype in both canine and human retinas.

The findings reported in this study have several important implications for the development of therapeutic approaches for retinal degeneration in humans. Among these, the use of survival factors (e.g., ciliary neurotrophic factor [CNTF] and brain-derived neurotrophic factor [BDNF]) as well as a gene-silencing approach, via ribozymes or siRNA, are currently being investigated in our laboratory. The results of this present study suggest that a first strategy should consist in initiating therapy before the burst of photoreceptor cell death that occurs in the dog between 6 and 7 weeks of age. Delivering the therapeutic agent at approximately 4 weeks of age may prevent or delay the onset of photoreceptor degeneration. Intraocular injection of survival factors that are immediately biologically active is feasible at such a young

age. Alternatively, another potential strategy would be to target the rescue of the photoreceptor cells that survived the initial burst of cell death. Indeed, we have shown that after this event, the rate of cell death is considerably slowed down, and that even in the most advanced stages of disease, the morphology of the remaining photoreceptor cells is reasonably preserved. We have observed that some photoreceptors maintain their IS and OS and continue to express proteins involved in the phototransduction pathway unlike what has been reported in humans with more advanced retinitis pigmentosa caused by rhodopsin gene mutations.[30] From this perspective, 12 weeks of age may be an optimal time-window to initiate therapy because, at that age, approximately 60% of photoreceptor cells remain.

Another important aspect that future studies should address is whether rescuing photoreceptor cells also allows reversal of inner retinal changes that occur secondary to rod and cone disease and degeneration. Modification of the inner retina after photoreceptor degeneration does not appear to be dependent on the genetic cause of the disease. Indeed, in addition to the two-nucleotide deletion in *RPGR* ORF15 that occurs in the *XLPRA2* dog, recent studies have shown inner retina remodeling in the *rd* and *crx-/-* mice, two models of retinal degeneration caused, respectively, by a mutation in the *PDE6B* and *CRX* genes.[24,44] In addition to these morphologic changes, a switch in neurotransmitter sensitivity of rod bipolar cells has been demonstrated in the *rd* mouse.[45] All these recent findings suggest, that if a similar phenomenon occurs in the human with early stages of retinal degeneration, then novel therapeutic approaches must to be evaluated not solely on their protective effect on photoreceptor cells, but also on their capacity in maintaining functional synaptic connections between photoreceptor cells and inner retinal neurons.

In conclusion, we have characterized the structural changes that occur in the *XLPRA2* retina, an early-onset canine model of X-linked retinitis pigmentosa caused by a microdeletion in *RPGR* exon ORF15 with resultant frameshift. This is a valuable spontaneous animal model that may provide a better understanding of the retinal function of the RPGR protein and the pathogenic mechanisms that lead to photoreceptor death. It also may provide a tool to assess the *in vivo* efficacy of novel therapies.

REFERENCES

1. Yokoyama A, Maruiwa F, Hayakawa M, et al. Three novel mutations of the RPGR gene exon ORF15 in three Japanese families with X-linked retinitis pigmentosa. *Am J Med Genet* 2001;104:232-238.

2. Lorenz B, Andrassi M, Kretschmann U. Phenotype in two families with RP3 associated with RPGR mutations. *Ophthalmic Genet* 2003;24:89-101.

3. Sharon D, Sandberg MA, Rabe VW, et al. RP2 and RPGR mutations and clinical correlations in patients with X-linked retinitis pigmentosa. *Am J Hum Genet* 2003;73:1131-1146

4. Vervoort R, Lennon A, Bird AC, et al. Mutational hot spot within a new RPGR exon in X-linked retinitis pigmentosa. *Nat Genet* 2000;25:462-466.

5. Jacobson SG, Buraczynska M, Milam AH, et al. Disease expression in X-linked retinitis pigmentosa caused by a putative null mutation in the RPGR gene. *Invest Ophthalmol Vis Sci* 1997;38:1983-1997.

6. Mears AJ, Hiriyanna S, Vervoort R, et al. Remapping of the RP15 locus for X-linked cone-rod degeneration to Xp11.4-p21.1, and identification of a de novo insertion in the RPGR exon ORF15. *Am J Hum Genet* 2000;67:1000-1003.

7. Ayyagari R, Demirci FY, Liu J, et al. X-linked recessive atrophic macular degeneration from RPGR mutation. *Genomics* 2002;80:166-171.

8. Hong DH, Pawlyk BS, Shang J, et al. A retinitis pigmentosa GTPase regulator (RPGR)-deficient mouse model for X-linked retinitis pigmentosa (RP3). *Proc Natl Acad Sci U S A* 2000;97:3649-3654.

9. Hong DH, Pawlyk BS, Adamian M, et al. Dominant, gain-of-function mutant produced by truncation of RPGR. *Invest Ophthalmol Vis Sci* 2004;45:36-41.

10. Zhang Q, Acland GM, Wu WX, et al. Different RPGR exon ORF15 mutations in Canids provide insights into photoreceptor cell degeneration. *Hum Mol Genet* 2002;11:993-1003.

11. Zeiss CJ, Acland GM, Aguirre GD. Retinal pathology of canine X-linked progressive retinal atrophy, the locus homologue of RP3. *Invest Ophthalmol Vis Sci* 1999;40:3292-3304.

12. Aguirre GD, Yashar BM, John SK, et al. Retinal histopathology of an XLRP carrier with a mutation in the RPGR exon ORF15. *Exp Eye Res* 2002;75:431-443.

13. Hong DH, Pawlyk B, Sokolov M, et al. RPGR isoforms in photoreceptor connecting cilia and the transitional zone of motile cilia. *Invest Ophthalmol Vis Sci* 2003;44:2413-2421.

14. Mavlyutov TA, Zhao H, Ferreira PA. Species-specific subcellular localization of RPGR and RPGRIP isoforms: implications for the phenotypic variability of congenital retinopathies among species. *Hum Mol Genet* 2002;11:1899-1907.

15. Acland GM, Aguirre GD. Retinal degenerations in the dog: IV. Early retinal degeneration (erd) in Norwegian elkhounds. *Exp Eye Res* 1987;44:491-521.

16. Farber DB, Danciger JS, Aguirre G. The beta subunit of cyclic GMP phosphodiesterase mRNA is deficient in canine rod-cone dysplasia 1. *Neuron* 1992;9:349-356.

17. Clarke G, Collins RA, Leavitt BR, et al. A one-hit model of cell death in inherited neuronal degenerations. *Nature* 2000;406:195-199.

18. Acland GM, Aguirre GD, Ray J, et al. Gene therapy restores vision in a canine model of childhood blindness. *Nat Genet* 2001;28:92-95.

19. Zhang Y, Li A, Zhu X, et al. Cone arrestin expression and induction in retinoblastoma cells. Proceedings of the Ninth International Symposium on retinal Degeneration 2001;309-319.

20. Zhang Q, Beltran WA, Mao Z, et al. Comparative analysis and expression of CLUL1, a cone photoreceptor-specific gene. *Invest Ophthalmol Vis Sci* 2003;44:4542-4549.

21. Adamus G, Zam ZS, Arendt A, et al. Anti-rhodopsin monoclonal antibodies of defined specificity: characterization and application. *Vision Res* 1991;31:17-31.

22. Chong NHV, Alexander RA, Barnett KC, et al. An immunohistochemical study of an autosomal dominant feline rod/cone dysplasia (Rdy cats). *Exp Eye Res* 1999;68:51-57.

23. Fariss RN, Li ZY, Milam AH. Abnormalities in rod photoreceptors, amacrine cells, and horizontal cells in human retinas with retinitis pigmentosa. *Am J Ophthalmol* 2000;129:215-223.

24. Pignatelli V, Cepko CL, Strettoi E. Inner retinal abnormalities in a mouse model of Leber's congenital amaurosis. *J Comp Neurol* 2004;469:351-359.

25. Strettoi E, Porciatti V, Falsini B, et al. Morphological and functional abnormalities in the inner retina of the rd/rd mouse. *J Neurosci* 2002;22:5492-5504.

26. Haverkamp S, Haeseleer F, Hendrickson A. A comparison of immunocytochemical markers to identify bipolar cell types in human and monkey retina. *Vis Neurosci* 2003;20:589-600.

27. Mosinger JL, Yazulla S, Studholme KM. GABA-like immunoreactivity in the vertebrate retina: a species comparison. *Exp Eye Res* 1986;42:631-644.

28. Ochiishi T, Terashima T, Sugiura H, et al. Immunohistochemical localization of Ca2+/calmodulin-dependent protein kinase II in the rat retina. *Brain Res* 1994;634:257-265.

29. Mitrofanis J, Maslim J, Stone J. Ontogeny of catecholaminergic and cholinergic cell distributions in the cat's retina. *J Comp Neurol* 1989;289:228-246.

30. John SK, Smith JE, Aguirre GD, et al. Loss of cone molecular markers in rhodopsin-mutant human retinas with retinitis pigmentosa. *Mol Vis* 2000;6:204-215.

31. Aguirre GD, Rubin LF, Bistner SI. Development of the canine eye. *Am J Vet Res* 1972;33:2399-2414.

32. Miller WW, Albert RA, Boosinger TR, et al. Postnatal development of the photoreceptor inner segment of the retina in dogs. *Am J Vet Res* 1989;50:2089-2092.

33. Aguirre G, O'Brien P. Morphological and biochemical studies of canine progressive rod-cone degeneration. 3H-fucose autoradiography. *Invest Ophthalmol Vis Sci* 1986;27:635-655.

34. Zeng HY, Zhu XA, Zhang C, et al. Identification of sequential events and factors associated with microglial activation, migration, and cytotoxicity in retinal degeneration in rd mice. *Invest Ophthalmol Vis Sci* 2005;46:2992-2999.

35. Clarke G, Lumsden CJ, McInnes RR. Inherited neurodegenerative diseases: the one-hit model of neurodegeneration. *Hum Mol Genet* 2001;10:2269-2275.

36. Wen R, Cheng T, Song Y, et al. Continuous exposure to bright light upregulates bFGF and CNTF expression in the rat retina. *Curr Eye Res* 1998;17:494-500.

37. Liu C, Peng M, Laties AM, et al. Preconditioning with bright light evokes a protective response against light damage in the rat retina. *J Neurosci* 1998;18:1337-1344.

38. Mohand-Said S, Deudon-Combe A, Hicks D, et al. Normal retina releases a diffusible factor stimulating cone survival in the retinal degeneration mouse. *Proc Natl Acad Sci U S A* 1998;95:8357-8362.

39. Leveillard T, Mohand-Said S, Lorentz O, et al. Identification and characterization of rod-derived cone viability factor. *Nat Genet* 2004;36:755-759.

40. Li ZY, Kljavin IJ, Milam AH. Rod photoreceptor neurite sprouting in retinitis pigmentosa. *J Neurosci* 1995;15:5429-5438.

41. Li ZY, Wong F, Chang JH, et al. Rhodopsin transgenic pigs as a model for human retinitis pigmentosa. *Invest Ophthalmol Vis Sci* 1998;39:808-819.

42. Fei Y. Cone neurite sprouting: An early onset abnormality of the cone photoreceptors in the retinal degeneration mouse. *Mol Vis* 2002;8:306-314.

43. Milam AH, De Castro EB, Smith JE, et al. Concentric retinitis pigmentosa: clinicopathologic correlations. *Exp Eye Res* 2001;73:493-508.

44. Strettoi E, Pignatelli V. Modifications of retinal neurons in a mouse model of retinitis pigmentosa. *Proc Natl Acad Sci U S A* 2000;97:11020-11025.

45. Varela C, Igartua I, De la Rosa EJ, et al. Functional modifications in rod bipolar cells in a mouse model of retinitis pigmentosa. *Vision Res* 2003;43:879-885.

CHAPTER FIVE

CILIARY NEUROTROPHIC FACTOR (CNTF) FAILS TO RESCUE PHOTORECEPTORS AND CAUSES PERIPHERAL REMODELING IN *RPGR* MUTANT RETINA.

INTRODUCTION

Retinitis pigmentosa (RP) is a genetically heterogeneous group of diseases that constitutes one of the leading causes of blindness worldwide, with an incidence of approximately 1: 4,000.[1,2] Despite the identification over the past 20 years of more than 50 genes responsible for RP (http://www.sph.uth.tmc.edu/Retnet/), currently there is no treatment available that can either prevent, or slow-down the course of photoreceptor cell death. A promising therapeutic approach, for which proof of principle has been demonstrated in various animal models, is the use of corrective gene therapy.[3,4] Yet, such a strategy requires the identification of the mutated gene, and is therefore aimed at targeting diseases in a gene-specific manner.

An approach that could potentially bypass the inherent limitation of gene-based therapy is the use of neuroprotective agents that can rescue photoreceptors regardless of the genetic and/or environmental causes of the retinal degeneration. Over the past 15 years, numerous survival factors have been tested in a variety of animal models of RP (e.g. see [5-7]). Among these agents, ciliary neurotrophic factor (CNTF) has been shown to rescue photoreceptors in several rodents and large animal models (for review see [8]). Because of the inability for CNTF to cross the blood-retina barrier following systemic administration, the necessity for sustained bioavailablity of the agent in the eye, and the ocular side-effects associated with bolus intravitreal injection, a long-term intraocular delivery system has been developed.[9] This encapsulated cell-

based technology (ECT) allows for the continuous release of small quantities of CNTF into the vitreous, and was evaluated in experimental animal models,[10,11] and more recently in Phase I clinical trial in humans.[12]

Previous work has shown that CNTF delivered through intravitreal injections (Pearce-Kelling, unpublished study), or by means of an ECT device,[10] rescues photoreceptors in the *rcd1* dog, an early and rapidly progressing large animal model of RP caused by a stop mutation in *PDE6B.* The purpose of the present study was to determine whether intravitreal injections of recombinant human CNTF could provide a similar neuroprotective effect in *XLPRA2,* an early onset model of X-linked RP caused by a frameshift mutation in *RPGR* exon ORF15.[13] Recently, we reported the morphologic retinal changes, and the kinetics of photoreceptor cell death, that occur during the course of this disease.[14] Death of rods occurs in a biphasic manner, beginning as early as 4 weeks of age, and reaching a peak at 6-7 weeks. Following this initial burst, the rate of cell death is considerably slowed down, yet persists at an approximately constant rate for at least 9 months.

Based on these findings, the initial phase of cell death was selected as a time-window to evaluate the neuroprotective effect of CNTF. Results show that intravitreal injections of CNTF at the onset and/or peak of cell death do not provide any significant rescue in *XLPRA2,* but cause prominent remodeling in the peripheral retina.

METHODS

Expression and purification of recombinant CNTF protein

The open reading frame of human *CNTF* cDNA was PCR-cloned into the pQE30 expression vector (Qiagen, Valencia, CA), and fused to a 6x His tag at the amino-terminus to generate plasmid pQE-CNTF. Recombinant human CNTF protein was expressed in *E. coli* (XL-blue, Stratagene, La Jolla, CA), and purified by immobilized-

metal affinity chromatography on Ni-NTA Agarose columns (Qiagen) under native conditions. Eluted protein was buffer-exchanged to phosphate buffered saline (PBS), and the protein concentration determined by the BCA protein assay (Pierce, Rockford, IL). The CNTF solution was then diluted with PBS to a concentration of 0.4 µg/µl, sterile filtered (Acrodisc Syringe filter 0.2 µm, Pall Corporation, Ann Harbor, MI), and aliquots of 30 µl (12 µg) were stored at -80°C.

Animals

A total of 16 affected *XLPRA2*, 3 affected *rcd1*, and 1 non-mutant dog was used for this study. All animals were bred and housed at the Retinal Disease Studies Facility (RDSF, University of Pennsylvania, New Bolton Center, Kennett Square, PA). Their genotype was determined either from the known status of their progenitors, or from genetic testing for the disease-causing mutation.[13,15] All animals underwent an initial ocular examination that confirmed the absence of clinically evident abnormalities. Twelve *XLPRA2* dogs were used to evaluate the neuroprotective effect of CNTF on photoreceptors, and the animals were allocated to one of the following treatment groups:

- Treatment Group #1 (n = 3): one single injection of CNTF at 4 weeks of age (see below), termination at 8 weeks of age (Inj. 4wk; Ter. 8 wk).
- Treatment Group #2 (n = 3): injection of CNTF at 4 and 8 weeks of age, termination at 12 weeks of age (Inj. 4 & 8 wk; Ter. 12 wk).
- Treatment Group #3 (n = 3): injection of CNTF at 7 and 10 weeks of age, termination at 14 weeks of age (Inj. 7 & 10 wk; Ter. 14 wk.).
- Treatment Group #4 (n = 3): one single injection of CNTF at 12 weeks, termination at 15.6 weeks of age (Inj. 12 wk; Ter. 15.6 wk).

As positive controls for the biological activity of CNTF, we treated 3 *rcd1* dogs (*rcd1* control goup) following a protocol that achieves photoreceptor rescue in this model (CNTF injection at 7 and 10 weeks of age, termination at 14 weeks of age). This work, reported in abstract form but never published, served as a basis for choosing the dose of CNTF that was administered in this study, and was evaluated in *XLPRA2* dogs (treatment Group #3). A single non-mutant dog also was treated in the same way to verify whether any potential CNTF-mediated biological effects are disease-specific, or also occur in the physiologically normal retina.

Because we observed marked peripheral remodeling in the retinas of *XLPRA2* dogs treated with CNTF, a separate set of studies was carried out to further characterize these alterations. For this, 4 affected *XLPRA2* dogs were used following protocols detailed below (see under “Histologic procedures”, and “Cell proliferation assays” sections).

All intravitreal injections were performed in eyes that had their pupils previously dilated by topical application of atropine, phenylephrine and tropicamide. Under general anesthesia (isoflurane), dogs underwent a 1 minute massage of their globes to reduce the intraocular pressure (IOP). A 29-gauge needle mounted on an insulin syringe was then inserted in the supero-temporal quadrant approximately 5 mm behind the limbus, and the tip was directed towards the center of the vitreous to inject in the left eye (OS) 12 µg of CNTF in 0.1 M PBS (Total volume injected:30 µl). The right eye (OD) served as a control, and was injected with 30 µl of the PBS diluent. Immediately following the injections, both eyes were examined by slit-lamp biomicroscopy and indirect ophthalmoscopy to verify that no lesions were caused to the lens and/or retina during the procedure. All animals underwent additional ocular examinations 2-4 days following the intravitreal injections and subsequently, at least once a week, for the remaining of the treatment period. This included IOP

measurements by applanation tonometry (TonoPen XL, Medtronic Ophthalmics, Jacksonville, FL). At the end of the treatment period, the animals were euthanatized by intravenous injection of pentobarbital sodium, enucleated, and the eyes processed as indicated below. All procedures involving animals were done in compliance with the ARVO Statement for the Use of Animals in Ophthalmic and Vision Research.

Histologic procedures

The eyes of the 16 dogs (12 *XLPRA2*, 3 *rcd1*, 1 non-mutant) used in the assessment of CNTF's photoreceptor rescue effect were processed after enucleation as previously published.[14] A slit was made at the level of the *ora serrata*, and the entire globe was fixed for 3 hours in 4% paraformaldehyde in 0.1 M PBS at 4°C. The posterior segment was isolated and fixed for an additional 24 hours at 4°C in 2% paraformaldehyde. The tissue then was trimmed into four pieces that extended from the optic disc to the *ora serrata* along the superior, inferior, nasal, and temporal meridians. Following sequential cryoprotection for 24 hours in solutions of 15% and 30% sucrose in PBS at 4°C, the tissues were embedded in optimal cutting temperature (OCT) medium. Cryosections were cut at 7 or 10 µm thickness, air-dried, and stained with hematoxylin & eosin (H&E), or used for immunohistochemistry (see below). The anterior segments of some animals were post-fixed in Bouin's solution, and paraffin embedded. Paraffin sections were cut at 6 µm thickness, H&E stained, and used to examine the pathology in the cornea, iris and lens.

Retinal cryosections stained with H&E were examined by light microscopy (Axioplan; Carl Zeiss Meditec GmbH, Oberkochen, Germany) in contiguous fields extending from the optic disc to the *ora serrata* with 10X and 40X objectives. For each animal, quantitative evaluation of the outer nuclear layer (ONL) thickness was done on sections from the 4 meridians of both eyes at 3 specific locations: S1, 2000 ±

500 µm from the optic disc; S3, 2000 ± 500 µm from the *ora serrata*; and S2, midway ± 500 µm between these 2 points. At each of these sites, the number of rows of nuclei in the ONL was counted in at least 3 representative areas and averaged. The field that was viewed with the 40X objective covered a retinal length of 290 µm. Significant alterations in the ONL, that included an abnormal increase in thickness, were observed in the retinal periphery of CNTF-injected eyes. Since these changes frequently involved and extended beyond site S3, we excluded ONL data collected at this site, and restricted the analysis of photoreceptor rescue to the central (S1) and mid-peripheral (S2) regions of the retina. For each quadrant, the average ONL thickness (mean of ONL thickness at S1 and S2) was calculated, and compared to that of the contralateral eye. The paired Student t-test was used to analyze the differences in ONL thickness between the CNTF- and the PBS-injected eyes. Statistical analysis was performed using a commercial software (Statistix 8; Analytical Software, Tallahassee, FL).

To better characterize the peripheral retinal alterations observed following CNTF treatment, and determine the cause of the increase in ONL thickness, we examined in semi-thin plastic sections the retinal morphology of two additional *XLPRA2* dogs that were injected intravitreally with CNTF. One dog was treated following the same protocol as for Group #1 (Inj. 4 wk, Ter. 8 wk); the second dog received the same treatment as Group #2 (Inj. 4 & 8 wk; Ter 12 wk). Eyes were collected, fixed, and trimmed as described above, and processed for epoxy resin embedding as previously reported.[14] Retinal sections extending along all 4 meridians were cut at 1 µm with glass knives using a supercut microtome (Reichert Jung model 2065; Leica, Deerfield, IL), and stained with azure II-methylene blue with or without paraphenylenediamine counterstain. For each meridian, the site of highest ONL thickness in the peripheral retina of the CNTF-injected eyes was located, and its

distance from the *ora serrata* measured. This was used to locate the corresponding site in the contralateral PBS-injected eye. Using the 40X objective, digitally captured images (Spot 4.0 camera; Diagnostic Instruments, Inc., Sterling Heights, MI) that encompassed a 290 µm length of retina, were printed to manually count the total number of photoreceptor nuclei at these two sites. For each meridian, the counts were performed in triplicate on sequential sections, and the values averaged.

Immunohistochemistry

Fluorescence immunohistochemistry on 7 or 10 µm thick retinal cryosections of dogs from all four treatment groups was used to examine CNTF-mediated modifications with cell-specific markers. Cryosections were air-dried, blocked in a solution containing 10% normal serum from the appropriate species, and incubated overnight at 4°C with the primary antibody. Primary antibodies used in this study are listed in Table 5.1. Species-specific secondary antibodies conjugated to fluorochromes (Alexa Fluor, Invitrogen, Carlsbad, CA, 1: 200 dilution) were then applied to the sections for 1 hour. The antibodies were used at the appropriate dilution in 1.5% normal serum, 0.25% Triton X-100, 0.05% sodium azide in PBS. DAPI stain was used to label cell nuclei. Slides were mounted with a medium composed of polyvinyl alcohol and DABCO (1,4 diazabicyclo-[2.2.2]octane) (Gelvatol; Sigma-Aldrich, St. Louis, MO), and examined with an epifluorescence microscope (Axioplan; Carl Zeiss Meditec). Digitally captured images were imported into a graphics program (Photoshop; Adobe, Mountain View, CA) for display. When double fluorescence immunohistochemistry was done, primary antibodies (followed by their secondary) were applied sequentially.

In order to determine whether the α subunit of the CNTF receptor (CNTFRα) is expressed in normal and mutant photoreceptors during postnatal retinal maturation, as well as during the course of retinal degeneration, archival collections of normal and

Table 5.1 List of primary antibodies used.

Antigen	Host	Source, catalog # or name	Working concentration	Specificity
Rod opsin	Mouse monoclonal	Paul Hargrave, R2-12N	1:300	OS of rods
Rod opsin	Mouse monoclonal IgG1	Chemicon, MAB5316	1:1,000	OS of rods
Human cone arrestin	Rabbit polyclonal	Cheryl Craft, LUMIF	1:10,000	Cone photoreceptors
Protein Kinase C (PKCα)	Mouse monoclonal IgG2b	BD Biosciences, 610107	1:100	Rod bipolar cells
Goα	Mouse monoclonal IgG1	Chemicon, MAB3073	1:5,000	ON (rod and cone) bipolar cells
Calretinin	Rabbit polyclonal	Sigma, C7479	1:500	Horizontal, amacrine, ganglion cells
CRALBP	Rabbit polyclonal	John Saari	1:1,500	Müller cells, RPE
Glial fibrillary acidic protein (GFAP)	Rabbit polyclonal	DakoCytomation, Z0334	1:1,000	Astrocytes, Müller cells (reactive)
CNTFRα	Rabbit polyclonal	Hermann Rohrer	1:2,000	IS of rods & cones, INL, GCL
Bromodeoxyuridine (BrdU)	Mouse monoclonal IgG1	Chemicon, MAB4072	1:100	Cells that have incorporated BrdU
Ki67	Mouse monoclonal IgG1	BD Biosciences, 550609	1:20	Proliferating cells

mutant retinas developed by our lab were used. These included retinas of normal, *rcd1*, and *XLPRA2* dogs (age: 4-24 weeks); some of these tissues have been used in previous studies.[14] Enzymatic immunohistochemistry was performed on 7 µm thick cryosections from the superior meridian of these retinas as previously described.[16] A rabbit protein A-purified polyclonal antibody raised against a large fragment of the chicken CNTFRα recombinant protein (1:2,000 dilution; kindly provided by H. Rohrer)[17] was used for this study. This antibody cross reacts in the dog as well as in other mammalian species.[16,18]

Cell proliferation assays

To determine whether the increase in ONL thickness in the retinal periphery could be explained by a proliferative event, we conducted BrdU pulse-labeling experiments in two XLPRA2 dogs. At 4 weeks of age both dogs were anesthetized with isoflurane and injected intravitreally in the left eye with 30 µl of a 0.1 M PBS solution containing 12 µg of CNTF and 10 µg of 5-Bromo-2'-Deoxyuridine (Sigma, St-Louis, MO); the contralateral eye was injected with 30 µl of a 0.1 M PBS solution containing 10 µg of BrdU. The dose of BrdU injected was extrapolated from the dose used in chick eyes.[19] Twenty four hours later, one dog was euthanatized and the eyes processed as described below. The second dog was re-injected under isoflurane anesthesia in both eyes with 30 µl of a 0.1 M PBS solution containing 10 µg of BrdU at 24 and 96 hours following the initial injection. At 5 weeks of age, this animal was killed, and the eyes collected. Following enucleation, the anterior and posterior segments were separated and the vitreous was gently removed from the posterior eyecup. The tissues were then fixed for 30 min in 4% paraformaldehyde with 3% sucrose in 0.1 M PBS at 4°C. Following three washes in PBS, tissues were cryoprotected, trimmed and embedded in OCT as described above. Immunohistochemical detection of BrdU incorporation was

done on 7 µm thick cryosections that were pretreated in 4 M HCl for 10 min, followed by overnight incubation with the primary monoclonal anti-BrdU antibody (see Table 5.1). BrdU-positive cells were counted throughout the entire length (i.e. from optic disc to *ora serrata*) on a least three retinal sections for each of the superior, inferior and temporal meridians. Values for each meridian were averaged and expressed as the number of BrdU-positive cells per unit length of retina. The unit length was set at 10,000µm. Expression of the nuclear cell proliferation marker Ki67 (see Table 5.1) was also examined in the retinas of these two dogs by immunohistochemistry.

RESULTS

Clinical findings and CNTF-mediated side effects.

Ocular examinations performed immediately after the intravitreal injections did not reveal any lesions caused by the procedure. Yet, several ocular abnormalities were visible clinically within a few days following intravitreal injection of CNTF in both *XLPRA2* and *rcd1* dogs (Table 5.2). None of these changes were seen in any of the PBS-injected eyes. Therefore, the following description only applies to the CNTF-treated eyes.

Clinical signs of uveitis were the first to appear, and consisted mainly of miosis, intraocular hypotension, and occasional iridal changes (see below). Aqueous humor flare was not detected by slit lamp biomicroscopy during the first week following the injection. Later, examination of the aqueous humor transparency was hampered by development of corneal haze (see below). Miosis that was refractory to dilatation with topical mydriatics was seen in all dogs that were reexamined 2 days after the first CNTF injection, and persisted for approximately 2 weeks.

In 2 *XLPRA2* dogs (treatment Group # 4) that had lightly pigmented irides, vascular engorgement was seen 48 hours following injection. Anterior displacement of

Table 5.2 Summary of clinical findings observed in eyes following intravitreal injection with CNTF (OS) or PBS (OD). Numbers for each category reflect the number of dogs affected in each treatment group.

	Group 1		**Group 2**		**Group 3**		**Group 4**		**rcd1 control**	
Clinical observations	OD (n = 3)	OS (n = 3)	OD (n = 3)	OS (n = 3)	OD (n = 3)	OS (n = 3)	OD (n = 3)	OS (n = 3)	OD (n = 3)	OS (n = 3)
Miosis	0	3	0	3	0	3	0	3	0	3
Iris vascular congestion	0	0	0	0	0	0	0	2	0	0
Iris hyperpigmentation	0	3	0	3	0	0	0	0	0	0
Intraocular hypotension	0	3	0	3	0	3	0	3	0	3
Corneal epitheliopathy	0	3	0	3	0	3	0	3	0	3
Cataract	0	3	0	3	0	3	0	2	0	3

the iris, causing a reduction in anterior chamber depth, was also seen 2 days post-injection in 2 *rcd1* dogs. An increase in iris pigmentation was observed in 1 dog (treatment Group #3), and in 3 dogs from (treatment Group #2), respectively, at 17 and 51 days after the 1st injection of CNTF. Combined IOP values of *XLPRA2* (all treatment groups) and *rcd1* dogs, measured between post-injection days 2-4, were significantly lower ($P<0.0001$, paired Student t test) in CNTF- injected (mean: 7.1 mm Hg , min:4 mm Hg, max: 12 mm Hg; n= 15) versus PBS-injected (mean: 13.5 mm Hg, min:8 mm Hg, max:22 mm Hg; n= 15) eyes. All CNTF-injected eyes were hypotensive (IOP < 8 mm Hg, or IOP at least 5 mm Hg lower than in the PBS-treated eye) after the first or second injection. A steep decrease in IOP was seen during the first 4-7 days following CNTF injection, but values returned to pre-injection levels within 20 days. In PBS-injected eyes, a slight increase in IOP occurred that remained within normal levels (19.2 ± 5.9)[20] was observed for 10-14 days following injection. Similarly, IOP values returned to pre-injection values within approximately 20 days. Figure 5.1 illustrates the IOP changes observed in a subset of the experimental dogs.

Corneal epithelial abnormalities were observed by external and slit-lamp examination in 15/16 of the eyes injected with CNTF (Figure 5.2 A). Discrete lesions that caused a hazy patch in the corneal epithelium could be observed in some animals as early as 3-4 days following CNTF injection. By post-injection day 11, the corneal epithelial haze was present in all 15 affected animals. These epithelial changes progressed with time, and could involve more than 75% of the corneal surface.

However, a peripheral band located in the superior part of the cornea was never affected, and remained optically clear. The lesions persisted throughout the entire treatment period, and were never associated with corneal ulceration. Histological examination revealed thinning of the epithelium with attenuation of the

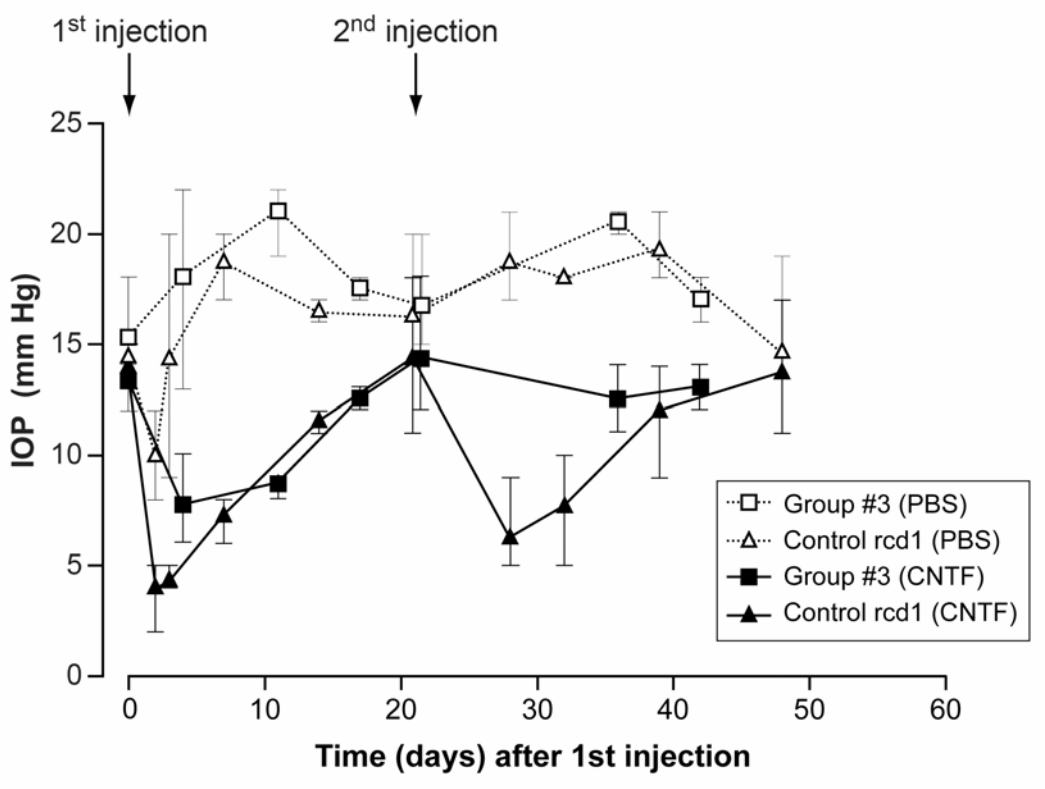

Figure 5.1 Values (mean, and range) of intraocular pressure in CNTF- and PBS-treated eyes. Data is provided for *XLPRA2* (n=3), and *rcd1* (n=3) dogs that were injected at 7 and 10 weeks of age. Pre-injection values of intraocular pressure are indicated at time 0. In the days following both CNTF injections a decrease in IOP was observed. The intraocular hypotension was transient, since IOP values returned to pre-injection values within approximately 20 days.

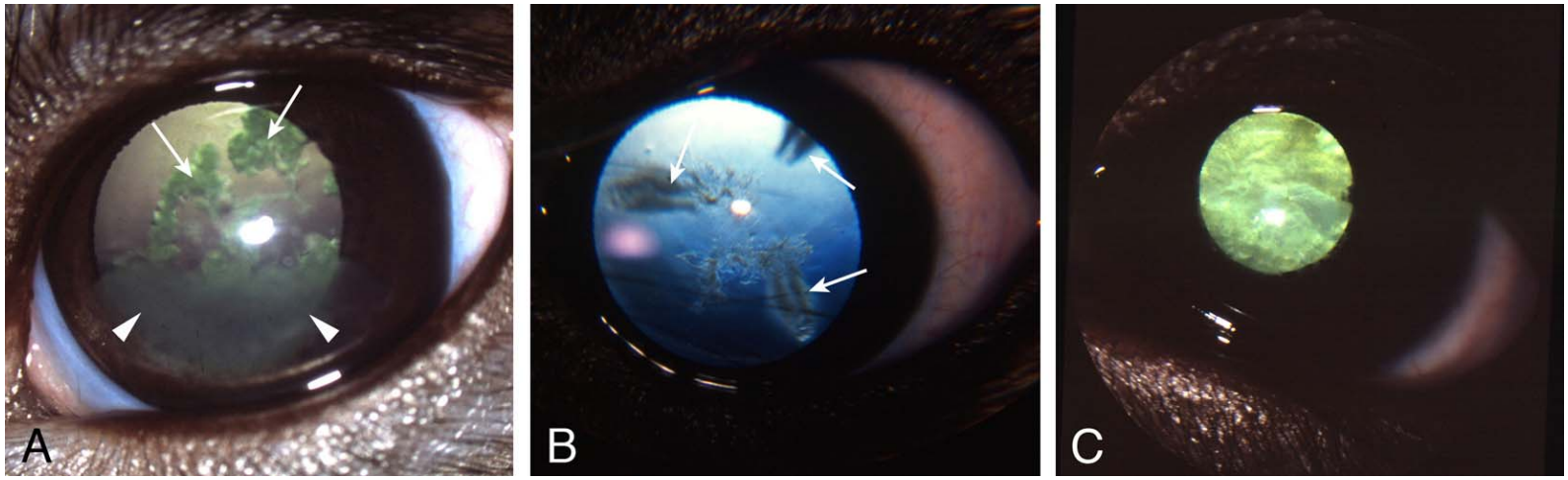

Figure 5.2 Ocular lesions caused by intravitreal injection of CNTF. (**A**) Corneal epithelial haze (*arrowheads*), and posterior subcapsular cataracts (*arrows*) 7 weeks post-injection. A corneal haze and sutural cataract had been detected in this dog 11 days following the first CNTF injection. (**B**) The earliest lens changes involved the extremities of the posterior Y sutures (arrows). (**C**) Immature cataract with anterior and posterior cortical opacification.

basal and suprabasilar (wing) cell layers (Figure 5.3 A, B). No corneal abnormalities were observed in any of the PBS-injected eyes.

Cataracts were commonly observed following CNTF injection (15/16 eyes). Examination of the lens was hampered during the first 2 weeks by the intense miosis and difficulty in fully dilating the pupil. By post-injection day 14, posterior sutural cataracts could be observed in CNTF-injected eyes of *XLPRA2* (8/12 eyes), *rcd1* (3/3 eyes), and non-affected (1/1 eye) dogs (Figure 5.2 B). Cataracts often progressed by involving the posterior and anterior cortex (Figure 5.2 C). Histological examination of some cataractous lenses confirmed the predominant involvement of the posterior suture lines and cortex (Figure 5.3 C, D). No lenticular opacities were detected in any of the PBS-injected eyes.

A thorough funduscopic examination was difficult to conduct in the CNTF-injected eyes, initially because of the associated miosis, and later on due to the loss of transparency of the ocular media caused by corneal epitheliopathy and lens opacities. In those animals in which areas of the fundus were visible, no abnormalities were detected. One exception was seen in the non-mutant control dog that had multiple small “doughnut” shaped foci scattered throughout both the tapetal and non-tapetal regions of the fundus (data not shown). Although this was an isolated observation in this study, we saw a similar type of lesion in a normal dog injected with a similar dose of CNTF in a previous pilot study.

Lack of photoreceptor rescue in *XLPRA2* with CNTF

The average ONL thickness in each quadrant was determined as a means of assessing the photoreceptor survival effect of CNTF. Using this measure, there was no statistically significant difference in any of the 4 treatment groups between the CNTF and PBS-injected eyes (Figure 5.4 and 5.5). The mean difference in ONL thickness of

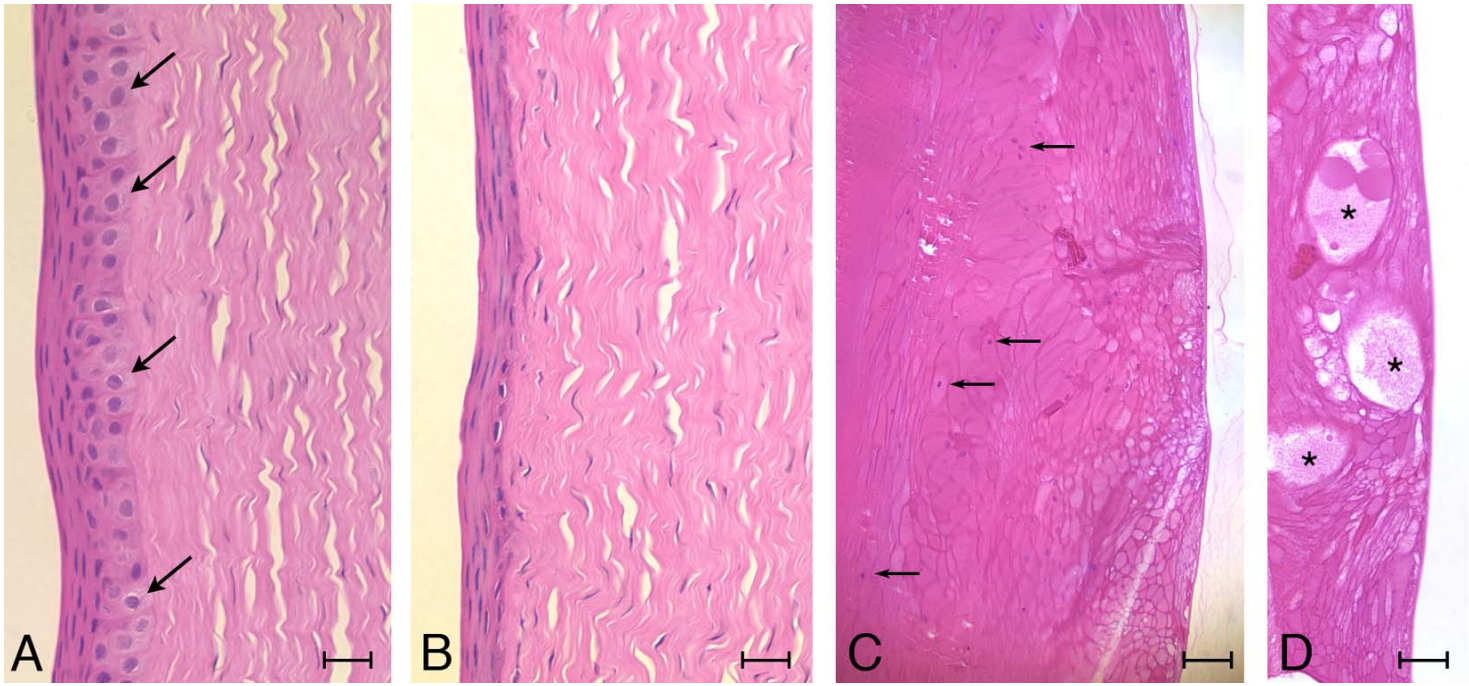

Figure 5.3 Histological lesions of the cornea and lens present after intravitreal injection of CNTF. (**A**) Normal aspect of the corneal epithelium in a PBS-injected eye. Note the presence of normal basal cells (*arrows*). (**B**) Cornea of the contralateral eye that was injected with CNTF. Note the thinning of the corneal epithelium due to the loss of the basal and suprabasilar (wing) cells. (**C**) Cataract caused by CNTF. Swelling and disorganization of lens fibers was observed in the posterior cortex, and was associated with the retention of lens fiber nuclei (*arrows*). (**D**) High magnification of the posterior subcapsular region of the same lens as in (C). Note the presence of large vacuoles that contain eosinophilic material (*asterisks*), and swollen lens fibers. H&E stain; scale bars: (**A**, **B**) 20 µm; (**C**) 80 µm; (**D**) 40 µm.

0.79 rows of nuclei (Group #1: 0.98 ± 0.52; Group #2: 0.77 ± 0.69; Group #3: 0.94 ± 0.63; Group #4: 0.48 ± 0.51) between the CNTF versus PBS-treated eyes also was not biologically relevant. Based on the kinetics of photoreceptor cell loss,[14] a difference of at least 2 rows of nuclei (treatment Groups #1 and #3), 3 rows of nuclei (Group #2), and 1 row of nuclei (Group #4), would have been expected in both the superior and inferior meridians if CNTF had caused a complete rescue of photoreceptors from the time of the first injection. Further confirming the absence of any significant neuroprotective effect of CNTF in the *XLPRA2* retina was the presence of morphological alterations at the level of the photoreceptor inner (IS) and outer (IS) segments that were characteristic of progression of the disease. Disruption of the OS, shortening and broadening of the IS, and reduction of the subretinal space was seen in all groups, either CNTF- or PBS-treated, and suggested that the natural course of the disease had not been arrested or modified.

In the *rcd1* control group, we observed a statistically significant rescue of photoreceptors with CNTF (Figure 5.4 and 5.5) The mean (± SD) difference in ONL thickness between the CNTF and PBS injected retinas was of 1.5 ± 0.56 rows of nuclei, and consistent with findings previously observed (Pearce-Kelling, unpublished). In the 7 week-old *rcd1* retina, the ONL has already lost approximately 40% - 50% of its photoreceptors, and has an average thickness of 5 to 6 rows of nuclei along the superior meridian.[21] In this study, the mean ONL thickness of the superior retina at 14 weeks of age was 4.4 and 2.5 rows of nuclei in the CNTF- and PBS-injected eyes, respectively. This indicates that although statistically significant, there is not a total rescue of photoreceptor cells in this model following an intravitreal injection of CNTF at 7 and 10 weeks of age.

To determine whether the lack of CNTF-mediated rescue in *XLPRA2* could be explained by the absence of expression of the α subunit of the CNTF

Figure 5.4 Scatter plots comparing the mean ONL thickness (measured as rows of nuclei) along the four meridians of eyes injected with CNTF or PBS. No statistically significant difference in ONL thickness was seen in any of the *XLPRA2* treatment Groups #1 - #4. CNTF caused a statistically significant increase in ONL thickness in *rcd1*. No major difference was seen in the single normal control dog. *: < 0.05; **: < 0.001; ND: not determined; OS: left eye; OD: right eye.

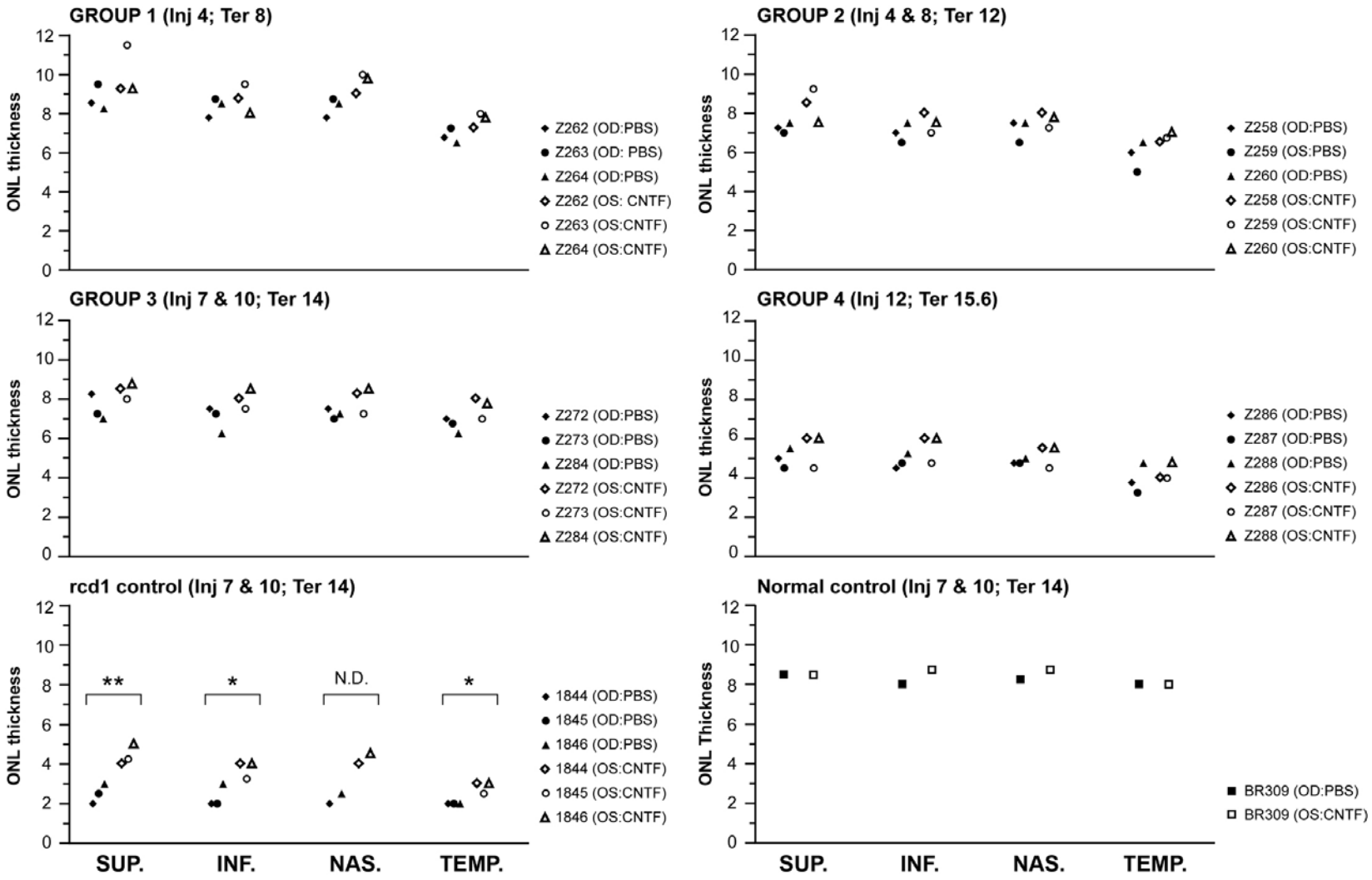
GROUP 1 (Inj 4; Ter 8)
ONL thickness
Z262 (OD:PBS)
Z263 (OD: PBS)
Z264 (OD:PBS)
Z262 (OS: CNTF)
Z263 (OS:CNTF)
Z264 (OS:CNTF)
GROUP 2 (Inj 4 & 8; Ter 12)
ONL thickness
Z258 (OD:PBS)
Z259 (OS:PBS)
Z260 (OD:PBS)
Z258 (OS:CNTF)
Z259 (OS:CNTF)
Z260 (OS:CNTF)
GROUP 3 (Inj 7 & 10; Ter 14)
ONL thickness
Z272 (OD:PBS)
Z273 (OD:PBS)
Z284 (OD:PBS)
Z272 (OS:CNTF)
Z273 (OS:CNTF)
Z284 (OS:CNTF)
GROUP 4 (Inj 12; Ter 15.6)
ONL thickness
Z286 (OD:PBS)
Z287 (OD:PBS)
Z288 (OD:PBS)
Z286 (OS:CNTF)
Z287 (OS:CNTF)
Z288 (OS:CNTF)
rcd1 control (Inj 7 & 10; Ter 14)
ONL thickness
**
*
N.D.
*
1844 (OD:PBS)
1845 (OD:PBS)
1846 (OD:PBS)
1844 (OS:CNTF)
1845 (OS:CNTF)
1846 (OS:CNTF)
SUP.
INF.
NAS.
TEMP.
Normal control (Inj 7 & 10; Ter 14)
ONL Thickness
BR309 (OD:PBS)
BR309 (OS:CNTF)
SUP.
INF.
NAS.
TEMP.

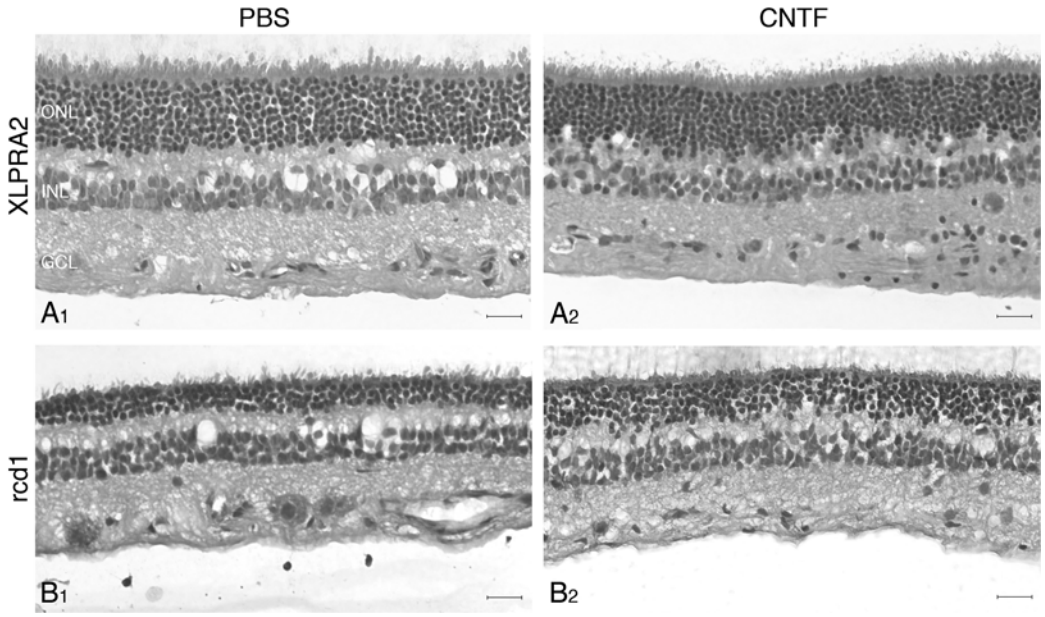

Figure 5.5 Illustration of the effect of CNTF on outer nuclear layer thickness in the mid-peripheral retina of a 14 week-old *XLPRA2* (**A2**) and *rcd1* (**B2**) dog. Contralateral eyes served as controls and were injected with PBS (**A1**, **B1**). CNTF caused an increase in the number of photoreceptor nuclei in *rcd1* (compare **B2** to **B1**), but no differences were seen in *XLPRA2* (compare **A2** with **A1**). CNTF often caused the vitreal border of the ONL to appear wavy (**A2**, **B2**). On these cryosections, RPE separation from the neuroretina was an artifact. H&E stain; scale bars: 20 µm.

receptor, immunolocalization of CNTFRα was done on retinas from *XLPRA2* as well as in *rcd1* and normal dogs, at ages ranging from 4 to 24 weeks. The pattern of labeling was similar to that previously reported for the normal adult canine retina.[16], and was characterized by an intense staining of the IS, inner nuclear layer (INL), ganglion cell layer (GCL) and nerve fiber layer (NFL). At the earliest age examined (4 weeks; Figure 5.6 A1-A3), CNTFRα-immunoreactivity was present in both rod and cone IS. With progression of both diseases, the shortening of rod IS, and their subsequent disappearance, photoreceptor labeling was restricted to the remaining cone IS (Figure 5.6 B2, C2, C3).

CNTF causes peripheral remodeling in XLPRA2 retinas.

A consistent finding in all 4 quadrants of CNTF-injected eyes of *XLPRA2* dogs enrolled in treatment Groups #1, #2, and #3 was abnormal changes in the retinal periphery. These alterations included a loss of IS and OS, an increase in ONL thickness, and misplaced rod-like nuclei in the INL (Figure 5.7 and Table 5.3). These changes were disease- (*XLPRA2*) and age-specific, since they were not present in either the *rcd1* control group, the single non-mutant dog, or the *XLPRA2* mutants treated for the first time at 12 weeks of age (Group #4).

A remarkable feature associated the with peripheral ONL remodeling was the loss of both photoreceptor IS and OS that caused, in some areas, the retinal pigment epithelium (RPE) to be in direct apposition with the external limiting membrane (ELM) (Figure 5.7 A2, B2, C2). This loss of the photoreceptor layer (PRL) extended over distances that were usually shorter, although occasionally equal, than the lengths over which an increase in ONL was noted. In animals from Group #4, there was never a complete loss of the PRL, yet loss of OS and significant shortening of IS was occasionally seen (Figure 5.7 D2).

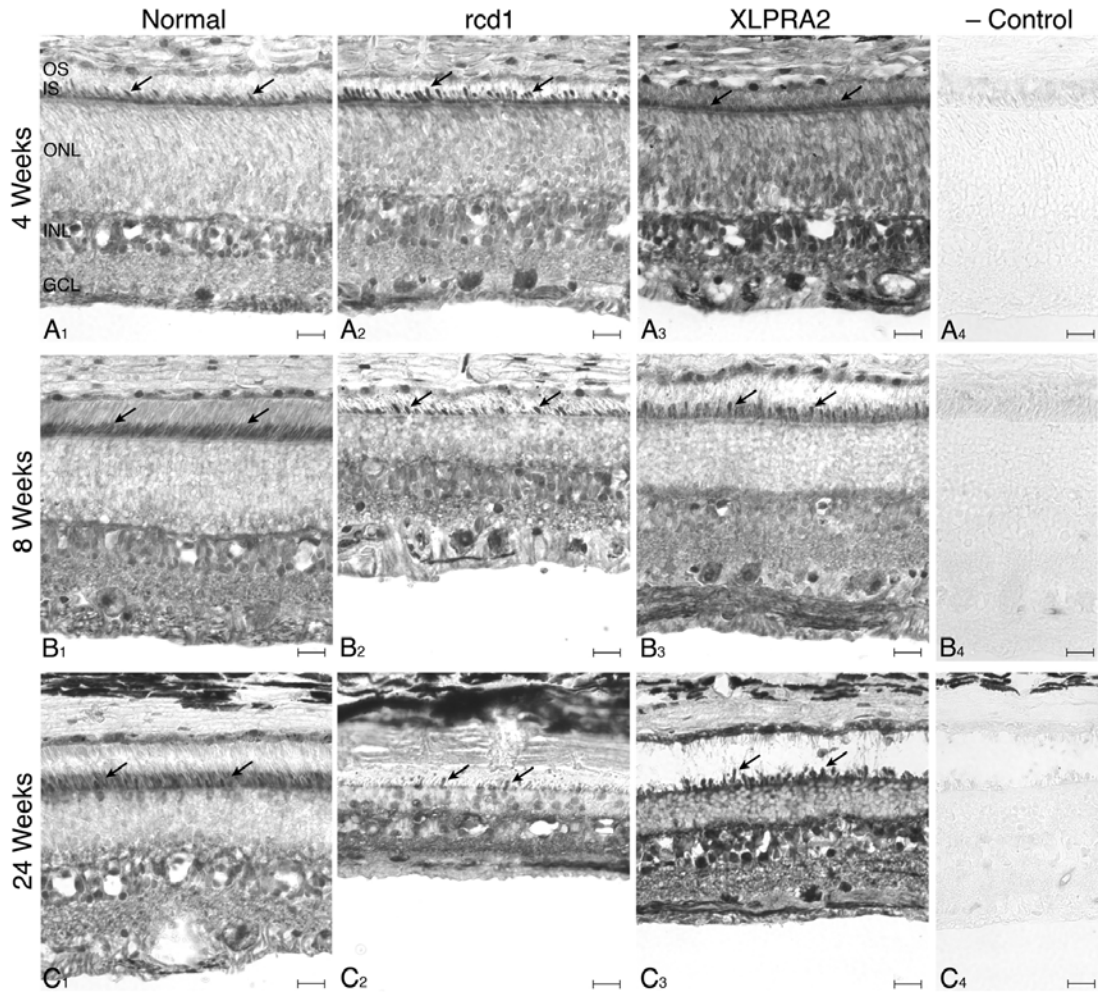

Figure 5.6 Immunohistochemical localization of CNTFRα in the retinas of normal, *rcd1*, and *XLPRA2* dogs of different ages. Strong immunoreactivity for CNTFRα was seen in the GCL, INL and inner segments (IS, *arrows*) in the normal and mutant retinas at 4 weeks of age (**A1-A3**). At 8 weeks of age, intense labeling is seen throughout the IS of rods and cones in the normal retina (**B1**). In the mutant retinas, labeling persists in the IS of both rods and cones in *XLPRA2* (**B3**), but is essentially limited to cone IS in *rcd1* which is the predominant cell class remaining in the PRL at this stage of disease (**B2**). (**C1-C3**) At 24 weeks of age, CNTFRα-positive cone IS and somas are still seen in *rcd1* and *XLPRA2* despite substantial loss of photoreceptors. Negative controls (**A4**, **B4**, **C4**) were *XLPRA2* retinas that were treated with the omission of the primary antibody. Scale bars: 20 μm.

Figure 5.7 Illustration of the morphologic changes observed in the peripheral retina of *XLPRA2* dogs following intravitreal injection with CNTF. An example from each of the 4 treatment groups is shown at the site where the measured ONL thickness was maximal. This same location in the contralateral (PBS-injected eye) is shown for comparison. The boxed areas in the low power photographs are shown in higher magnification. (**A1**, **A2**) Inferior periphery (1,000 µm from the *ora serrata*) in an 8 week-old dog (Z263; Group #1; Inj. 4 weeks; Ter. 8 weeks). (**B1**, **B2**) Superior periphery (3,900 µm from the *ora serrata*) in a 12 week-old dog (Z 259; Group #2; Inj. 4 & 8 weeks; Ter. 12 weeks). (**C1**, **C2**) Temporal periphery (550 µm from the *ora serrata*) in a 14 week-old dog (Z272; Group #3; Inj. 7 & 10 weeks; Ter. 14 weeks). (**D1**, **D2**) Superior periphery (680 µm from the *ora serrata*) in a 15.6 week-old dog (Z288; Group #4; Inj. 12 weeks; Ter. 15.6 weeks). Note the prominent increase in ONL thickness in dogs from Groups #1-3 (**A2**, **B2**, **C2**), and the misplacement of rod-like nuclei in the INL (**A2**, **B2**; *arrows*). No significant difference in ONL is seen in Group #4 (**D1**, **D2**). A loss of the photoreceptor (PRL) layer is seen in Groups #1-3, which causes the external limiting membrane to be in direct contact with the retinal pigment epithelium (**A2**, **B2**, **C2**; *asterisks*). In Group #4, short inner segments persist in the PRL (**D2**, *arrows*). Cryosections; H&E stain; scale bars: 100 µm.

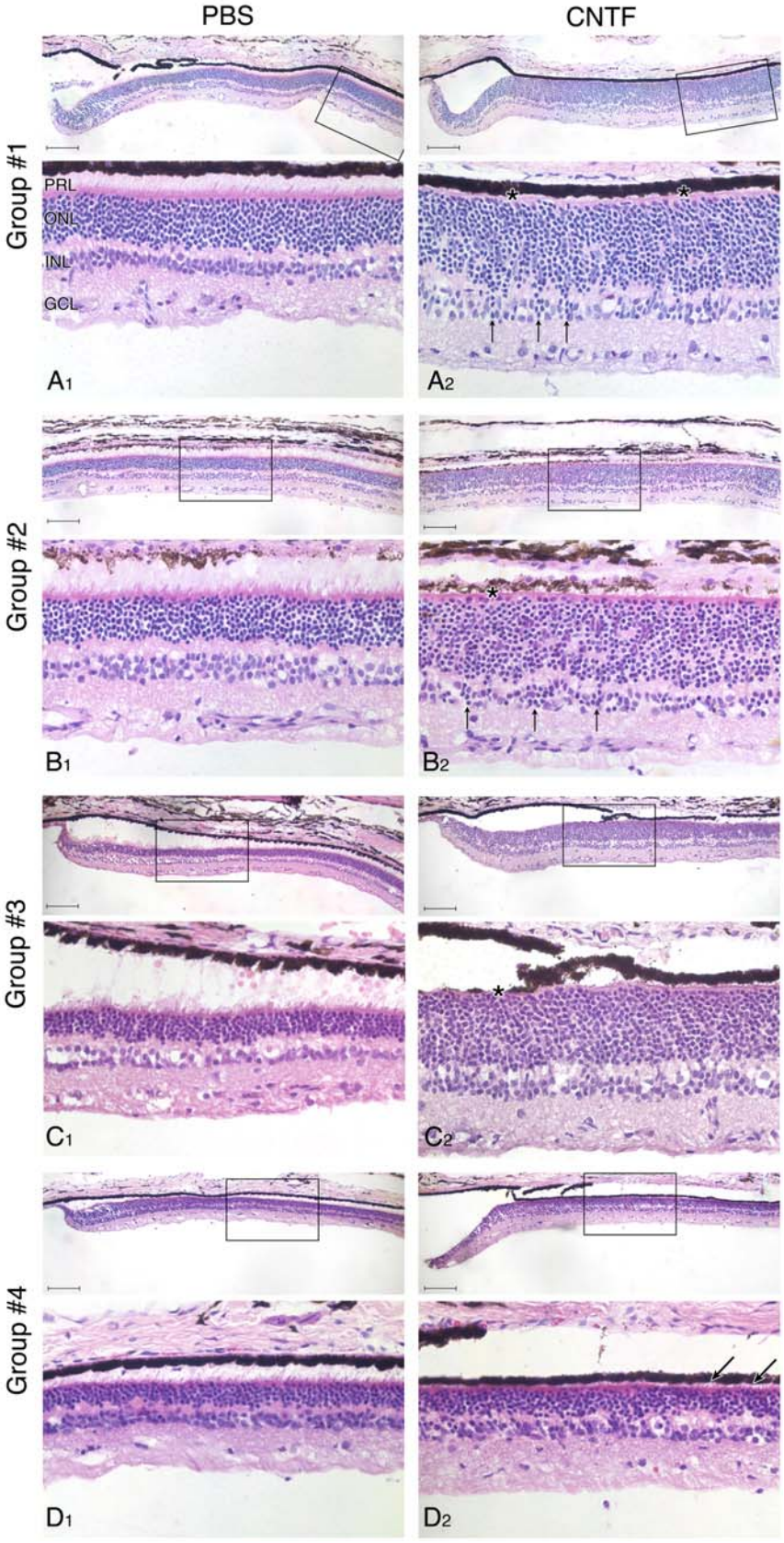
PBS
CNTF
Group #1
PRL
ONL
INL
GCL
A1
A2
Group #2
B1
B2
Group #3
C1
C2
Group #4
D1
D2

Table 5.3 Increase in ONL thickness and loss of IS and OS in the *XLPRA2* peripheral retina after CNTF treatment.
SUP: superior meridian; INF: Inferior meridian; NAS: Nasal meridian; TEMP: Temporal meridian; ONL: outer nuclear layer; IS: inner segment; OS: outer segment.
L: length of retina (measured in µm from the ora serrata) over which there is an increase in ONL thickness in the CNTF-treated eye in comparison to the PBS-treated eye.
D: distance from the ora serrata (measured in µm) of the site of highest ONL thickness in the peripheral retina of the CNTF-treated eye.
R: ratio of ONL thickness in the CNTF-treated eye over the ONL thickness in the PBS-treated eye at distance D from the ora serrata.
l:Length of retina (measured in µm from the ora serrata) over which there is a loss of IS and OS in the CNTF-treated eye in comparison to the PBS-treated eye.

		Group 1 (Inj 4; Ter 8)			Group 2 (Inj 4&8; Ter 12)			Group 3 (Inj 7&10; Ter 14)			Group 4 (Inj 12; Ter 15.6)		
	ID	Z262	Z263	Z264	Z258	Z259	Z260	Z272	Z273	Z274	Z286	Z287	Z288
	L	3,200	4,700	1,300	5,200	5,800	4,500	2,650	2,200	2,700	0	0	0
	D	2,350	3,400	1,000	3,550	3,900	3,800	1,500	2,000	2,150	None	None	None
SUP	R	1.48	1.67	1.85	1.59	1.87	1.85	2.03	1.22	2.77	None	None	None
		(68/46)	(87/52	(72/39)	(62/39)	(71/38)	(63/34)	(67/33)	(44/36)	(72/26)			
	l	2,300	3,300	700	3,800	3,900	3,800	1,900	2,200	2,700	0	0	0
	L	2,000	1,800	1,000	3,000	3,200	1,400	1,900	1,400	1,500	0	0	0
	D	1,250	1,000	400	2,000	1,350	550	650	1,100	1,350	None	None	None
INF	R	2.05	1.83	1.69	1.61	2.40	2.27	2.35	1.41	2.26	None	None	None
		(80/39)	(75/41)	(44/26)	(61/38)	(72/30)	(68/30)	(61/26)	(41/29)	(43/19)			
	l	1,350	1,200	300	2,100	1,350	600	400	1,400	1,200	0	0	0
	L	/	/	/	/	/	/	1,300	1,200	1,150	/	/	0
	D	/	/	/	/	/	/	700	1,100	900	/	/	None
NAS	R	/	/	/	/	/	/	2.77	1.53	2.24	/	/	None
								(61/22)	(46/30)	(56/25			
	l	/	/	/	/	/	/	800	1,200	950	/	/	0
	L	800	500	/	750	900	850	1,000	1,400	900	0	0	0
	D	600	450	/	500	650	600	550	1,100	600	None	None	None
TEMP	R	1.53	1.44	/	1.24	2.28	3	2.5	1.46	2.17	None	None	None
		(52/34)	(46/32)		(36/29)	(57/25)	(69/23)	(60/24)	(38/26)	(39/18)			
	l	650	300	/	600	500	550	700	700	600	0	0	0

When combining results from all 4 meridians of treatment Groups #1, #2, and #3, the mean distance from the *ora serrata* over which an increase in ONL thickness could be observed in the CNTF-treated eye was 2,075 µm (min: 500 µm; max: 5,800 µm). The longest expanse of altered ONL was seen in the superior meridian, and then in the inferior meridian. The peripheral ONL remodeling was most extensive in animals from treatment Group #2. The increase in ONL thickness was associated with an increase in spacing between nuclei, such that the density of photoreceptors appeared to be reduced following CNTF injection. Because of this, and due to the misalignment of layers of photoreceptor nuclei, the thickness of the ONL was measured in micrometers rather than in number of rows of nuclei. This was done at the site of highest ONL thickness. If, an equal increase in ONL thickness was observed throughout an extended length of ONL, the area that was selected for analysis was the one located the furthest distance from the *ora serrata*. At that site, there was a 1.94 fold average increase (min: 1.22; max: 3) in ONL thickness in comparison to the corresponding region of the PBS-treated eye (Figure 5.7 and Table 5.3).

Finally, misplacement of rod-like nuclei in the outer plexiform layer (OPL) and INL caused a disorganization of the typical layering of the retina. A wavy aspect of the vitreal edge of the ONL was responsible for the frequent loss of a clear delimitation by the OPL of both nuclear layers (Figure 5.7 A2, B2).

To determine the nature of the cell population(s) responsible for this apparent increase in cell number in the ONL, immunohistochemical studies were performed using several cell-specific markers on *XLPRA2* retinas from all 4 treatment groups. The results confirm that the overwhelming majority of cells present in the peripheral ONL, and migrating to the INL of CNTF-treated eyes (Groups #1-3), are rod opsin-positive (Figure 5.8 A2). Although we have previously reported in *XLPRA2* a mislocalization of rod opsin to the soma and axons of rods,[14] (see Figure 5.8 A1) this

was more pronounced in retinas examined 4 to 8 weeks after CNTF treatment. In addition, in contrast to what is seen in the untreated *XLPRA2* retina,[14] there was absence of rod opsin labeling in rod OS and IS in the periphery, thus, further confirming the loss of these structures following CNTF treatment (Figure 5.8 A2). The use of a cone arrestin antibody also confirmed the presence of heterotopic cone somas in the middle and inner portions of the ONL. These cells had neither an axon nor an IS (Figure 5.8 A2). One week following the injection of CNTF in a 4 week-old *XLPRA2* retina, the migration of cone somas down their axon was seen in the periphery (Figure 5.8 B3).

Rod opsin and cone arrestin immunoreactivities were also examined in *XLPRA2* retinas 1 and 7 days following an injection of CNTF, and a significant decrease in intensity of labeling was seen in comparison to the PBS-injected eye. (Figure 5.8 B1, B2). This decrease in rod opsin and cone arrestin expression which was more pronounced 1 week post-CNTF injection was seen throughout the entire length of the retinal sections, but was most prominent in the periphery. This reduction in immunoreactivity was not present 4 weeks after the injection.

Peripheral remodeling of the retina also involved cells of the INL. The use of cell markers for bipolar cells showed significant dendritic sprouting into the peripheral ONL, as well as heterotopia of PKCα-positive cells (a marker for rod bipolar cells) (Figure 5.8 C1, C2). Similarly, radial extension into the ONL of processes originating from calretinin-immunoreactive horizontal cells was observed in the peripheral retina (Figure 5.8 D1, D2). CNTF treatment also caused misplacement in the ONL of the somas of some CRALBP-positive Müller cells (Figure 5.8 E1, E2). Glial Fibrillary acid protein (GFAP) immunoreactivity was also examined and showed a similar labeling of the entire cell body of Müller cells (data not shown) in both CNTF- and PBS-treated

Figure 5.8 Immunohistochemical characterization of CNTF-mediated remodeling of the peripheral retina of *XLPRA2*. (**A1**, **A2**, **B1**, **B2**) Double immunofluorescence labeling of rods and cones with, respectively, anti-rod opsin (*green*) and anti-cone arrestin (*red*), in a 12 week-old dog, 8 weeks after the first CNTF injection (Group # 2; **A1**, **A2**), and in a 5 week-old animal one week post-CNTF injection (**B1**, **B2**). No labeling is seen at the level of the PRL due to the loss of inner and outer segments (**A2**; *asterisks*).The majority of the cells found in the ONL are rod opsin-positive due to the increased mislocalization caused by CNTF (**A2**). Rod opsin immunoreactive cells are seen displaced in the INL (*arrows*), and cone arrestin-labeled somas are present within the thickened ONL (*arrowheads*). One week following CNTF injection, there is a significant decrease in rod opsin and cone arrestin expression (compare **B2** with **B1** which were taken at the same exposure settings). Digitally increasing the red fluorescent signal in an area of (**B2**) shows the displacement of cone somas (*arrowheads*) down their respective axons (*arrows*; **B3**). (**C1**, **C2**) Double immunofluorescence labeling of ON bipolar cells with anti-Goα (*red*), and rod bipolar cells with anti-PKCα (*green*) in a 12 week-old dog 8 weeks after the first CNTF injection (Group # 2). DAPI (*blue*) was used as a nuclear counterstain. Rod bipolar cells are co-labeled with both antibodies and appeared yellow-orange, whereas ON cone bipolar cells were only labeled with anti-Goα and appeared *red*. Note the neuritic sprouting extending into the ONL (*arrows*), and the presence of Goα- and PKCα-positive somas in the ONL (*arrowheads*) of the CNTF-treated eye. (**D1**, **D2**) Immunofluorecence labeling of horizontal and amacrine cells with anti-calretinin in a 12 week-old dog (Group #2) 8 weeks after the first CNTF injection. There are radial extensions into the ONL of neurite sprouts origination from the horizontal cells (*arrows*) in the CNTF-treated eye. (**E1**, **E2**) Immunofluorescence labeling of Müller cells with anti-CRALBP in a 12 week-old dog (Group #2) 8 weeks after the first CNTF injection. Müller cell somas are seen displaced into the ONL *(arrowheads*) in the CNTF-treated eye. Note the intense normal CRALBP labeling in the RPE. Scale bars: 20 μm.

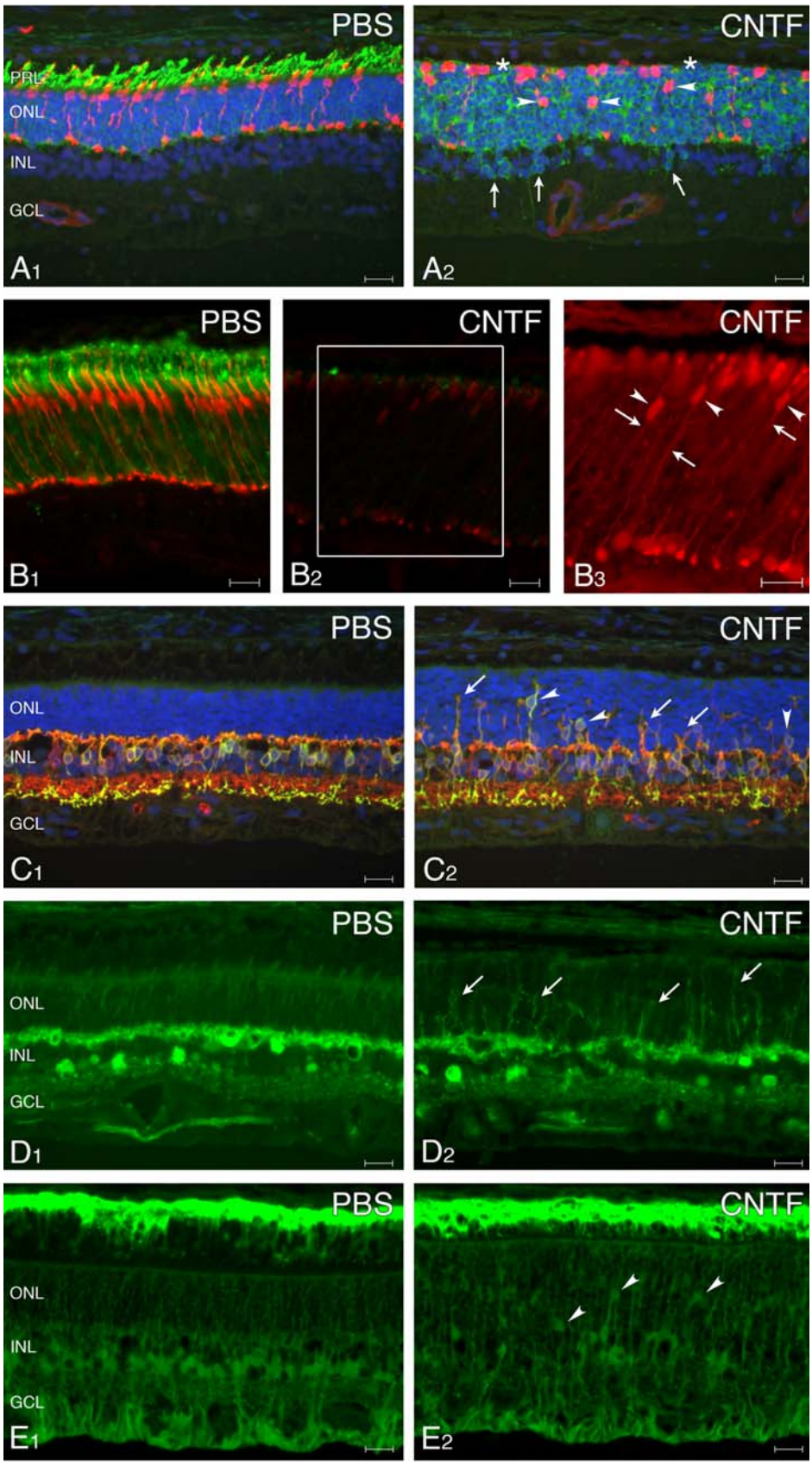
PBS
CNTF
PRL
ONL
INL
GCL
A1
A2
B1
B2
B3
C1
C2
D1
D2
E1
E2

eyes. This is not surprising since increase in GFAP expression in Müller cells is known to occur at the ages examined.[14]

CNTF causes an increase in cell number in the peripheral *XLPRA2* retina.

To determine whether the thickening of the ONL was caused solely by an increased internuclear spacing, or by a higher number of ONL cells, plastic embedded retinal sections of two *XLPRA2* dogs were examined; each dog was treated using the same protocols as for Group #1 (Inj. 4 wk; Ter. 8 wk), and Group #2 (Inj. 4 & 8 wk; Ter. 12 wk), respectively. These 1-µm thick sections permitted individual cell counts (Figure 5.9) which could not be done on the thicker (7 or 10 µm) cryosections where substantial overlap of nuclei occurred. Examination of the peripheral retina of the CNTF-treated eyes confirmed that there was more space between the photoreceptor nuclei, although it could not be determined whether this resulted from intra- or extracellular swelling. Elevation of the external limiting membrane, suggesting cytoplasmic swelling of photoreceptors or Müller cell processes, has been reported in both *rcd1* and non-mutant dogs implanted with a long-term CNTF release device.[22] This was not observed in the current study. In addition to heterotopic rod nuclei in the INL (Figure 5.9 C2; arrows), there were cells with larger nuclei within the thickness of the ONL (arrowheads). These nuclei contained fewer chromatin clumps than rods, and resembled that of cones. Nuclear count in both CNTF- and PBS-injected eyes was done at the site of highest ONL thickness as described above. Although statistical analysis could not be done due to the limited number of observations, we observed a consistently higher number of cells in the CNTF-treated peripheral retina (Table 5.4).

To determine how early following an injection of CNTF an increase in ONL thickness is observed in the peripheral *XLPRA2* retina, and to determine if this is

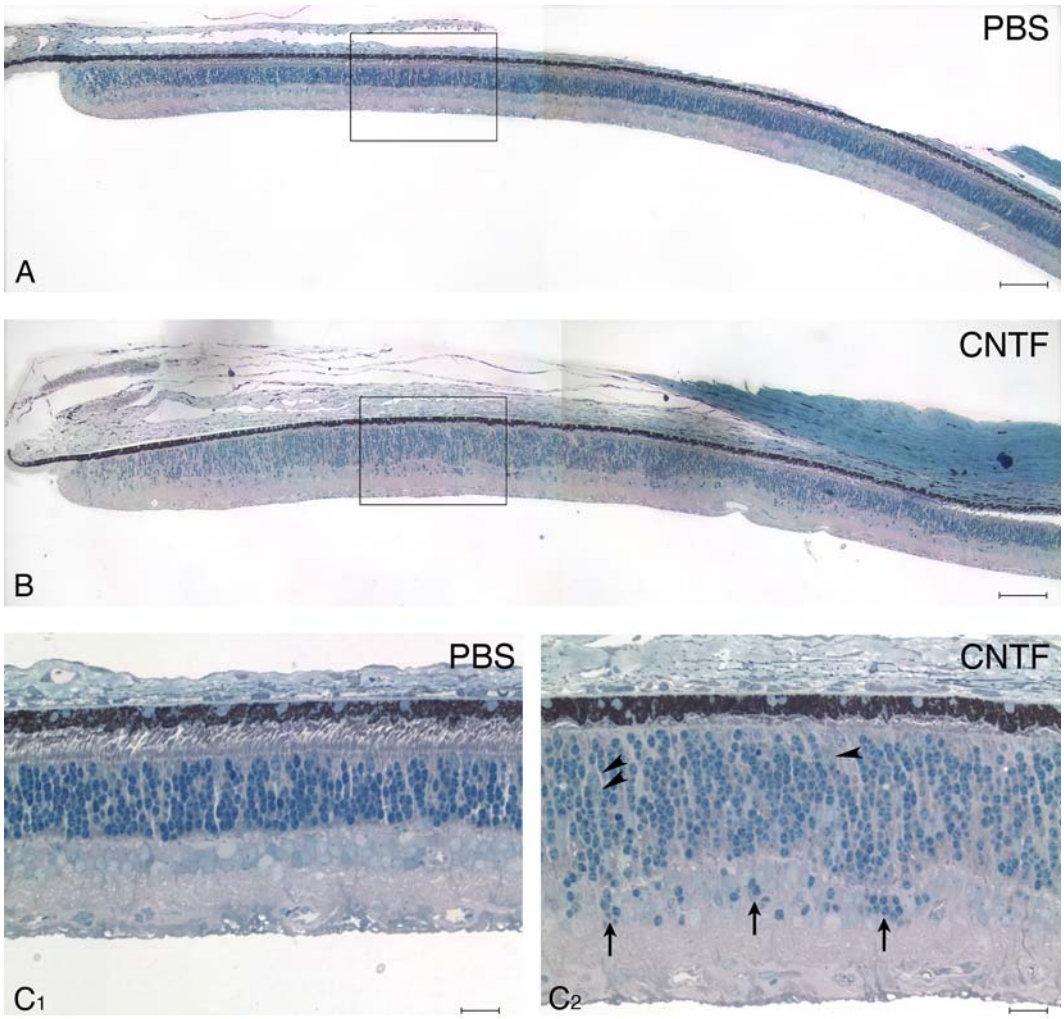

Figure 5.9 Changes in the ONL of the inferior periphery in an 8 week-old *XLPRA2* dog following intravitreal injection of CNTF (PBS in the contralateral eye) at 4 weeks of age. Note the increase in ONL thickness (Compare **A** and **B**). The 1 µm-thin epoxy resin sections enabled counts of individual cells in the ONL (**C1**, **C2**). Rod-like nuclei were seen in the INL (*arrows*), and larger euchromatic nuclei with a cone-type morphology were found in deeper layers of the ONL (*arrowheads*). Azure II-methylene blue stain with PPDA counterstain; scale bars: (**A**, **B**) 100 µm; (**C1**, **C2**) 20 µm.

Table 5.4 ONL nuclear count (mean [min; max]) in a 40X microscope field (290 µm in length) of the peripheral *XLPRA2* retina treated with CNTF or PBS. (Note: rod-like nuclei present in the INL were also included in this count)

Dog: meridian	**PBS-injected**	**CNTF-injected**	**% increase**
Z265:	(Inj. 4 wk; Ter. 8 wk)	(Inj. 4 wk; Ter. 8 wk)	
Superior	483 [469 ; 498]	552 [546 ; 556]	14
Inferior	362 [360 ; 366]	544 [533 ; 553]	50
Temporal	398 [391 ; 406]	530 [520 ; 548]	33
Z261:	(Inj. 4 & 8 wk; Ter. 12 wk)	(Inj. 4 & 8 wk; Ter. 12 wk)	
Superior	363 [341 ; 384]	424 [411 ; 431]	17
Inferior	298 [280 ; 318]	421 [400 ; 445]	41
Temporal	321 [313 ; 331]	393 [376 ; 416]	22

Figure 5.10 Evidence for cell proliferative events in the peripheral ONL of *XLPRA2* following intravitreal injection of CNTF. (**A**-**D**) One week after CNTF injection there was increased ONL thickness in a 5 week-old dog. Note also the extended loss of the PRL (**B**, and **C**$_2$, *asterisks*). (**D**$_1$-**D**$_3$) Fluorescence immunohistochemical labeling for BrdU (*green*) shows incorporation in the ciliary epithelium of the *pars plana* (**D**$_1$, **D**$_2$, *arrowheads*), and in cells located at the retinal margin (**D**$_1$, **D**$_2$, *arrows*) in both the CNTF- and PBS-injected eye. (**D**$_3$) BrdU incorporation was detected in cells located in the INL (*arrowhead*), GCL and NFL in both eyes, but few BrdU-positive cells were seen only in the ONL of the CNTF-treated eye (*arrow*).
(**E**$_1$, **E**$_2$) Fluorescence immunohistochemical labeling for the nuclear cell marker of proliferation Ki67 (*red*). (**E**$_2$) Ki67-positive cells were seen exclusively in the ONL of the CNTF-treated eye (arrows), but Ki67 positive cells were found in other retinal layers in both PBS-and CNTF-injected eyes. Scale bars: (**A**, **B**) 100 µm; (**C**$_1$-**E**$_2$) 20 µm.

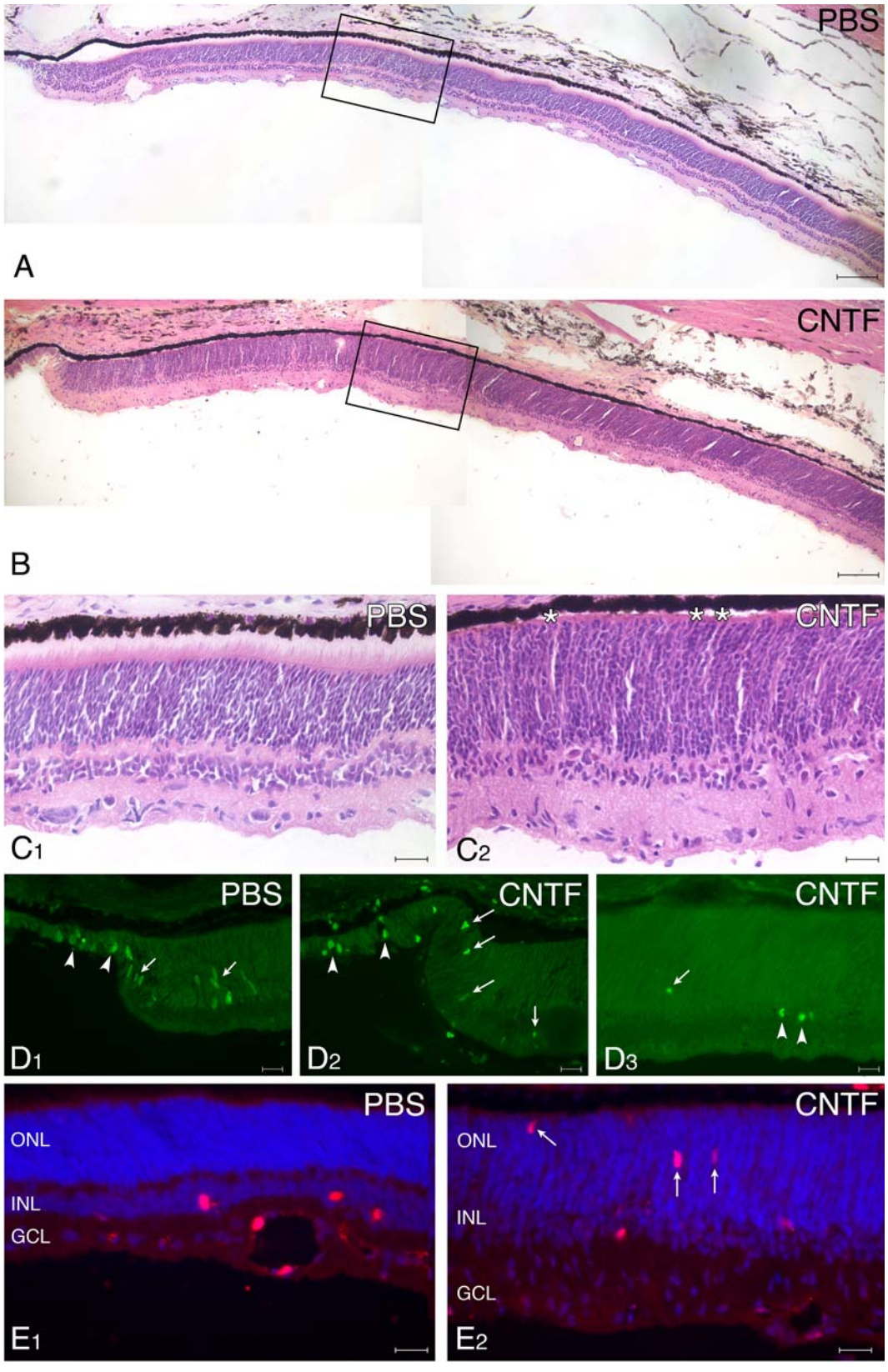
PBS
A
CNTF
B
PBS
C1
CNTF
C2
PBS
D1
CNTF
D2
CNTF
D3
PBS
ONL
INL
GCL
E1
CNTF
ONL
INL
GCL
E2

caused by cell proliferation, BrdU pulse labeling and Ki67 immunohistochemical studies were performed in two dogs. No major differences in ONL thickness, BrdU incorporation, or Ki67 immunolabeling were observed 24 hours following CNTF injection (data not shown). Yet, a major increase in ONL thickness was observed in the dog whose retina was collected one week post-CNTF administration (Figure 5.10 A, B). Although BrdU incorporation was seen in cells located at the peripheral retinal margin (Figure 5.10 D1, D2), and in the NFL, GCL, and INL throughout the entire length of the retina of both CNTF- and vehicle-treated eyes, there was a higher number of BrdU-positive nuclei with CNTF (Table 5.5). Indeed, combining results from three meridians, a mean of 47 and 135 cells per 10,000 μm of retina length, was found in the PBS- and CNTF-injected eyes, respectively. In addition, rare BrdU-positive cells were found exclusively in the ONL of the CNTF-treated retina (Figure 5.10 D3). A similar finding was observed with Ki67 (Figure 5.10 E2).

Table 5.5 Number of BrdU-positive cells per unit length of retina (10,000 μm) following CNTF or PBS injection in a 5 week-old *XLPRA2* dog. Mean [minimum; maximum] values were obtained from at least three sections for each of the meridians.

Meridian	**PBS-injected**	**CNTF-injected**
Superior	43 [39; 47]	138 [122; 161]
Inferior	54 [41; 65]	101 [97; 104]
Temporal	45 [34; 55]	165 [140; 187]

DISCUSSION

XLPRA2 is an early onset model of retinitis pigmentosa characterized by an early burst of photoreceptor cell death that begins at 4 weeks of age and reaches a peak at 7 weeks. This event is followed by a more gradual loss of rods and later of cones that persists for over 9 months.[14] An attempt to rescue photoreceptors from this initial phase of cell death with intravitreal injections of CNTF failed to promote in *XLPRA2* a similar neuroprotective effect as seen in the *rcd1* dog.[10] A peculiar set of findings that were exclusively observed in *XLPRA2* consisted of remodeling of the retinal periphery and an increase in cell number in the ONL. In addition, ocular toxic effects that involved the cornea, lens, and uveal tract were seen in both mutants and normal dogs.

Intravitreal injection of survival factors in animal models of RP has been used routinely to establish proof of principle of their photoreceptor rescue properties.[5] Yet, a recognized limitation to this route of administration for the treatment of retinal degenerations is the short half-life of these agents, and their associated ocular side-effects.[23-26] In this study, corneal epitheliopathy, cataracts, and clinical signs of uveitis were observed within a few days following a single intravitreal injection of 12 μg of CNTF. Similar clinical findings were found in the *rcd1* dog (Pearce-Kelling, unpublished) and *Rdy* cat[27] treated with Axokine® (Regeneron, Tarrytown, NY), a recombinant mutein of human CNTF. These side-effects appear to be dose-related because they are not observed in *rcd1* dogs that are intravitreally implanted with a long-term delivery device that releases a daily dose approximately 1000 fold lower.[10]

Several hypotheses may explain the absence of a positive rescue effect in photoreceptors of the *XLPRA2* dog: 1) A lack of activation of intracellular signaling pathways may be responsible for the absence of a survival response. This study showed that the α subunit of the CNTF receptor (CNTFRα) was expressed throughout the course of retinal degeneration in *rcd1* and *XLPRA2*, but we did not investigate

whether CNTF triggered any cell signaling pathways. Therefore, it is not known whether the binding of CNTF to CNTFRα activates the same molecular signaling cascades in both diseases. 2) The activation of anti-apoptotic molecules may not interfere with the molecular mechanisms of cell death that are involved in *XLPRA2*. Identifying the key molecular events that occur in different models of photoreceptor degeneration may reveal a spectrum of cell death pathways that respond differentially to survival factors. This may be the basis for the difference in response between *rcd1* and *XLPRA2*, and could explain CNTF's positive rescue effect in the *rd/rd*, *nr/nr* and Q344 ter mice, and its absence in the *rds/rds*, *pcd/pcd*, P23H and VPP mice.[28] 3) In the mutant, there may be activation of a stimulus so detrimental to the cell's homeostasis that its effects can not be countered by the survival factor. We intentionally chose to target the initial burst of photoreceptor cell death that occurs between 4 and 7 weeks of age in *XLPRA2*[14] as an approach to inhibit as early as possible the onset of the disease, and rescue the highest number of cells. However, this may not have been the optimal time-window for therapy, if the putative toxic gain of function caused by the *RPGR* frameshift mutation is at its highest level during this period. 4) A rapid elimination of CNTF from the eye may prevent prolonged activation of a rescue response. Despite the absence of any published pharmacokinetic study on the rate of clearance of intravitreally-injected CNTF, it is assumed that it is eliminated from the eye in less than 24 hours, as shown for pigment epithelium-derived factor (PEDF).[7] If achieving photoreceptor rescue in *XLPRA2* requires the continuous activation of pro-survival signaling pathways, then sustained bioavailability of CNTF through the use of a long-term delivery device may be necessary in this disease.

Quantitative methods were not used to measure the levels of expression of rod opsin and cone arrestin, yet immunohistochemical results suggested that CNTF caused

a rapid but transient decrease in the expression of these two proteins. This was seen as early as 24 hours following the injection, and was more pronounced 7 days later. This negative regulation in the expression of phototransduction proteins by CNTF has been also reported in the normal rat,[29] the *rd* mouse,[30] and in the *rcd1* dog.[22] Such an effect may be responsible for the electroretinographic alterations reported in rat and mouse models of retinal degeneration, as well as in the normal albino rabbit following intraocular delivery of CNTF. [31-34]

A striking finding was the prominent remodeling that occurred in the peripheral retina of *XLPRA2* dogs following intravitreal injection of CNTF. These retinal alterations consisted of loss of IS and OS, neuronal neuritic sprouting, heterotopia of retinal cells, and increase in the number of rods that contributed to the thickening of the ONL. The changes were disease- and age-specific. Indeed, they were only observed in *XLPRA2* dogs, and only if the first intravitreal injection of CNTF was done no later than at 7 weeks, an age at which the normal canine retina is reaching full maturation.[35]

The disorganization in the normal retinal layering was associated with the loss of inner and outer segments, which has been also observed by others.[29,33] Although IS are beginning to bud in the 4 week-old canine peripheral retina, IS and OS are fully formed when the retina has reached maturity at 7-8 weeks of age. CNTF, therefore, may have prevented the formation of IS and OS when injected at 4 weeks of age (treatment Groups #1 and #2), and caused their loss when injected later in 7 week-old dogs (treatment Group #3). Numerous reports have shown that CNTF causes a transient arrest in rod differentiation in the developing retina.[30,36,37] Our findings suggest that CNTF may not only arrest photoreceptor maturation in the *XLPRA2* dog, but also cause them to dedifferentiate. This is not unexpected since CNTF has recently

been shown to induce the dedifferentiation of adult human myoblasts into multipotent progenitor cells.[38]

CNTF is known to elicit the formation of new neuritic processes in rodent motor neurons.[39,40] More recently, it was reported that gene delivery of CNTF in a feline model causes neurite extension from rods, bipolar, and horizontal cells.[41] We observed in this study a similar effect in the *XLPRA2* dog. This may be caused by an alteration in neurotransmission at the synaptic terminal between rods, horizontal, and bipolar cells, as a result of a negative regulation on the phototransduction pathway. Another feature of the retinal remodeling that took place in the periphery was heterotopia of some rod, cone, bipolar, and Müller cell somas. Although we could not determine whether these rods and bipolar cells had migrated to an ectopic location, or whether these were newly generated neurons, we do provide evidence that displaced cones represented somas that had moved down the cone axon.

The most prominent feature of the peripheral remodeling was the abnormal increase in ONL thickness that has also been reported in normal rabbits implanted with ECT devices secreting a high dose (22ng/day) of CNTF.[11] In the present study, the thickened ONL could be seen extending several millimeters away from the *ora serrata*, and was detected as early as one week following CNTF administration. Although this was undoubtedly associated with some degree of intra- and/or extracellular swelling, an increase in the number of rod opsin-positive cells was the major contributing factor. The extent of the increase in cell number could not be explained only by a rescue effect. The use of cell proliferation markers confirmed that CNTF caused a higher number of cells to enter the cell cycle. Yet, the number of BrdU- or Ki67-positive cells that were found in the ONL was limited, and could not account completely for the supernumerary nuclei seen in this layer. The most plausible explanation for this discrepancy has to do with the period of cell proliferation, and the

time-points at which tissues were collected. It is indeed possible that, despite doing repeated injections of BrdU, a high enough concentration may not have been attained at the optimal time for its incorporation. Similarly, one week following CNTF injection, the great majority of these cells may have exited the cell cycle and were no longer be Ki67-positive. Addressing this issue would require determining the precise time of onset of the cell proliferation, and performing additional BrdU pulse-labeling experiments. This will be the subject of future studies.

The increased number of cells in the ONL raises the question of their origin. Although there is recent evidence for the presence of retinal progenitor cells at the retinal margin of $ptc^{+/-}$ mice,[42] monkeys, and humans,[43] it is unlikely that neurogenesis in this zone may account for all the additional cells that are seen over distances as far as 5,000 µm from the *ora serrata*. Recently, a pool of mitotic retinal progenitor cells was found distributed in the central retina of the adult $Chx10^{-/-}$ mouse.[44] Therefore, it may be possible that in *XLPRA2*, CNTF induces proliferation of such precursor cells.[45] Finally, another possibility is that CNTF causes rods to dedifferentiate and subsequently re-enter the cell cycle. The elimination of CNTF from the eye would cause the cells to stop proliferating, and assume a differentiated phenotype.

In summary, this study shows that intravitreal injection of CNTF does not prevent the early phase of cell death that occurs in a canine model of X-linked retinitis pigmentosa caused by a frameshift mutation in *RPGR* exon ORF15. Whether CNTF can rescue photoreceptors from the later phase of degeneration now needs to be addressed. This should provide further evidence as to whether human patients with similar mutations in *RPGR* would be expected to respond to this specific neuroprotective agent. CNTF also caused substantial remodeling in the peripheral retina of *XLPRA2* dogs. These peripheral alterations are most likely dose- and disease-specific. In addition, they were only observed when CNTF was injected before the

canine retina had reached full maturation. Therefore, although this may not be an issue for adult human patients treated with sustained release of CNTF,[12] peripheral retinal changes observed in normal adult rabbits,[11] and the suggestion that endogenous secretion of CNTF may be the cause of cell proliferation in humans with mutations in the *NR2E3* gene[46] warrants further investigation.

REFERENCES

1. Boughman JA, Conneally PM, Nance WE. Population genetic studies of retinitis pigmentosa. *Am J Hum Genet* 1980;32:223-235.

2. Puech B, Kostrubiec B, Hache JC, et al. Epidemiology and prevalence of hereditary retinal dystrophies in the Northern France. *J Fr Ophtalmol* 1991;14:153-164.

3. Acland GM, Aguirre GD, Ray J, et al. Gene therapy restores vision in a canine model of childhood blindness. *Nat Genet* 2001;28:92-95.

4. Pang JJ, Chang B, Kumar A, et al. Gene therapy restores vision-dependent behavior as well as retinal structure and function in a mouse model of RPE65 Leber congenital amaurosis. *Mol Ther* 2006;13:565-572.

5. LaVail MM, Unoki K, Yasumura D, et al. Multiple growth factors, cytokines, and neurotrophins rescue photoreceptors from the damaging effects of constant light. *Proc Natl Acad Sci U S A* 1992;89:11249-11253.

6. Frasson M, Picaud S, Leveillard T, et al. Glial cell line-derived neurotrophic factor induces histologic and functional protection of rod photoreceptors in the rd/rd mouse. *Invest Ophthalmol Vis Sci* 1999;40:2724-2734.

7. Cayouette M, Smith SB, Becerra SP, et al. Pigment epithelium-derived factor delays the death of photoreceptors in mouse models of inherited retinal degenerations. *Neurobiol Dis* 1999;6:523-532.

8. Beltran WA. Cellular and molecular studies of ciliary neurotrophic factor mediated neuroprotection in the canine retina. 2006, PhD dissertation. Field of *Comparative Biomedical Sciences*. Cornell University; Ithaca, NY.

9. Thanos CG, Bell WJ, O'Rourke P, et al. Sustained secretion of ciliary neurotrophic factor to the vitreous, using the encapsulated cell therapy-based NT-501 intraocular device. *Tissue Eng* 2004;10:1617-1622.

10. Tao W, Wen R, Goddard MB, et al. Encapsulated cell based delivery of CNTF reduces photoreceptor degeneration in animal models of retinitis pigmentosa. *Invest Ophthalmol Vis Sci* 2002;43:3292-3298.

11. Bush RA, Lei B, Tao W, et al. Encapsulated cell-based intraocular delivery of ciliary neurotrophic factor in normal rabbit: dose-dependent effects on ERG and retinal histology. *Invest Ophthalmol Vis Sci* 2004;45:2420-2430.

12. Sieving PA, Caruso RC, Tao W, et al. Ciliary neurotrophic factor (CNTF) for human retinal degeneration: Phase I trial of CNTF delivered by encapsulated cell intraocular implants. *Proc Natl Acad Sci U S A* 2006;103:3896-3901.

13. Zhang Q, Acland GM, Wu WX, et al. Different RPGR exon ORF15 mutations in Canids provide insights into photoreceptor cell degeneration. *Hum Mol Genet* 2002;11:993-1003.

14. Beltran WA, Hammond P, Acland GM, et al. A frameshift mutation in *RPGR* exon ORF15 causes photoreceptor degeneration and inner retina remodeling in a model of X-linked retinitis pigmentosa. *Invest Ophthalmol Vis Sci* 2006;47:1669-1681.

15. Ray K, Baldwin VJ, Acland GM, et al. Cosegregation of codon 807 mutation of the canine rod cGMP phosphodiesterase beta gene and rcd1. *Invest Ophthalmol Vis Sci* 1994;35:4291-4299.

16. Beltran WA, Zhang Q, Kijas JW, et al. Cloning, mapping, and retinal expression of the canine ciliary neurotrophic factor receptor α (CNTFRα). *Invest Ophthalmol Vis Sci* 2003;44:3642-3649.

17. Holst A, Heller S, Junghans D, et al. Onset of CNTFRα expression and signal transduction during neurogenesis in chick sensory dorsal root ganglia. *Dev Biol* 1997;191:1-13.

18. Beltran WA, Rohrer H, Aguirre GD. Immunolocalization of ciliary neurotrophic factor receptor α (CNTFRα) in mammalian photoreceptor cells. *Mol Vis* 2005;11:232-244.

19. Fischer AJ, Reh TA. Identification of a proliferating marginal zone of retinal progenitors in postnatal chickens. *Dev Biol* 2000;220:197-210.

20. Gelatt KN, MacKay EO. Distribution of intraocular pressure in dogs. *Vet Ophthalmol* 1998;1:109-114.

21. Schmidt SY, Aguirre GD. Reductions in taurine secondary to photoreceptor loss in Irish setters with rod-cone dysplasia. *Invest Ophthalmol Vis Sci* 1985;26:679-683.

22. Zeiss CJ, Allore HG, Towle V, et al. CNTF induces dose-dependent alterations in retinal morphology in normal and rcd-1 canine retina. *Exp Eye Res* 2005.

23. Faktorovich EG, Steinberg RH, Yasumura D, et al. Photoreceptor degeneration in inherited retinal dystrophy delayed by basic fibroblast growth factor. *Nature* 1990;347:83-86.

24. Faktorovich EG, Steinberg RH, Yasumura D, et al. Basic fibroblast growth factor and local injury protect photoreceptors from light damage in the rat. *J Neurosci* 1992;12:3554-3567.

25. Lewis GP, Erickson PA, Guerin CJ, et al. Basic fibroblast growth factor: a potential regulator of proliferation and intermediate filament expression in the retina. *J Neurosci* 1992;12:3968-3978.

26. Perry J, Du J, Kjeldbye H, et al. The effects of bFGF on RCS rat eyes. *Curr Eye Res* 1995;14:585-592.

27. Chong NH, Alexander RA, Waters L, et al. Repeated injections of a ciliary neurotrophic factor analogue leading to long-term photoreceptor survival in hereditary retinal degeneration. *Invest Ophthalmol Vis Sci* 1999;40:1298-1305.

28. LaVail MM, Yasumura D, Matthes MT, et al. Protection of mouse photoreceptors by survival factors in retinal degenerations. *Invest Ophthalmol Vis Sci* 1998;39:592-602.

29. Song Y, Zhao L, Liu Y, et al. Negative regulation of phototransduction machinery by CNTF is likely through the photostasis mechanism. ARVO 2005; E-abstract #163.

30. Caffe AR, Soderpalm AK, Holmqvist I, et al. A combination of CNTF and BDNF rescues rd photoreceptors but changes rod differentiation in the presence of RPE in retinal explants. *Invest Ophthalmol Vis Sci* 2001;42:275-282.

31. Liang FQ, Aleman TS, Dejneka NS, et al. Long-term protection of retinal structure but not function using RAAV.CNTF in animal models of retinitis pigmentosa. *Mol Ther* 2001;4:461-472.

32. Bok D, Yasumura D, Matthes MT, et al. Effects of adeno-associated virus-vectored ciliary neurotrophic factor on retinal structure and function in mice with a P216L rds/peripherin mutation. *Exp Eye Res* 2002;74:719-735.

33. Schlichtenbrede FC, MacNeil A, Bainbridge JW, et al. Intraocular gene delivery of ciliary neurotrophic factor results in significant loss of retinal function in normal mice and in the Prph2Rd2/Rd2 model of retinal degeneration. *Gene Ther* 2003;10:523-527.

34. Bush RA, Kononen L, Machida S, et al. The effect of calcium channel blocker diltiazem on photoreceptor degeneration in the rhodopsin Pro23His rat. *Invest Ophthalmol Vis Sci* 2000;41:2697-2701.

35. Farber DB, Danciger JS, Aguirre G. The beta subunit of cyclic GMP phosphodiesterase mRNA is deficient in canine rod-cone dysplasia 1. *Neuron* 1992;9:349-356.

36. Neophytou C, Vernallis AB, Smith A, et al. Müller-cell-derived leukaemia inhibitory factor arrests rod photoreceptor differentiation at a postmitotic pre-rod stage of development. *Development* 1997;124:2345-2354.

37. Schulz-Key S, Hofmann HD, Beisenherz-Huss C, et al. Ciliary neurotrophic factor as a transient negative regulator of rod development in rat retina. *Invest Ophthalmol Vis Sci* 2002;43:3099-3108.

38. Chen X, Mao Z, Liu S, et al. Dedifferentiation of adult human myoblasts induced by CNTF in vitro. *Mol Biol Cell* 2005;16:3140-3151.

39. Gurney ME, Yamamoto H, Kwon Y. Induction of motor neuron sprouting in vivo by ciliary neurotrophic factor and basic fibroblast growth factor. *J Neurosci* 1992;12:3241-3247.

40. Siegel SG, Patton B, English AW. Ciliary neurotrophic factor is required for motoneuron sprouting. *Exp Neurol* 2000;166:205-212.

41. Sethi CS, Schlichtenbrede F, Lewis GP, et al. Subretinal CNTF gene delivery in a feline model: Cell transfection and morphological sequelae. ARVO 2005;E-abstract #5217.

42. Moshiri A, Reh TA. Persistent progenitors at the retinal margin of ptc+/- mice. *J Neurosci* 2004;24:229-237.

43. Cuenca N, Angulo A, Martinez-Navarrete G, et al. Neurogenesis of photorecetors in the adult monkey and human retina. ARVO 2005;E-abstract #575.

44. Dhomen NS, Balaggan KS, Pearson RA, et al. Absence of chx10 causes neural progenitors to persist in the adult retina. *Invest Ophthalmol Vis Sci* 2006;47:386-396.

45. Zhang SS, Liu MG, Kano A, et al. STAT3 activation in response to growth factors or cytokines participates in retina precursor proliferation. *Exp Eye Res* 2005;81:103-115.

46. Jacobson SG, Sumaroka A, Aleman TS, et al. Nuclear receptor NR2E3 gene mutations distort human retinal laminar architecture and cause an unusual degeneration. *Hum Mol Genet* 2004;13:1893-1902.

CHAPTER SIX

CONCLUSION

Among the various therapeutic strategies aimed at maintaining vision in human patients affected with retinitis pigmentosa, the intravitreal long-term delivery of ciliary neurotrophic factor appears as one of the most promising approaches to rescue photoreceptors prior to cell death. Over the past recent years, proof of principle of CNTF's neuroprotective effect on photoreceptors and the results of preclinical safety studies in large animal models using the ECT-CNTF device have led to the testing of this therapeutic approach in 10 human patients with RP in a Phase I clinical trial. With Phase II clinical trial now being planned in humans with ARMD and RP, there is an increasing need for a better understanding of the mechanism of action by which CNTF promotes a survival response in photoreceptor cells.

The work presented in this thesis began to address this issue by characterizing the site of expression of the receptor for CNTF (CNTFRα) in the mammalian retina. This hopefully has contributed at resolving what used to be a matter of debate in the field of retinal cell biology. Our results (**Chapter 2**) show that CNTFRα is expressed by both rods and cones in the normal adult canine retina, thus implying that the photoreceptor survival effect observed in *rcd1* dogs treated with CNTF may be occurring through a direct mechanism of action. We also demonstrate that this finding is not specific to the dog but is also seen in the following non-rodent species: cat, sheep, pig, horse, monkey, and in human (**Chapter 3**). In the rat and mouse, immunolocalization of CNTFRα is not found in photoreceptor cells. These results imply therefore that the canine retina may be a more relevant model system than the rodent retina to characterize CNTF-mediated signaling pathways in photoreceptors.

A common assumption in using neuroprotective survival factors as a potential treatment for RP is that these agents should be capable of rescuing photoreceptors and curing all forms of RP regardless of the genetic cause of the disease. To begin addressing this issue we evaluated whether CNTF could rescue photoreceptors in *XLPRA2*, an early and rapidly progressive canine model for X-linked retinitis pigmentosa that was recently identified. We selected this model because the severity of disease is comparable to that of *rcd1*, yet the causative mutations are different. For this purpose, we first characterized the morphologic retinal changes that occur during the course of the disease and determined the kinetics of photoreceptor cell death (**Chapter 4**). Our results show a burst of photoreceptor cell death at an early stage of the disease which is responsible for a significant loss of photoreceptor cells. These findings suggest that this period of increased risk of cell death might be an optimal therapeutic time-window to test the neuroprotective effects of CNTF in this model. Intravitreal injections of CNTF during this acute and initial phase of cell death failed to protect photoreceptors in *XLPRA2*. In addition, significant remodeling is observed in the peripheral retina of the *XLPRA2* dogs treated with CNTF, while no such abnormality is observed in non-mutant and *rcd1* retinas.

In summary, several elements are strongly in favor of pursuing the development of this therapeutic strategy. These include the proof of principle of CNTF's photoreceptor rescue effect in small and large animal models of RP caused by mutations in different genes, the existence of an encapsulated cell therapy device that allows the prolonged intravitreal release of small and therapeutically active doses of CNTF, and the very encouraging results of a Phase I clinical trial in humans using this technology. Yet, some recent observations following the intraocular delivery of CNTF in animal models of RP ought to draw our attention. We and others have found that CNTF can down-regulate the expression of phototransduction proteins, which may

explain a reduction in retinal function as assessed by electroretinography. The absence of any rescue effect in some rodent models of retinal degeneration, as well as in the *XLPRA2* dog following intravitreal injections of CNTF, suggests that some forms of RP will most likely not be responsive to this survival factor either. A possibility is that only a limited number of forms of RP that share a common pathogenic mechanism and/or signaling pathway of cell death will be responsive to a particular survival factor. If this is proven to be correct, the ultimate strategy for treating RP may consist in matching a neuroprotective agent or a combination of these factors with a particular form of RP. Finally, our findings and those from other groups suggest that CNTF has the potential for causing cell dedifferentiation and proliferation. While this may be explained by a dose effect or by the age at which the intravitreal injections were done in the case of the *XLPRA2* dog, it is critical to assess that prolonged intravitreal delivery of CNTF does not cause a similar effect in the human eye.